

UC Santa Barbara

UC Santa Barbara Electronic Theses and Dissertations

Title

Essays on Environmental Markets and Marine Conservation

Permalink

<https://escholarship.org/uc/item/3d7838qv>

Author

Villaseñor-Derbez, Juan Carlos

Publication Date

2022

Peer reviewed|Thesis/dissertation

University of California
Santa Barbara

Essays on Environmental Markets and Marine Conservation

A dissertation submitted in partial satisfaction
of the requirements for the degree

Doctor of Philosophy
in
Environmental Science and Management

by

Juan Carlos Villaseñor-Derbez

Committee in charge:

Professor Christopher Costello, Chair
Professor Steven Gaines
Professor Kyle Meng
Professor Fiorenza Micheli

September 2022

The Dissertation of Juan Carlos Villaseñor-Derbez is approved.

Professor Steven Gaines

Professor Kyle Meng

Professor Fiorenza Micheli

Professor Christopher Costello, Committee Chair

June 2022

Essays on Environmental Markets and Marine Conservation

Copyright © 2022

by

Juan Carlos Villaseñor-Derbez

A mis padres. Sin su apoyo, cariño y ejemplo de dedicación esto no habría sido posible.

Acknowledgements

Financial support for my degree was provided by the International Doctoral Fellowship by Consejo Nacional de Ciencia y Tecnología and UCMexUS, the Latin American Fisheries Fellowship, Dissertation Fellowship from the UC's Institute on Global Conflict and Cooperation, Schmidt Environmental Solutions Fellowship, and the Graduate Division at the University of California, Santa Barbara.

My work benefited from discussions with Darcy Bradley, Christopher Free, Renato Molina, Andrew Plantinga, and members of the Gaines Lab, the Costello Lab, and the Environmental Markets Lab.

Curriculum Vitæ

Juan Carlos Villaseñor-Derbez

Education

- 2022 Ph.D. in Environmental Science and Management (Expected), University of California, Santa Barbara.
- 2017 Masters of Environmental Science and Management, University of California, Santa Barbara.
- 2015 B.Sc. in Oceanography, Universidad Autónoma de Baja California, Mexico

Publications

2022

- **Villaseñor-Derbez, J. C.**, Amador-Castro, I. G., Hernandez-Velasco, A., Torre, J., Fulton, S. (2022). Two Decades of Community-Based Marine Conservation Provide the Foundations for Future Action. *Frontiers in Marine Science*
- Wintergalen E., Molina R., Oyanedel R., **Villaseñor-Derbez, J.C.**, Fulton S. Opportunities and challenges for livelihood resilience in urban and rural Mexican small-scale fisheries. (in press). *Ecology and Society*.
- Wilson M. W., Lawson J. M., Rivera-Hechem M. I., **Villaseñor-Derbez J. C.**, Gaines, S. D. Evaluating Conditions for Moored Fish Aggregating Device Fisheries Development in the Caribbean and Bermuda. (2022). *Frontiers in Marine Science*

2021

- Millage K.D., **Villaseñor-Derbez, J.C.**, Bradley D., Burgess M., Lenihan H., Costello C. (2021). SelfFinanced Marine Protected Areas. *Environmental Research Letters*
- Tuholske C., Halpern B., Blasco G., **Villaseñor-Derbez J.C.**, Frazier M., Caylor K.K. (2021). Mapping global inputs and impacts from human sewage in coastal ecosystems. *PLoS ONE*
- Ramírez-Valdez A., Rowell T. J., Dale K., Craig M., Allen L., **Villaseñor-Derbez J.C.**, Cisneros-Montemayor A., Hernández-Velasco A., Torre J., Hofmeister J., Erisman B. (2021) Asymmetry across international borders: Research, fishery and management trends and economic value of the giant sea bass (*Stereolepis gigas*). *Fish & Fisheries*.
- Lynham J., Nikolaev A., Rainor, J., Vilela T., **Villaseñor-Derbez J.C.** (2021). Reply to "Catch rate composition affects assessment of protected area impacts". *Nature Communications*.

2020

- Wilson M. W., Lawson J. M., Rivera-Hechem M. I., **Villaseñor-Derbez J. C.**, Gaines, S. D. (2020). Status and trends of moored fish aggregating device (MFAD) fisheries in the Caribbean and Bermuda. *Marine Policy*.
- Lynham J., Nikolaev A., Rainor, J., Vilela T., **Villaseñor-Derbez J.C.** (2020). Economic Impact of Two of the Largest Protected Areas on Earth. *Nature Communications*.
- **Villaseñor-Derbez J.C.**, Lynham J., Costello C. (2020). Environmental Market Design for Large-Scale Marine Conservation. *Nature Sustainability*.

2019

- **Villaseñor-Derbez J.C.**, Aceves-Bueno E., Fulton S., Suarez-Castillo A., Hernández-Velasco A., Torre J., Micheli F. (2019). An interdisciplinary evaluation of community-based TURF-reserves. *PLoS ONE*.
- O'Hara C., **Villaseñor-Derbez.**, J.C., Ralph G., Halpern B. (2019). Mapping status and conservation of global at-risk marine biodiversity. *Conservation Letters*.
- **Villaseñor-Derbez J.C.**, Fitzgerald S. (2019). Spatial variation in allometric growth of invasive lionfish has management implications. *PeerJ*

2018

- Peake, J., Bogdanoff A.K., Layman C.A., Castillo B., Chapman J., Dahl K., Patterson W., Eddy C., Ellis R., Faletti M., Higgs N., Johnston M., Muñoz R., Sandel V., **Villaseñor-Derbez J.C.**, Morris Jr. J.A. (2018). Feeding ecology of invasive lionfish (*Pterois volitans* and *Pterois miles*) in the temperate and tropical western Atlantic. *Biological Invasions*. DOI: 10.1007/s10530-018-1720-5
- **Villaseñor-Derbez J.C.** Faro C., Wright M., Martínez J., Fitzgerald S., Fulton S., Mancha-Cisneros M.M., McDonald G., Micheli F., Suárez A., Torre J., Costello C. (2018). A user-friendly tool to evaluate the effectiveness of no-take marine reserves. *PLoS ONE*. DOI: 10.1371/journal.pone.0191821

2016

- Hernández-Velasco A.J., Fernández-Rivera Melo F.J., Melo-Merino, S.M. **Villaseñor-Derbez, J.C.** (2016). Occurrence of *Holacanthus clarionensis* (Pomacanthidae), *Stegastes leucorus*, and *S. acapulcoensis* (Pomacentridae) at Isla Magdalena B.C.S., Mexico. *Marine Biodiversity Records*. DOI: 10.1186/s41200-016-0062-1

2015

- Ramírez-Valdez A., Dominguez-Guerrero I., Palacios-Salgado D.S., Cota-Nieto J.J., Hinojosa-Arango G., Correa-Sandoval F., Reyes-Bonilla H., **Villaseñor-Derbez J.C.**, Hernandez A., Aburto-Oropeza, O. (2015). The nearshore fishes of the Cedros archipelago and their biogeographic affinities, northeastern Pacific. *CalCOFI Reports*

- Dreyfus M., Mejía-Trejo A., **Villaseñor-Derbez J.C.** (2015). Analysis of null sets (no catch) made by the Mexican tuna seine fleet (2000-2013). *Ciencias Marinas*. DOI: 10.7773/cm.v41i2.2471

2014

- Villaseñor-Derbez J.C. & Herrera-Pérez R. (2014). Brief description of prey selectivity and ontogenetic changes in the diet of the invasive lionfish *Pterois volitans* (Actinopterygii, Scorpaenidae) in the Mexican Caribbean. *Pan-American Journal of Aquatic Sciences*, 8(2):131-135

Teaching

Teaching Assistant for graduate-level courses

2020

- ESM 206 – Introduction to Environmental Data Science & Statistics with Dr. Allison Horst (100+ students)
- ESM 201 – Ecology of Managed Ecosystems with Dr. David Tilman (86 students)

2019

- ESM 201 – Ecology of Managed Ecosystems with Dr. David Tilman (82 students)

Guest Lecturer

2020

- ESM 206 – Data Analysis and Statistics: “Package-less” coding: Coding in base R (100+ students)
- EEMB 168 – Conservation Ecology: Marine Conservation in Practice (100+ students)

2018

- ESM 244 – Adv. Data Analysis and Statistics: The development cycle of web-based apps (70 students)

Data Science Workshops

2021

- EcoDataScience Workshop: GNU make and Makefiles for continuous development (and reproducibility)

2019

- EcoDataScience Workshop : Collaborative workflows with git and GitHub

- LAFF workshop: Coding ecological models in R

2017

- EcoDataScience Workshop: Introduction to R Markdown

Technical Workshops

2019

- Evaluation and budgeting of Marine Reserves in Mexico

2018

- 2018 Empirical valuation of Marine Reserves effectiveness

2017

- A general approach and tool to evaluate the effectiveness of no-take marine reserves
- Empirical valuation of Marine Reserves effectiveness

2015

- REEFCheck California monitoring techniques

Mentoring

Master's Group Theses Mentored (Client in parentheses)

2020

- Marine Extractive Reserve performance in Brazil (World Wildlife Fund Brazil) Students: Peyton Moore, Ruben Sanchez-Ramirez, Dylan Glave, Elliott Matthews

2019

- Assessing Brazil's Marine Aquaculture Potential (World Wildlife Fund Brazil) Students: Caio Della Colleta Vianna, Eva Marrero, Kirby Bartlett, Anna Calle, Sandra Fogg

2018

- Economic quantification of delaying management in the Midriff Islands, Mexico (Comunidad y Biodiversidad) Students: Edaysi Bucio, Seleni Cruz, Vienna Saccomanno, Juliette Verstaen, Valeria Tamayo
- Insurance instruments to leverage natural infrastructure for climate change resilience Students: Mario Colon, Daniel Elkin, Lauren Kaapcke, Madison Meltzer, Casey Moorhead

2017

- Creating Effective Marine Reserves (Fundación Claudia y Roberto Hernández) Students: Fabio Castagnino, Roxanne Diaz, Denise Garcia, Sarah Salem, Camila Vargas

High school students (Placement)

2018

- Alex Reulbach. Small-scale variation in the diet of invasive lionfish. (Marine Biology, UNC)
- Alisha Naidu. Ontogenetic habitat shifts in invasive lionfish. (Computer Science, Williams College)
- Joseph Sausville. Optimal marine reserve design to maximize economic and conservation benefits

Grants and Awards

Research Grants

2021

- Environmental Solutions Research Grant (\$20,000). Schmidt Family Foundation. Incentives for Equitable and Cost-effective Marine Conservation
- Dissertation Fellowship (\$25,000). UC Institute on Global Conflict and Cooperation. Designing Conservation Markets for International Cooperation

2020

- H. William Kuni Research Award (\$14,950). Economic and Ecological responses to global economic shutdowns in coral reef communities. With Erin Winslow and Nathaniel Grimes

2019

- Mohamed bin Zayed Species Conservation Fund (\$11,500). Unveiling the Ecology of Giant Sea Bass (*Stereolepis gigas*). With Arturo Ramírez-Valdez and Kyla Blincow

2018

- H. William Kuni Research Award (\$15,000). The proliferation of Fish Aggregating Devices (FADs) in the Caribbean Sea. With Molly Wilson, Julia Lawson, and Ignacia Rivera

2017

- PADI Foundation Research Grant (\$6,600) Natural history of the giant sea bass (*Stereolepis gigas*) in Mexican waters. With Arturo Ramírez-Valdez and Paula Sgarlatta.

Fellowships, scholarships, and awards

2019

- Best presentation. Integrated Marine Biosphere Research. Awarded best presentation at the Future Oceans Conference

2017

- Doctoral Fellowship (\$61,194). UC Mexus. Complimentary funding to complete a Ph.D in Environmental Sciences
- Latin American Fisheries Fellowship (\$57,400) University of California, Santa Barbara Complimentary funding to complete a Ph.D in Environmental Sciences
- International Student's Doctoral Fellowship (\$146,619). Consejo Nacional de Ciencia y Tecnología (CONACyT). Four years of funding to complete a 5-year Ph.D. in Environmental Sciences
- Honorable Mention. Integrated Marine Biosphere Research. Runner-up for best student project at the IMBeR ClimEco6 Summer School

2015

- Latin American Fisheries Fellowship (\$42,000). University of California, Santa Barbara. Complimentary funding to complete a Master in Environmental Science and Management
- CONACyT International Student's Master's Fellowship (\$64,946). Mexican Government. Funding to complete a Master in Environmental Science and Management

2014

- Pedro Mercado Sánchez National Oceanography Award. Asociación Mexicana de Oceanólogos. For the best undergraduate research project presented at the XVIII National Oceanography Conference
- Honorable Mention. CONACyT. Runner-up for best student paper at the 2nd State Meeting of Young Researchers
- Distinguished Student of the Oceanography program. Facultad de Ciencias Marinas, Universidad Autónoma de Baja California. Ranked first in academic performance for the overall major in 2014

2013 Best presentation. CONACyT. For the best student paper at the 1st State Meeting of Young Researchers.

- Best presentation. Facultad de Ciencias Marinas, Universidad Autónoma de Baja California. 1st Place for the best undergraduate presentation at the XXI Student Conference

2012

- Honorable mention. Facultad de Ciencias Marinas, Universidad Autónoma de Baja California. 2nd Place for the best undergraduate presentation at the XX Student Conference
- Distinguished Student of the Oceanography program. Facultad de Ciencias Marinas, Universidad Autónoma de Baja California. Ranked first in academic performance for the overall major in 2012

Academic Appointments

- 2020 - 2022 Graduate Student Researcher. Environmental Markets Lab, UCSB.
- 2019 - 2020 Graduate Student Researcher. National Center for Ecological Analysis and Synthesis, UCSB.
- 2015 - 2016 Data analyst. Mexican Tuna Purse Seine Fleet Research Trust
- 2013 - 2013 Research Intern. Fundación para el Estudio y Conservación de Condrictios, SQUALUS
- 2013 - 2013 On-board scientific observer. Fisheries Ecology Lab, CICESE
- 2012 - 2012 Oceanographic Cruise Research Intern. Oceanography Department, CICESE
- 2011 - 2015 Research Assistant. Kelp Forest Ecology Research Group, UABC

Academic Service

Referee Activity

Ecological Modeling, Frontiers in Marine Science, Gulf and Caribbean Research, Bulletin of Marine Science, Nature Sustainability, Marine Policy

Committees

- 2020 Faculty Search. Assistant Professor in Environmental Data Science. Bren School of Environmental Science & Management, UCSB
- 2019 Dean's Advisory Council. Bren School of Environmental Science & Management, UCSB
- 2018 PhD Symposium organization committee. Bren School of Environmental Science & Management, UCSB
- 2014 Student Conference Organizer. Facultad de Ciencias Marinas, UABC
- 2013 Student Council. Facultad de Ciencias Marinas, UABC

Working groups and panels

2021

- Data Science communities in Santa Barbara. Master of Environmental Data Science Program, UCSB

2019

- Palau's National Marine Sanctuary: Managing Ocean Change and Supporting Food Security. NCEAS

2017

- Marine Spatial Planning in Baja California: Connecting MPA networks in a trans-boundary context. COBI
- Defining Socioeconomic and Ecological indicators for to evaluate marine protected areas. COBI / TNC

Conference Presentations

2019

- Villaseñor-Derbez J.C., Rivera-Hechem M.I., Wilson, M. W., Lawson, J. M., Gaines, S. D. Status and trends of moored fish aggregating device (MFAD) fisheries in the Caribbean and Bermuda. 72nd GCFI
- Villaseñor-Derbez J.C., Lynham J., Costello C. Change in behavior and effort redistribution after implementation of Large Scale Marine Protected Areas. Future Oceans2

2018

- Villaseñor-Derbez, J.C., Aceves-Bueno E., Fulton, S., Suarez-Castillo, A., Hernández-Velasco, A., Torre, J., Micheli, F. Effectiveness of community-based marine reserves in small-scale fisheries. 3rd World Small-Scale Fisheries Conference

2017

- J.C. Villaseñor-Derbez, C. Faro, M. Wright, J. Martínez, C. Costello. A general approach and tool to evaluate the effectiveness of no take marine reserves. 28th International Congress for Conservation Biology.

2014

- J.C. Villaseñor-Derbez, A. Ramírez-Valdez, G. Montaña-Moctezuma, G. Torres-Moye. Because size matters: Differences in size structure of exploited and unexploited fish populations along the coasts of Baja California, Mexico. XIV National Ichthyology Meeting and III Latin-American Ichthyology Symposium.
- Ramírez-Valdez A., Montaña-Moctezuma G., Torres-Moye G., Aburto-Oropeza O., Villaseñor-Derbez J.C. Biogeographic relationships of fish communities associated to Kelp Forests off the coasts of Baja California, Mexico. XIV National Ichthyology Meeting and III Latin-American Ichthyology Symposium.

- J.C. Villaseñor-Derbez, A. Ramírez-Valdez, G. Montaña-Moctezuma, G. Torres-Moye. Effects of recreational fisheries over sizes and biomasses of fish associated to Kelp Forests. 2nd State Meeting of Young Researchers.
- J.C. Villaseñor-Derbez, A. Ramírez-Valdez, G. Montaña-Moctezuma, G. Torres-Moye. Latitudinal distribution of sizes of fish associated to Kelp Forests off the coasts of Baja California, Mexico. XVIII National Oceanography Conference.
- J.C. Villaseñor-Derbez, A. Ramírez-Valdez, G. Montaña-Moctezuma, G. Torres-Moye. Latitudinal distribution of sizes of fish associated to Kelp Forests off the coasts of Baja California, Mexico. XXII Student Conference at the Marine Sciences School and 1st National Student Conference on Marine and Environmental Sciences.
- J.C. Villaseñor-Derbez. Description of feeding habits and ontogenetic changes in the invasive lionfish *Pterois volitans* (Linnaeus, 1758) diet off the coasts of Playa del Carmen, Quintana Roo. 1st Student Conference of Biological Sciences.

2013

- J.C. Villaseñor-Derbez, G. Montaña-Moctezuma, G. Torres-Moye y A. Ramírez-Valdez. Community relationships of fish associated to Kelp Forests off the coasts of Baja California, Mexico. 1st State Meeting of Young Researchers
- J.C. Villaseñor-Derbez, G. Montaña-Moctezuma, G. Torres-Moye y A. Ramírez-Valdez. Community relationships of fish associated to Kelp Forests off the coasts of Baja California, Mexico. XXI Student Conference at the Marine Sciences School

2012

- J.C. Villaseñor-Derbez. Contribution to knowledge of diet and biometrics of the invasive lionfish [*Pterois volitans* (Linnaeus 1758)] off the coasts of Playa del Carmen, Quintana Roo, Mexico. XIII National Ichthyology Meeting and 1st Latin-American Ichthyology Symposium

Abstract

Essays on Environmental Markets and Marine Conservation

by

Juan Carlos Villaseñor-Derbez

Humanity depends on the ocean for jobs, subsistence, and way of life. Yet, many of our activities directly or indirectly threaten the marine environment. Environmental markets are one way to regulate these negative externalities. Environmental markets have been frequently used in land, water, and atmospheric contexts, but their application to the marine environment is rare and their interaction with other institutions remains understudied. Here, I combine theory from environmental economics and ecology with modern data science techniques and computer simulation to study three types of links between environmental markets and marine conservation. My first chapter explores how an existing market for fishing effort interacts with a nation's incentive to engage in marine conservation in the form of Marine Protected Areas. In my second chapter, I propose, design, and analyze a global market for marine conservation, where nations can trade conservation obligations. Finally, my third chapter studies the implied carbon costs of human-induced whale mortality, thus providing a way to connect cetacean conservation and carbon markets. Together, these essays show how seemingly benign nuances in market design features and ecological processes are pivotal in determining the incentives for marine conservation.

Contents

Curriculum Vitae	vi
Abstract	xv
List of Figures	xviii
List of Tables	xxiv
1 Introduction	1
1.1 Introduction	2
1.2 Notes on reproducibility	4
1.3 Permissions and Attributions	5
2 Environmental market design for large-scale marine conservation	7
2.1 Introduction	9
2.2 Methods	12
2.3 Results	22
2.4 Discussion	30
3 A global market for marine conservation	33
3.1 Introduction	35
3.2 Methods	39
3.3 Results	44
3.4 Discussion	49
4 The implied carbon cost of human-induced whale mortality	53
4.1 Introduction	55
4.2 Methods	58
4.3 Results	69
4.4 Discussion and Conclusions	77

A	Supplementary materials for Ch. 2	81
A.1	Supplementary methods	81
A.2	Supplementary figures	82
B	Supplementary materials for Ch. 3	93
C	Supplementary materials for Ch. 4	102
	Bibliography	109

List of Figures

2.1	Map of the Exclusive Economic Zones (EEZs) and Marine Protected Areas in the PNA, the bottom-left inset provides a reference for the area. Parties to the Nauru Agreement (PNA) are shown in blue, while empty polygons indicate all others. A red line outlines the three EEZs of Kiribati. The solid red polygons show The Phoenix Islands Protected Area (PIPA) implemented in 2015 and the proposed Palau National Marine Sanctuary (PNMS) to be implemented in 2020. Land masses are shown in gray. Labels indicate ISO3 country codes for PNA members (PLW: Palau, PNG: Papua New Guinea, FSM: Federal States of Micronesia, SLB: Solomon Islands, NRU: Nauru, MHL: Marshal Islands, KIR: Kiribati, TUV: Tuvalu, TKL: Tokelau).	11
2.2	Cost of spatial closures in a vessel-day fishery. Each line represents a possible value of within-country stock movement (θ ; line colors), with $\theta = 0$ representing a stock that doesn't move to $\theta = 1$ depicting a stock that continuously moves between the reserve and the fishing zone. The revenue losses to Country 1 (vertical axis) are relative to a fishery with no spatial closures, and are shown as a function of reserve size (R ; horizontal axis), from no reserve ($R = 0$) to closing the entire Exclusive Economic Zone ($R = 1$). Costs are shown for Country 1 when there is no trading (a) and when trading is allowed (b; note the change in axis limits). Costs avoided by trading are shown in (c). Dashed red line in (a) is a 1:1 line. When trading between countries occurs, 88.5% to 99.2% of revenue losses can be avoided.	24

2.3	<p>Costs of a spatial closure for Country 1 under different allocation rules. Each line represents the revenue losses for a combination of allocation rules (α; line type) and movement (θ; color) for different reserve sizes (R; horizontal axis). A value of $\alpha = 1$ implies that allocations are based entirely on historical effort, while a value of $\alpha = 0$ implies a 100% biomass-based allocation rule. A value of $\theta = 0$ represents a stock that doesn't move, and $\theta = 1$ depicts a stock that continuously moves between the reserve and the fishing zone. The proportion of the Exclusive Economic Zone closed to fishing is given by R. An effort-based allocation and low within-country movement values result in the highest costs. Cost can be minimized for all movement values if allocation is based on biomass within each country's waters.</p>	25
2.4	<p>Change in spatial footprint of fishing activity by 318 tuna purse seiners. Black lines show Exclusive Economic Zones (EEZ), and red line outlines the Phoenix Island Protected Area (PIPA). Panels a and b show the normalized change in average fishing hours through time for displaced (panel a; $n = 64$) and non-displaced vessels (panel b; $n = 254$). Panel c shows the difference between a and b, highlighting areas where displaced vessels redistributed to, relative to non-displaced vessels. Note that displaced vessels allocate more hours to the Gilbert Islands and Line islands (part of Kiribati's EEZs), but also Tuvalu and the high seas surrounding PIPA and Kiribati's EEZ.</p>	27
2.5	<p>Effort displacement and license revenues. Panels (a) and (b) show AIS-derived annual vessel-days for Kiribati and for all Parties to the Nauru Agreement (PNA) by 318 tuna purse seine vessels. Annual effort is broken down by displaced ($n = 64$) and non-displaced ($n = 254$) vessels. The dashed horizontal lines represent the total allowable vessel-days in Kiribati (11,000 days [1]) and the PNA (45,000 vessel-days). Panel (c) shows annual revenue from fishing license fees by country and year (2008 - 2016) and panel (d) shows the correspondence between FFA-reported revenues and AIS-derived vessel-day observations (2012 - 2016). The dashed line in panel (d) represents line of best fit, and the shaded area represents the standard error around the regression. Colors in panels (c) and (d) are given by ISO3 country codes for PNA members (PLW: Palau, PNG: Papua New Guinea, FSM: Federal States of Micronesia, SLB: Solomon Islands, NRU: Nauru, MHL: Marshal Islands, KIR: Kiribati, TUV: Tuvalu, TKL: Tokelau).</p>	28

3.1	Stylized conservation supply curves and market outcomes, which are assumed to be linear for illustrative purposes. MC_1 and MC_2 indicate the marginal costs curves to each nation. The opaque triangles labeled TC_1 and TC_2 indicate the total costs to each nation. The solid triangles labeled S_1 and S_2 indicate the savings to each nations under a market.	37
3.2	Conservation supply curves for 186 coastal nations. Note the large heterogeneity in potential conservation benefits and marginal costs of conserving.	44
3.3	Map of savings. The color indicates whether a firm buys (blue) or sells (red) conservation credits, and the hue indicates the magnitude of the savings, similar to the area of the stylized "savings triangles" described in Fig 3.1C.	46
3.4	Gains from trade of a market for marine conservation under four bubble policies. The y-axis shows the difference between the total costs under market and total costs under BAU, relative to the total costs under BAU. The x-axis shows the bubble policy implemented, with numbers in parentheses indicting the number of bubbles implemented under each policy. .	48
3.5	Gains from trade (y-axis) for a range of conservation targets (10% to 99%; x-axis), under four different bubble policies (colors). Each line shows the percent of the costs that can be avoided by allowing trade between nations within each segment. The dashed horizontal lines mark the often-cited conservation targets of 10%, 30%, and 50%.	49
4.1	Fate of removed whales determine cost. A) Implied costs (y-axis) of whale mortality due to harvesting (blue) or shipstrikes (red) across age-ranges. Panel B shows the difference between the red and blue lines in panel A. Panel C) shows the differences in Carbon contributions (y-axis) for a whale harvested at a given age (x-axis) for the three different contribution pathways. The difference is calculated as Carbon under the mortality scenario minus the Carbon under the BAU scenario. The dotted vertical line indicates the age at maturity (α_m), the dashed vertical line indicates $a_{m50} = a_0 + \frac{\ln(0.5)}{-k}$ the age at which organisms reach 50% of the theoretical maximum mass (m_∞) according to the von Bertalanfy weight-at-age relationship, and the solid vertical line shows the maximum age (α). . . .	72
4.2	Difference in Carbon sequestration pathways ($C_{mrt} - C_{bau}$) for two selected runs under each mortality source scenario. Positive values indicate greater sequestration under the given mortality scenario, relative to BAU. The simulations were selected to show the pathway of simulations where a whale is removed from the first age class ($\alpha = 1$) and the terminal age class ($\alpha = 97$). The panel on the left shows a scenario where the whale sinks, the panel on the right shows a scenario where the whale does not sink.	73

4.3	Comparison of value of somatic growth and reproductive growth. Panel A) shows the implied Carbon cost for Carbon stored in a whale's body (x-axis) and the inter-generational Carbon sequestration potential due to reproduction and growth (y-axis), exclusive of in-body Carbon of the harvested whale for each harvested age (marker size). Panel B shows the in-body Carbon value of a harvested whale as a percent of the total value of a whale (y-axis).	73
4.4	Implied costs (y-axis) for ten different initial population sizes (colors) across all possible age-classes (x-axis). The circle markers indicate the highest value along each line; the age at which costs are largest for a given initial population size. The dotted vertical line indicates the age at maturity (α_m), the dashed vertical line indicates $a_{m50} = a_0 + \frac{\ln(0.5)}{-k}$ the age at which organisms reach 50% of the theoretical maximum mass (m_∞) according to the von Bertalanfy weight-at-age relationship, and the solid vertical line shows the maximum age (α).	74
4.5	Implied Carbon cost of human-induced whale mortality for five species of baleen whales. Panel A) shows the mean (\pm SD) implied Carbon cost resulting from 1000 simulations where one organism is randomly removed from the population. The age at which an organism is removed is proportional to the age-class-specific abundance. Panel B) shows the kernel density distribution (using a bandwidth of 5 years) of ages at which mortality is induced by species.	76
4.6	Whale catch from the International Whaling Commission. Panel A) shows a time series of catch since the moratorium on whaling came into place (1985). Panel B) shows the number of whales caught in 2020 for each species.	79
A.1	Vessel-day prices with conservation and no trading. Vessel-day prices (vertical axis) are shown for a combination of reserve sizes (R in the horizontal-axis) and different within-country movement (θ) for the country with spatial closure and other countries (left - right, respectively) when there is no trading.	82
A.2	Change in revenues to non-conserving countries. Relative change in revenue for countries 2 - 9 (vertical axis) for a combination of reserve sizes (R in the horizontal-axis) and different within-country movement (θ) when there is no trading.	84
A.3	Vessel-day prices with conservation and trading. PNA-wide vessel-day prices (vertical axis) with trading, for a combination of reserve sizes (R in the horizontal-axis) and different within-country movement (θ).	85

A.4	Effort and revenues to the conserving country with and without trading. Effort and revenue in Country 1 are shown for a combination of reserve sizes (R), different within-country movement (θ), and with and without trading. With trading, the relative drop in effort is always larger than the relative drop in revenue as R increases. The exact opposite relationship holds without trading: effort remains fixed as revenue declines with increasing R	86
A.5	Vessel characteristics for 318 tuna purse seiners. Distribution of observable characteristics by vessel for displaced ($n = 64$), non-displaced vessels ($n = 254$).	87
A.6	Total revenues for all PNA countries combined.	88
A.7	Financial indicators for PNA countries. A) Total annual purse seine catch by EEZ and, B) Total annual value of purse seine catch by EEZ. Vertical dashed line in both plots denotes implementation of PIPA.	89
A.8	Annual country-level vessel-days for all PNA countries by 318 tuna purse seiners.	90
A.9	Annual fishing effort (hours) on a 1-degree grid around PIPA (red polygon) and Kiribati (black polygons).	91
A.10	Longline and purse seine vessel-days in Palau during 2018 at a 0.5 degree resolution.	92
A.11	Time series of the annual proportion of longline and purse seine vessel-days within the proposed PNMS boundaries.	92
B.1	Construction of our measure of conservation benefits using a 0.5 x 0.5 grid cell. Panel A) shows the Habitat Suitability Index (HSI_i), panel B) shows the area (α_i in Km^2), and panel C) shows the conservation benefit ($Q_i = HSI_i \times \alpha_i$) for each grid cell.	94
B.2	Median fisheries revenue (M USD; 2005 - 2015) along a 0.5 x 0.5 grid.	94
B.3	Benefit to cost ratio (log-10 transformed HSI-weighted KM^2 / M USD) on a 0.5 x 0.5 grid cell.	95
B.4	Histogram of habitat suitability index "HSI"	95
B.5	Spatial distribution of the four bubble policies intersected with the Exclusive Economic Zones of 186 coastal nations. A) Shows a global bubble policy, where all nations participate in a single market. B) Shows the oceans are divided into four market segments on the basis of geographic hemispheres. C) Shows the 12 biogeographic realms defined by Spalding et al., 2007, and D) shows the sub-division of realms into 60 provinces.	96
B.6	Conservation supply curves for nations across four hemispheres.	97
B.7	Conservation supply curves for nations across 12 biogeographic realms.	98
B.8	Conservation supply curves for nations across 60 biogeographic provinces.	99

B.9	A market-based approach relocates some Marine Protected Areas. Colors on the map indicate whether a grid cell is protected regardless of strategy, protected only under unilateral conservation, or protected only under a market (yellow).	100
B.10	Differences in surface area (y-axis) needed to meet a given conservation target (x-axis). The top panel shows change in area relative to BAU, and is represented as a percentage. The bottom panel shows the absolute difference. Each line shows a bubble policy.	101
C.1	Age-specific population trajectories (y-axis) in time (x-axis) for five baleen whale species. Age structure becomes stable (slopes are parallel for across age classes). Note how Minke whales do not achieve stable age distribution.	104
C.2	Stable age distributions for five baleen whale species. The x-axis shows age, the y-axis shows the proportion of individuals contained in each age class.	105
C.3	Reproductive value (y-axis) by age (x-axis) for five baleen whale species.	106
C.4	Time series of relative abundance (abundance normalized by carrying capacity) for five whale populations. The these population trajectories are used as a baseline for the subsequent simulations where human-induced whale mortality is introduced.. . . .	107
C.5	Contribution of whales to the carbon cycle through time. Note that the sequestration plot shows annual values, not the cumulative sequestration.	108

List of Tables

2.1	Model parameters.	17
4.1	Demographic and mass-at-age parameters for five baleen whale species. K represent the pre-whaling biomass (in thousand tonnes) estimates used as carrying capacity. N_0 are the present day (2011) estimates of abundance. α_m is the age at maturity, α is the maximum age attained, μ is the fecundity, σ_{juv} and σ_{adt} are the juvenile and adult survival rates, and m_∞ , k , and a_0 are the von Bertalanfy parameters for mass-at-age conversions. All parameters come from Pershing et al., 2010.	63
4.2	Other model parameters.	63
4.3	Summary of experiments (rows), scenarios (columns), and simulations (cells) used to explore the costs of human-induced whale mortality. This protocol is applied to all five baleen whale species. Note that human-induced mortality is not present in the Business As Usual (BAU) column.	68
A.1	Mean values on observable characteristics by vessel for displaced ($n = 64$), and non-displaced vessels ($n = 254$). Numbers in parentheses indicate standard deviation. The last column contains the difference in means (t-scores), with asterisks indicating significant differences as indicated by a two-tailed t-test (* $p < 0.1$; ** $p < 0.05$; *** $p < 0.01$).	82
A.2	Proportion of vessel flags by group. Note that we do not observe the flag for two vessels (0.78%) in the non-displaced group.	83
C.1	Annual Social Cost of Carbon, 2020-2050 (in 2020 dollars per metric ton of CO ₂) for three different discount rates. Model output by the Interagency Working Group reports values in five-year increments, they then use linear interpolation to fill-in missing years (Interagency Working Group, 2021).	103

Chapter 1

Introduction

1.1 Introduction

As an Environmental Scientist, I am broadly interested in design and evaluation of policy interventions in the marine realm, the behavioral responses of humans, and their environmental and economic outcomes. Working at the intersection of conservation planning and environmental economics, I combine Ecological and Economic theory, Data Science, Econometric techniques, and large data sets on environmental measures and human activities to answer policy-relevant questions. For some projects, I *evaluate* past policy interventions by using observational data, natural experiments, and cutting-edge Econometric techniques to estimate causal effects. For others, I *predict* the economic and environmental impacts of policy interventions by combining computer simulation and mathematical modelling of coupled bio-economic systems. This dissertation contains three essays that use this second approach to study environmental markets in marine conservation.

Humanity depends on the ocean for livelihood, subsistence, and way of life. Yet, many of our activities create externalities that threaten the marine environment. In attempting to regulate these impacts, regulators have implemented a diverse array of institutions. These range from command-and-control rules that dictate, for example, the total allowable catch that can be extracted from a given stock, to the implementation of Marine Protected Areas to spatially as a way of space-based management. Notably, the use of market-based institutions in the ocean is limited and understudied. Here, I study how environmental markets interact with other institutions (Ch. 2), the potential for developing new markets (Ch. 3), and the ecosystem services of populations (Ch. 4). I use simulation modeling and quantitative methods to explore how environmental markets can incentivize conservation in the marine environment.

In my first paper I explore how existing environmental markets for fishing effort

interact with a nation's incentive to engage in marine conservation in the form of Marine Protected Areas. Specifically, I look at the vessel-day scheme used by the Parties to the Nauru Agreement (PNA) and the Phoenix Island Protected Area (PIPA) implemented by Kiribati in 2015. I develop a bespoke spatial bio-economic model of a market for fishing effort, fisheries and conservation to simulate the effect of different design features (transferability and allocation of rights). I then use vessel-tracking data and a large-scale spatial closure to corroborate model predictions. I find that between-country transferable fishing rights and a biomass-based allocation rule reduce the costs of displacing fishing effort and can incentivize large-scale conservation. I also find that vessels displaced by PIPA largely relocated to outside of Kiribati and into the waters of other PNA countries, consistent with the model's predictions.

In my second paper, I propose, design, and analyze a new global market for marine conservation. Similar to a cap-and-trade market used to regulate pollution emissions, nations receive conservation obligations in the form of Marine Protected Area coverage targets and engage in voluntary trade to efficiently allocate their obligations. I combine theory from ecology and economics to build conservation supply curves, simulate a global market for marine conservation, and estimate the gains from trade. I find that global market reduces the costs of conserving 30% of the ocean by 98%. Segmenting the market using biogeographic regionalization to implement bubble policies brings the cost-savings down to 76-98% relative to BAU, depending on the number of bubble policies.

Finally, the third paper, explores the link between climate change mitigation strategies and whale conservation by estimating the implied carbon cost of human-induced whale mortality. I combine an age-structured model of whale populations and quantify their contributions to the carbon cycle. I find that the cost is driven population dynamics rather than somatic growth, and that it depends largely on the species, source of mortality and the age of the individual, but values range between $\$3,820 \pm 1,440$ (M \pm

SD) for Minke whales and $\$51,700 \pm 16,000$ for Fin whales.

1.2 Notes on reproducibility


All code necessary to reproduce each of the chapters can be found in the central GitHub repository at https://github.com/jcvdav/markets_and_conservation. The repository contains three git submodules, one for each chapter. All code is written in R, and were last run using R version 4.1.2 (2021-11-01) [2]. The submodules for Chapters 3 and 4 use renv to create an isolated and independent environment with a list of R libraries used by each project.

The reproducibility protocol is different for each chapter, representing the progressive evolution of the tools incorporated in my workflow. Chapter 2 uses a combination of source scripts to layout the basic dependencies of the modelling and data processing steps. These are then called by an Rmarkdown document. Chapter 3 uses only R scripts, sequentially numbered to indicate the order in which they run. Finally, Chapter 4 uses the GNU make protocol, which uses a file called the makefile, which lists each of the non-source files and how to compute it from other files.

1.3 Permissions and Attributions

- Chapter 2 and appendix A are the result of a collaboration with John Lynham and Christopher Costello, and contains material from: Villaseñor-Derbez, J. C., Lynham, J., & Costello, C. Environmental market design for large-scale marine conservation. Nature Sustainability, published 2020, Springer Nature Limited.

4/28/22, 8:06 AM Rightslink® by Copyright Clearance Center



Home
Help ▾
Live Chat
Sign in
Create Account

Environmental market design for large-scale marine conservation

Author: Juan Carlos Villaseñor-Derbez et al
Publication: Nature Sustainability
Publisher: Springer Nature
Date: Jan 6, 2020

Copyright © 2020, The Author(s), under exclusive licence to Springer Nature Limited

Author Request

If you are the author of this content (or his/her designated agent) please read the following. If you are not the author of this content, please click the Back button and select no to the question "Are you the Author of this Springer Nature content?".

Ownership of copyright in original research articles remains with the Author, and provided that, when reproducing the contribution or extracts from it or from the Supplementary Information, the Author acknowledges first and reference publication in the Journal, the Author retains the following non-exclusive rights:

- To reproduce the contribution in whole or in part in any printed volume (book or thesis) of which they are the author(s).
- The author and any academic institution, where they work, at the time may reproduce the contribution for the purpose of course teaching.
- To reuse figures or tables created by the Author and contained in the Contribution in oral presentations and other works created by them.
- To post a copy of the contribution as accepted for publication after peer review (in locked Word processing file, of a PDF version thereof) on the Author's own web site, or the Author's institutional repository, or the Author's funding body's archive, six months after publication of the printed or online edition of the Journal, provided that they also link to the contribution on the publisher's website.
- Authors wishing to use the published version of their article for promotional use or on a web site must request in the normal way.

If you require further assistance please read Springer Nature's online [author reuse guidelines](#).

For full paper portion: Authors of original research papers published by Springer Nature are encouraged to submit the author's version of the accepted, peer-reviewed manuscript to their relevant funding body's archive, for release six months after publication. In addition, authors are encouraged to archive their version of the manuscript in their institution's repositories (as well as their personal Web sites), also six months after original publication.

v1.0

BACK
CLOSE WINDOW

© 2022 Copyright - All Rights Reserved | Copyright Clearance Center, Inc. | [Privacy statement](#) | [Terms and Conditions](#)
Comments? We would like to hear from you. E-mail us at customer@copyright.com

https://s100.copyright.com/AppDispatchServlet/formTop 1/1

2. Content of chapter 3 and appendix B are the result of a collaboration with Christopher Costello.
3. Content of chapter 4 benefited from comments from Renato Molina.

Chapter 2

Environmental market design for large-scale marine conservation

Abstract

It is commonly agreed that marine conservation should expand dramatically around the world. However, most countries have yet to implement large-scale no-take Marine Protected Areas (MPAs). When a country closes a large fraction of its waters to fishing, it stands to lose significant fishery revenue. While biodiversity and spillover fishing benefits may far exceed these losses, benefits from large-scale MPAs typically accrue to other countries or the high seas. To overcome this dilemma, we simulate and test an international fisheries management scheme with transferable fishing rights that incentivizes, rather than hinders, large-scale marine conservation. By combining a bioeconomic model of cross-country trading of fishing rights with vessel-level tracking data before and after a large-scale conservation action is implemented, we show that transferable fishing rights and a biomass-based allocation rule are pivotal to incentivize conservation under this market-based setting. Our work focuses on the Vessel-Day Scheme, an environmental market employed by the Parties to the Nauru Agreement (a group of nine Pacific Island Nations) to manage their tuna fisheries, and where large-scale conservation interventions have taken place. Overall, these results provide a template for how to incentivize countries to engage in large-scale marine conservation within a market-based setting.

2.1 Introduction

Recognizing the need to protect marine biodiversity and ecosystem services, various international bodies have committed to dramatically expand marine protection around the world by protecting 30% of the oceans [3, 4], with a focus on no-take Marine Protected Areas (MPAs) [5, 6]. While most MPAs implemented to date have been small, it is widely-recognized that very large MPAs must also be part of the strategy if we are to meet these goals. But would any country rationally close 30%, 80% or even 100% of its waters to fishing if this means losing all fishing revenue from within the closed area? At first glance, the answer is probably “no”. Losing this important source of revenue would cripple many fishing-dependent economies, particularly the Pacific Island nations who are viewed by many as viable candidates for large closures [7]. On the other hand, the closure may generate substantial “spillover” of larvae and adult fish [8, 9] and other benefits into adjacent waters which could, in principle, offset these losses. The problem with this argument is that for very large MPAs, these spillover benefits could accrue to other nations and the high seas [10], with no obvious mechanism for the conserving country to recoup them. A viable solution may lie in international fishing effort markets, where nations trade the right to fish across international boundaries. The design and effectiveness of fishing effort markets for fisheries management have been explored before [11, 12], but little attention has been given to the role these markets can play in conservation. Here, we will show how fishing effort markets can be designed (if new) or modified (if already existing) to incentivize implementation of large-scale MPAs.

We are motivated by a real-world but relatively understudied institution called the Parties to the Nauru Agreement (PNA). The PNA is a coalition of nine Pacific Island Nations that collectively manages tuna purse seine fishing in its members’ waters [12, 13] (Fig. 2.1). These waters account for 14.5 million km² (an area four times larger than

the continental US), and over 60% of skipjack tuna catch in the Western Central Pacific [12]. The PNA manages this tuna purse seine fishery using a vessel-day scheme (VDS) where total annual fishing effort is capped at around 45,000 vessel-days. Vessel-days are allocated across the nine nations, which then lease them to (mostly foreign) fishing vessels. A vessel-day grants a fishing vessel the right to fish for 24 hours within one of the nine Exclusive Economic Zones (EEZs) within the PNA. Member nations derive enormous benefits from leasing these fishing rights to foreign fleets, in some cases exceeding half of a country's GDP ¹. In addition to highly productive tuna fisheries, the PNA waters provide a wealth of ecosystem benefits, hence the focus on large-scale conservation efforts in the region [7]. In 2015, Kiribati, a PNA member, created the Phoenix Islands Protected Area, one of the largest protected areas on earth (408,250 km²), and Palau will close 80% of its national waters to fishing by January 2020. We draw from the PNA's market-based approach to managing tuna fisheries and build on it to show how an environmental market can be designed to incentivize conservation.

Not all market-based approaches to environmental management contain the same conservation incentives. A pervasive finding across a range of natural resources is that features of markets, such as the allocation of rights, can have implications for the market's functioning [14]. In the context of fishing effort markets, we find that two market design features are pivotal in determining the incentives for large-scale marine conservation: trading and allocation rules. But why would these design features of a fisheries market affect the incentives for conservation? Consider the incentives for a country to close 100% of its waters. Such a closure might benefit other countries through the spillover of fish from the protected area to the waters of neighboring countries. If the conserving country could trade the rights to that spillover to adjacent countries, this could offset the foregone fisheries revenue. But if the conserving country was not allowed to trade these rights,

¹<https://www.ffa.int/>

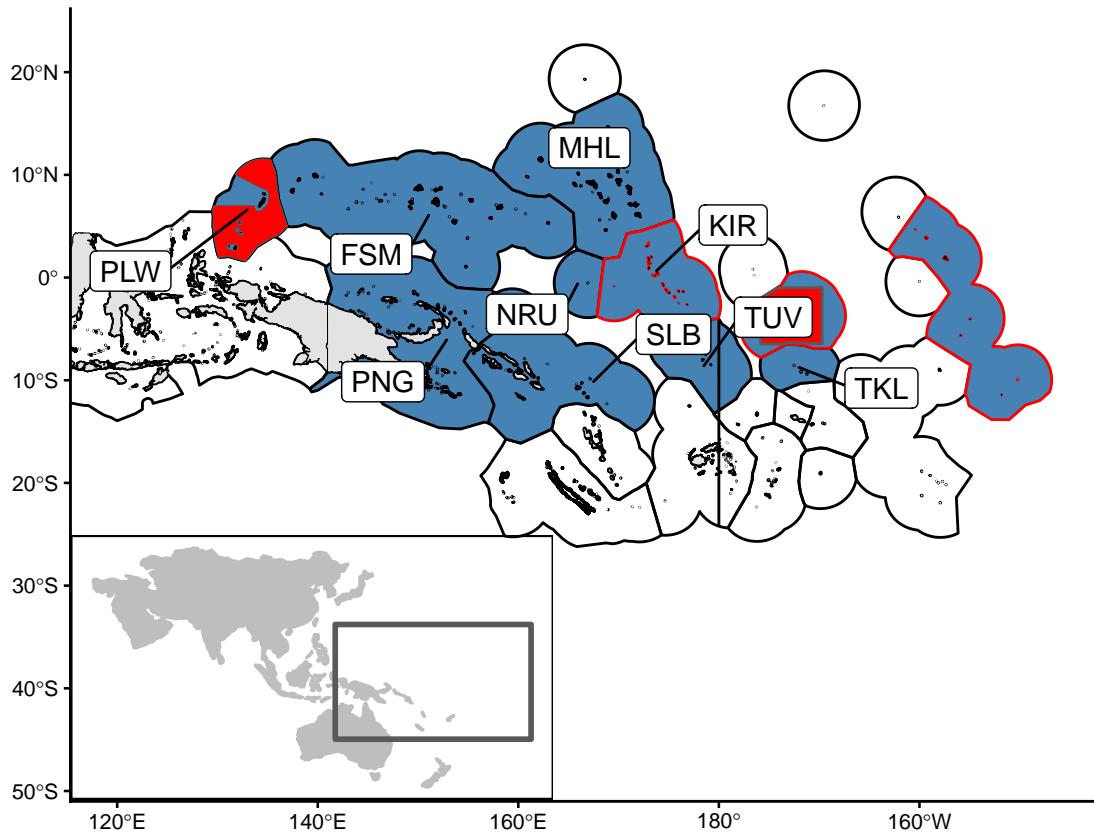


Figure 2.1: Map of the Exclusive Economic Zones (EEZs) and Marine Protected Areas in the PNA, the bottom-left inset provides a reference for the area. Parties to the Nauru Agreement (PNA) are shown in blue, while empty polygons indicate all others. A red line outlines the three EEZs of Kiribati. The solid red polygons show The Phoenix Islands Protected Area (PIPA) implemented in 2015 and the proposed Palau National Marine Sanctuary (PNMS) to be implemented in 2020. Land masses are shown in gray. Labels indicate ISO3 country codes for PNA members (PLW: Palau, PNG: Papua New Guinea, FSM: Federal States of Micronesia, SLB: Solomon Islands, NRU: Nauru, MHL: Marshall Islands, KIR: Kiribati, TUV: Tuvalu, TKL: Tokelau).

then it would lose all of its fishing revenue. The rules for how fishing rights are allocated across countries are equally important. Suppose rights are allocated each year based on the previous year's fishing effort: the more a country fishes, the more it gets allocated the next year. This would clearly disadvantage a conservation-minded country and, in fact, might reward undesirable behavior. In the following section, we will show how trading and allocation rules can shape the incentives that may facilitate or hinder large-scale conservation. We will then make use of vessel-tracking data to analyze a real-world case of large-scale marine conservation under fishing effort markets.

2.2 Methods

2.2.1 Bioeconomic model

We model a 10-country discrete-time meta-population system, where Country 1 considers a spatial closure. Countries 1 - 9 operate under a vessel-day scheme, and Country 10 represents the high seas and other areas not managed under a VDS. The stock of fish in each country is stationary within a single fishing season, but growth from escapement redistributes across all countries annually. The price of fish is p , and catchability is given by q (in mass of catch per unit effort and stock biomass; $\frac{Kg}{Vessel-DaysKg}$). These parameters are held constant across countries.

Fishery dynamics

In the absence of a reserve, the revenue for vessels in country i is given by pqE_iX_i , where E_i and X_i are effort (vessel-days) and stock size in country i at the beginning of a period. The input costs of fishing in country i are given by cE_i^β , where $\beta = 1.3$ matches commonly-used cost functions that assume marginal units of effort are increasingly costly

to apply [15]. Finally, the cost of access fees (when relevant), is given by $\pi_i E_i$, where π_i is the price of a vessel-day.

Country 1 considers a spatial closure by implementing a reserve as a fraction R of the total country ($R \in [0, 1)$). This closure reduces the amount of biomass available for harvest, because vessels can only target fish outside the reserve. Fish movement between the reserve and fishing areas also determines how much biomass is available for harvest. Fish move within a country based on θ , where $\theta = 0$ implies no movement within the country, and $\theta = 1$ implies that fish move so much that they can be caught from anywhere within the country. The proportion of biomass within country 1 that is available for harvest is therefore given by:

$$\Omega(\theta, R) = \begin{cases} \theta R + (1 - R), & \text{if } 0 \leq R < 1 \\ 0, & \text{if } R = 1 \end{cases}$$

Our parameterization of within-country fish movement implies that for a given country with stock size X_i , the total biomass available for harvest will be given by $\Omega_i X_i$ (Eq 2.2.1). Consider the case of a sessile fish with $\theta = 0$. If the country were to close 50% of its waters to fishing ($R = 0.5$), only 50% of the stock would be available for harvest (*i.e.* $(0 \times 0.5) + (1 - 0.5) = 0.5$). Now, consider the same closure is applied with a stock with high mobility, so $\theta = 0.9$. In this case, despite the closure, fish frequently move between the reserve and fishing grounds making 95% of biomass available for harvest (*i.e.* $(0.9 \times 0.5) + (1 - 0.5) = 0.95$). As derived in the bioeconomic model below, a vessel's willingness to pay to fish in a given patch will be determined by the amount of biomass available for harvest. Within-patch stock movement therefore plays an important role in determining a vessel's willingness to pay in the remaining open waters: a vessel will be willing to pay more to fish in waters where 95% of biomass is available for harvest, than

when only 50% of biomass is available for harvest. No biomass is available for harvest if the country decides to implement a reserve in the entirety of its waters (*i.e.* $R = 1$),

In country 1, profits from fishing are given by:

$$\Pi_1(E_1, X_1, R_1) = pqE_1X_1\Omega_1 - cE_1^\beta - \pi_1E_1$$

Since only Country 1 implements a reserve, $\Omega_{i \neq 1} = 1$. Therefore, we can generalize the profit equation to:

$$\Pi_i(E_i, X_i, R_i) = pqE_iX_i\Omega_i - cE_i^\beta - \pi_iE_i$$

The above equations imply that the marginal profit from the last unit of effort in a country is given by:

$$\Pi'_i(E_i) = \frac{\partial \Pi_i}{\partial E_i} = pqX_i\Omega_i - \beta cE_i^{\beta-1} - \pi_i \quad (2.1)$$

Note that $\pi_{10} = 0$ since vessels don't pay an access fee to fish in patch 10. In practice, the effort levels in each country are allocated by management (so E_1, E_2, \dots, E_9 are given) and the effort level on the high seas (E_{10}) is a result of open access dynamics. Therefore, we assume that effort continues to enter Country 10 until the profit from the last unit of effort is exactly zero, indicating that E_{10} is the value for which $\Pi'_{10}(E_{10}) = 0$. Setting Equation 2.1 (for $i = 10$) equal to zero and removing $\Omega_{10} = 1$ for simplicity, we can solve for E_{10} :

$$E_{10} = \left(\frac{pqX_{10}}{\beta c} \right)^{\frac{1}{\beta-1}} \quad (2.2)$$

Under VDS-operated countries, however, profits from the marginal unit of effort should equate to the price of fishing in the country. Therefore vessel-day price for coun-

tries under VDS ($i = (1, 9)$) is given by:

$$\pi_i = pqX_i\Omega_i - \beta cE_i^{\beta-1}$$

Solving for E_i we obtain:

$$E_i = \left(\frac{pqX_i\Omega_i - \pi_i}{\beta c} \right)^{\frac{1}{\beta-1}} \quad (2.3)$$

Equation 2.3 tells us the country-level effort for a given country-specific stock size (X_i) and vessel-day price (π_i). A vessel-day scheme establishes a cap on total effort allowed. This means that fishing effort from Countries 1 - 9 must add up to this limit (45,000 vessel-days). Therefore, total allowable effort in the fishery is given by:

$$\bar{E} = \sum_{i=1}^9 \left(\frac{pqX_i\Omega_i - \pi}{\beta c} \right)^{\frac{1}{\beta-1}} \quad (2.4)$$

In the above Equation, vessel-day price is the same across all countries when trading is allowed; the subindex is dropped for this parameter.

Stock dynamics

Country-level harvest is then determined by effort and stock size:

$$H_i = qE_iX_i\Omega_i \quad (2.5)$$

Therefore, escapement in country i in time period t is the difference between initial stock size and harvest given by $e_{i,t} = X_{i,t} - H_{i,t}$ and total escapement is $e_t = \sum_{i=1}^{10} e_{i,t}$. The entire stock then grows logistically according to:

$$X_{t+1} = e_t \times \exp \left(r \left(1 - \frac{e_t}{K} \right) \right) \quad (2.6)$$

where r and K are species-specific intrinsic growth and carrying capacity parameters (the slope $\frac{dX_{t+1}}{de_t}|_{e_t=0} = \exp(r)$). After the stock grows, a constant and country-specific fraction f_i of the total stock redistributes to country i , so:

$$X_{i,t+1} = f_i X_{t+1} \quad (2.7)$$

Vessel-day revenues

The vessel-day price that a country charges is given by π_i from Eqn 2.1. Therefore, country-level license revenues are given by:

$$\omega_i = \pi_i E_i \quad (2.8)$$

Equation 2.5 shows that low values of θ and $R > 0$ would decrease harvest and increase escapement in Country 1, for a given level of effort and stock size. This would lead to an increase in total stock size (Equation 2.6) and a benefit to all the other countries. But this would also cause the stock in the high seas (X_{10}) to increase, leading to increased effort being allocated to the high seas (Equation 2.2) and a loss of these potential rents. Thus, the spillover benefits of increasing R are never completely captured.

2.2.2 Model parameterization

We calibrate our model to loosely match the fishery dynamics observed for the VDS operated by the PNA. The table below contains the values used to parameterize the model.

Table 2.1: Model parameters.

Parameter	Value	Source
MSY	1.875600e+06	50th percentile from MSY in Table 8 of WCPFC Stock Assessment
B_{msy}	1.628000e+06	50th percentile from MSY in Table 8 of WCPFC Stock Assessment
K	6.876526e+06	50th percentile from MSY in Table 8 of WCPFC Stock Assessment
B_c/B_{msy}	0.51	50th percentile from MSY in Table 8 of WCPFC Stock Assessment
C_{now}	1.679444e+06	Catches from WCPFC Stock Assessment
B_{now}	3.507028e+06	Current Biomass (2012 - 2015 average)
r	0.57	From FishBase: Prior $r = 0.57$, 95 CL = 0.41 - 0.78
β	1.3	Standard [15]
p	1100	Mean between Thailand and Japan values (Value of WCPFC-CA Tuna Fisheries 2017 Report)
q	3.420000e-05	Estimated so that efforts match catches given biomass and vessel-day prices
c	1800	Estimated to match cost and revenue structures
f	0.1	Biomass is equally distributed between countries

Simulations

We run simulations under various market designs and test the model across a range of reserve sizes and within-country movement parameters. The first scenario does not allow trading. In this case, total allowable effort (\bar{E}) and biomass B_{now} are known and equally distributed among Countries 1-9. For Country 10, we solve for Eq 2.2 until biomass converges to match B_{now} . We then proceed to “close” a portion of Country 1, and calculate the vessel-day price in Country 1 given that only $X_i\Omega_i$ biomass is available for harvest. We compare vessel-day revenues of each scenario to a case with no reserve ($R = 0$). This produces a measure of the cost of implementing a spatial closure of size R in Country 1.

The second scenario allows trading. We start again by solving for the high seas to obtain total effort. Since a closure is not in effect and VDS-managed effort is equally distributed across the 9 countries, this equilibrium is the same as the first step above. We then implement a spatial closure in Country 1. This essentially lowers the price

fishers would be willing to pay to fish in a country with only biomass $X_i\Omega_i$, lowering demand for vessel-days in Country 1. Countries 2 - 9 have a higher demand for vessel days, and therefore a portion of vessel-days from Country 1 are sold to Countries 2 - 9. This increases effort in these countries, which reduces escapement and therefore biomass. This reduction in biomass in turn will modify the marginal profit and willingness to pay to fish in each country. We iterate this process until biomass stabilizes. Like before, we calculate vessel-day revenues to each country and compare them to a case with no reserve in Country 1.

Annual vessel-days are often allocated based on a combination of historical within-country effort and biomass. In the PNA, 60% of the allocation is calculated based on EEZ effort over the last seven years and 40% is calculated based on the 10-year average of each country's share of estimated biomass (of skipjack and yellowfin tuna) within its EEZ (see Article 12.5 of the 2012 Amendment to the Palau Agreement and in [16]). Trading vessel-days to other countries would imply that historical within-country effort declines through time. The allocated days to a country with a full spatial closure would eventually be reduced to just the 40% based on biomass.

In the trading scenario above, effort from Country 1 (with the reserve) is traded to other countries. This means that its allocation will decrease as purse seine effort in Country 1 is reduced. To analyze the consequences of different allocation rules when trading is allowed, we simulate a fishery 50 years into the future, and annually re-allocate vessel-days based on a 7-year running mean of country-level effort and biomass. At the end of every time period (a year), vessel-days are re-allocated to each country based on the following rule:

$$E_{i,t+1}^* = \left[\alpha \left(\frac{\sum_{\tau=0}^{\hat{\tau}} E_{i,t-\tau}}{\sum_{\tau=0}^{\hat{\tau}} \bar{E}_{t-\tau}} \right) + (1 - \alpha) \left(\frac{\sum_{\tau=0}^{\hat{\tau}} X_{i,t-\tau}}{\sum_{\tau=0}^{\hat{\tau}} \bar{X}_{t-\tau}} \right) \right] \bar{E}_{t+1}$$

where α is a weight on historical effort (E_i) and $1 - \alpha$ is the weight on historical biomass (B_i). We use $\hat{\tau} = 6$ to obtain a moving mean of 7 years for these measures. This allocation rule generally captures how the PNA distributes the total allowable effort to each party [17]. The difference between allocated days (E_i^*) and used days (determined by Equation 2.3) for Country 1 are the sales. We then calculate vessel-day revenues to each country over the 50-year time horizon and compare to a case where there is no reserve and allocations are based solely on biomass ($\alpha = 0$).

2.2.3 Empirical case study

Vessel tracking data and MPAs

Automatic Identification Systems (AIS) are on-board devices that provide at-sea safety and prevent ship collisions by broadcasting vessel position, course, and activity to surrounding vessels. These broadcast messages can be received by satellites and land-based antennas. We use AIS data provided by Global Fishing Watch [18] to track 318 tuna purse seiners that fished within the PNA. For every georeferenced position, we observe the time spent (defined as the time since the last position), and whether the vessel was actively fishing versus only transiting. Of the 318 tuna purse seine vessels that fished in PNA waters between 2012 and 2018, 64 “displaced” vessels fished within PIPA at least once prior to its implementation, the remaining 254 “non-displaced vessels” never fished in PIPA waters. Our dataset contains more than 37 million geo-referenced positions for these 318 tuna purse seiners. We use these data to calculate vessel-days (the metric used by the PNA), and to track the spatial redistribution of displaced vessels. A comparison of vessel characteristics between displaced and non-displaced vessels is presented in Supplementary Tables A.1-A.2 and Supplementary Figure A.5.

We use these data to calculate the number of vessel-days that the 318 purse seiners

spent fishing in each PNA country and in PNA waters as a whole (Fig. 2.5). The vessel-day equivalent of a day of fishing depends on vessel size, a measure used to control for effort creep. The Palau Arrangement for the Management of the Western Pacific Fishery Management Scheme² states that a day of activity by vessels smaller than 50 meters long counts as half a vessel-day, a day of activity by vessels 50 - 80 meters long counts as one vessel-day, and a day of activity by vessels larger than 80 meters counts as 1.5 vessel-days. Vessel length is an observable characteristic in our dataset, and therefore vessel-days calculated in our analyses correspond to the PNA definition of vessel-days.

We can also compare the location of fishing activity by displaced and non-displaced vessels before and after the implementation of PIPA to better understand the effort redistribution. Non-displaced vessels serve as a plausible control group that was not subject to a spatial closure but might have redistributed in response to changing environmental conditions, such as El Niño [19, 13].

We begin by filtering the data to keep only positions labeled as fishing events. We then create a gridded version of the data for each year and group (*i.e.* displaced and non-displaced) by binning the coordinates to a 1-degree grid and summing all fishing hours for a given grid cell. We use a 1-degree grid as a reasonable compromise between higher resolutions that would result in a more granular but noisy footprint, and the simple estimation of vessel-days at the EEZ-level (as in Supplementary Figure A.8, but represented spatially). This process results in 14 gridded datasets of fishing hours (7 years, for two groups). For each group of vessels, we then calculate the average fishing hours before (2012 - 2014, inclusive) and after (2015 - 2018, inclusive) the implementation of PIPA, resulting in 4 datasets of mean fishing effort (before and after for displaced and non-displaced vessels). We then calculate the change in effort allocation between these two periods (after minus before) for each group, and normalize the value of each grid cell

²pnatuna.com

by dividing it by the largest within-group absolute change:

$$h_i = \frac{(h_{i,a} - h_{i,b})}{\max(|(h_{i,a} - h_{i,b})|)} \quad (2.9)$$

Where, for a given group of vessels, i is a subindex for each cell, and a and b indicate after and before. The resulting gridded differences are shown in Fig. 2.4a-b. The redistribution by non-displaced vessels (Fig. 2.4b) therefore provides a baseline of redistribution. We then compare the changes of displaced vessels to those by non-displaced vessels (Fig. 2.4c). The spatial redistribution patterns of displaced vessels relative to non-displaced vessels suggest that some relocated to other waters in Kiribati (*i.e.* the Gilbert islands and Line islands), but also the Marshall Islands, Tuvalu, Nauru, and the high seas.

Revenues

We obtained information on revenues from the Pacific Islands Forum Fisheries Agency *Tuna Development Indicators 2016* report. Specifically, we use data compiled by the Pacific Islands Forum Fisheries Agency (FFA [20]) where annual revenues from license fees (for VDS and other access programs) are reported for each country (2008 - 2016; Fig. 2.5c; Supplementary Figures A.6-A.7). For countries in the PNA, these revenues show a combination of vessel-day license fees as well as joint-venture operations.

Shapefiles of Exclusive Economic Zones were obtained through Marine Ecoregions of The World, we use World EEZ v10 (2018-02-21) available for download at: marineregions.org. Shapefiles for Marine Protected Areas come from the World Database of Protected Areas, and were downloaded in March 2019 from: protectedplanet.net.

2.3 Results

2.3.1 Designing markets for conservation

To examine how market design incentivizes or hinders large-scale conservation, we develop a 10-country spatial bioeconomic model that mirrors the strategies and spatial connections among the nine PNA nations and the high seas. Countries 1 to 9 represent the PNA countries, which operate under a vessel-day scheme where vessel-days are capped for each country and closely tracked. “Country” 10 represents the high seas, where fishing days are unregulated and determined by prevailing economic conditions. We examine the effects of large-scale conservation in a single country (Country 1) under markets with and without trading between countries. In all cases, we solve the bioeconomic model for the equilibrium vessel-day price, fishing effort redistribution across countries, and fish stock that would be expected to occur in the market. We quantify the change in revenue to Country 1 and compare each scenario to a benchmark scenario without any conservation action. We simulate these outcomes across a range of reserve sizes and assumptions about within-country stock movement.

We first simulate a fishery where trading between countries is not allowed. This represents the status quo of any nation unilaterally engaging in large-scale conservation. Intuitively, we find that a spatial closure in Country 1 will always result in a loss in revenues to Country 1 (Fig. 2.2a). Higher within-country stock movement ($\theta = 0$ implies no within-country movement and $\theta = 1$ implies that fish are well-mixed within the fishing season) allows vessels to harvest the stock within the remaining open area, lowering the cost to Country 1. Even for a highly mobile stock where fish can move in and out of the reserve, a spatial closure reduces the amount of biomass that is available for harvest in the conserving country (*i.e.* biomass outside the reserve), which reduces vessels’ willingness to pay to fish in such waters (Supplementary Figure A.1). When countries cannot trade,

the costs of conservation are incurred by Country 1, but the benefits are received by the eight other countries (revenues increase between 0% and 7% each; Supplementary Figure A.2) and the high seas. This benchmark simulation highlights the misalignment of incentives, where a conservation-minded country incurs large costs and provides public benefits to other nations with no mechanism for recouping these benefits.

How does trading between countries change these results? We simulate the same fishery, but now allow for vessel-days to be traded across countries (as is the case for the PNA). As before, a closure in Country 1 lowers the value of vessel-days in that country (because the fishable area shrinks). But increased biomass in other countries causes their vessel day prices to increase. As a result, vessel-days from Country 1 are traded to Countries 2 to 9, until prices equalize across countries (Supplementary Figure A.3). Under this market design, revenue losses to Country 1 are less than 1%, compared to the base case with no reserve (Fig. 2.2b; note that the vertical axis now only ranges from 0 to 0.8% instead of from 0 to 100% as in Fig. 2.2a). This shows that, with trading, the relative revenue drop will always be smaller than the relative effort drop, and the opposite is observed when there is no trading (Supplementary Figure A.4). Overall, this shows that 88% to 99% of the costs of conservation can be avoided if markets are designed to allow trading (Fig. 2.2c).

We have shown that trading significantly reduces the costs of conservation. However, a new question arises. How should rights be re-allocated every year once a country starts closing its waters to fishing? Customarily, the allocation of fishing effort rights is a formula that combines historical fishing effort and biomass in a country's waters [12]. We test a range of allocation rules that weigh effort (α) and biomass ($1 - \alpha$) differently as the basis for ongoing rights allocation. We simulate a fishery operating with closures for 50 years and compare the resulting revenues to a fishery without any closures. We find that when allocation is based on historical effort only (*i.e.* $\alpha = 1$), implementing a

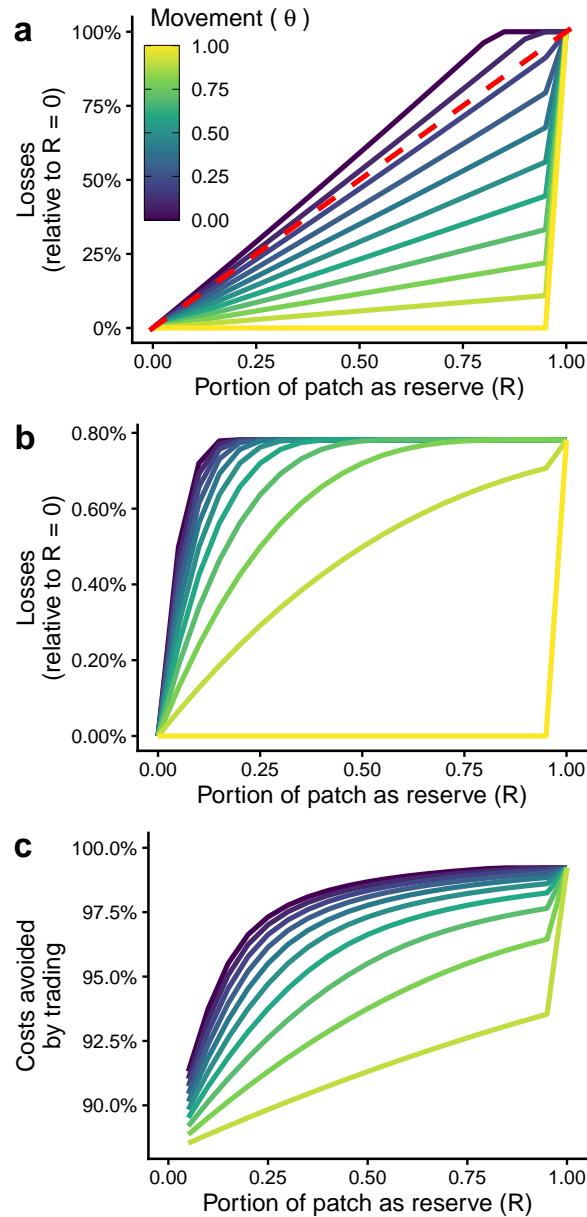


Figure 2.2: Cost of spatial closures in a vessel-day fishery. Each line represents a possible value of within-country stock movement (θ ; line colors), with $\theta = 0$ representing a stock that doesn't move to $\theta = 1$ depicting a stock that continuously moves between the reserve and the fishing zone. The revenue losses to Country 1 (vertical axis) are relative to a fishery with no spatial closures, and are shown as a function of reserve size (R ; horizontal axis), from no reserve ($R = 0$) to closing the entire Exclusive Economic Zone ($R = 1$). Costs are shown for Country 1 when there is no trading (a) and when trading is allowed (b; note the change in axis limits). Costs avoided by trading are shown in (c). Dashed red line in (a) is a 1:1 line. When trading between countries occurs, 88.5% to 99.2% of revenue losses can be avoided.

reserve results in long-term losses to the conserving country of up to 93.4%, depending on the size of reserve and stock movement (Fig. 2.3). However, a biomass-only allocation rule (*i.e.* $\alpha = 0$) results in revenue losses of up to 0.7%, essentially eliminating the costs of conservation. This result implies that if allocation is based purely on the biomass within a nation’s waters, and not on fishing intensity, the incentives for conservation can be sustained through time.

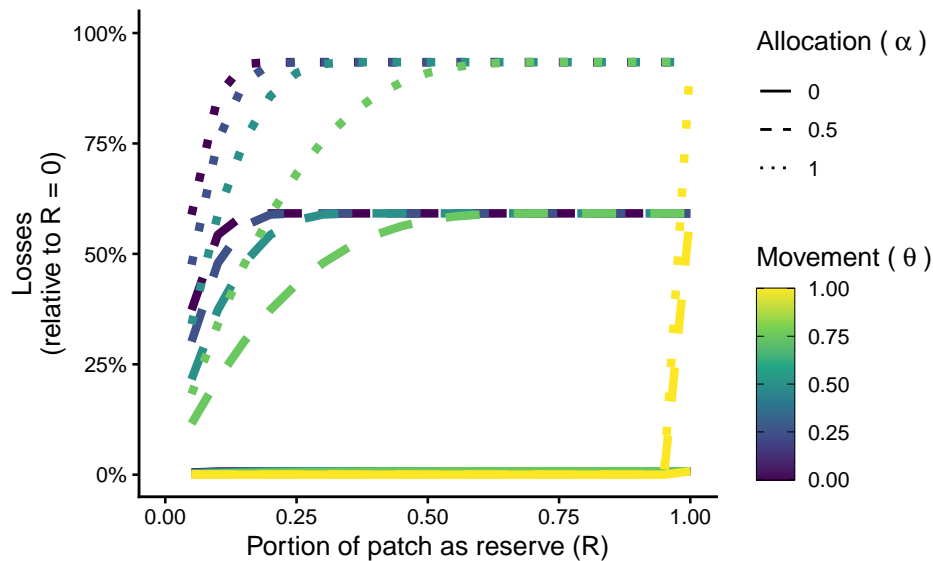


Figure 2.3: Costs of a spatial closure for Country 1 under different allocation rules. Each line represents the revenue losses for a combination of allocation rules (α ; line type) and movement (θ ; color) for different reserve sizes (R ; horizontal axis). A value of $\alpha = 1$ implies that allocations are based entirely on historical effort, while a value of $\alpha = 0$ implies a 100% biomass-based allocation rule. A value of $\theta = 0$ represents a stock that doesn’t move, and $\theta = 1$ depicts a stock that continuously moves between the reserve and the fishing zone. The proportion of the Exclusive Economic Zone closed to fishing is given by R . An effort-based allocation and low within-country movement values result in the highest costs. Cost can be minimized for all movement values if allocation is based on biomass within each country’s waters.

2.3.2 Markets and conservation in practice

A large-scale MPA was recently implemented in PNA waters, providing the ideal empirical setting to test our predictions. In January 2015, Kiribati closed 11.5% of its

EEZ to implement the Phoenix Islands Protected Area (PIPA), effectively displacing all fishing effort within its boundaries [21, 22]. By protecting important tuna spawning habitat [9], PIPA may provide important recruitment and biomass benefits to adjacent waters. We combine vessel-level tracking data [18] and country-level license revenue data reported by the Pacific Islands Forum Fisheries Agency (FFA) [20] to quantify the displacement of vessel-days and the likely costs of conservation. Of the 318 tuna purse seine vessels that fished in PNA waters between 2012 and 2018, 64 “displaced” vessels fished within PIPA at least once prior to its implementation and 254 “non-displaced vessels” never fished in PIPA waters but fished within PNA waters. We use the vessel-level tracking data to calculate vessel-days in the same way that the PNA does (see Methods for details). We present descriptive statistics on the redistribution of fishing activity before and after the implementation of PIPA.

Consistent with our model’s prediction, after PIPA was implemented, displaced vessels relocated largely outside of Kiribati, and into other PNA countries’ waters (Fig. 2.4). Indeed, from 2014 to 2015, displaced vessels spent 2,115 fewer vessel-days (a 25% reduction) in Kiribati, and 2,298 fewer vessel-days in PNA waters (a 17 % reduction; Fig. 2.5a-b). On the other hand, non-displaced vessels spent 4,656 additional days in Kiribati during 2015, and an additional 9,598 vessel-days in PNA waters. By 2018, we observe a net decrease of vessel-days within Kiribati, from 12,671 in 2014 to just 7,677 in 2018, with displaced vessels driving the decrease (Fig. 2.5a). However, aggregate effort at the PNA-level remains relatively constant and we do not observe a “fishing the line” effect (Supplementary Figures A.8 - A.9). The reduction in effort in Kiribati and constant effort at the PNA-level suggest that trading facilitated redistribution of effort within PNA waters, just as the model predicts.

The decrease of vessel-days in Kiribati could be alternatively (or jointly) explained by changes in oceanographic conditions that drive the distribution of target species and

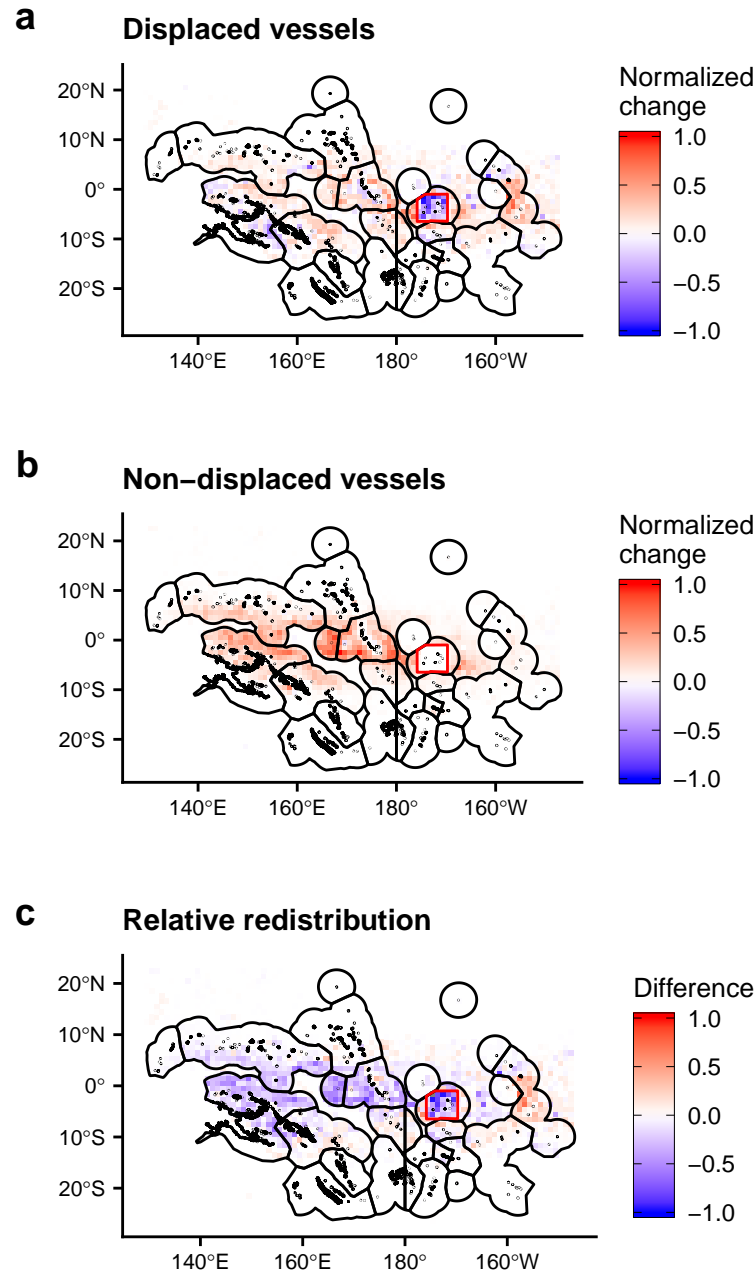


Figure 2.4: Change in spatial footprint of fishing activity by 318 tuna purse seiners. Black lines show Exclusive Economic Zones (EEZ), and red line outlines the Phoenix Island Protected Area (PIPA). Panels a and b show the normalized change in average fishing hours through time for displaced (panel a; $n = 64$) and non-displaced vessels (panel b; $n = 254$). Panel c shows the difference between a and b, highlighting areas where displaced vessels redistributed to, relative to non-displaced vessels. Note that displaced vessels allocate more hours to the Gilbert Islands and Line islands (part of Kiribati's EEZs), but also Tuvalu and the high seas surrounding PIPA and Kiribati's EEZ.

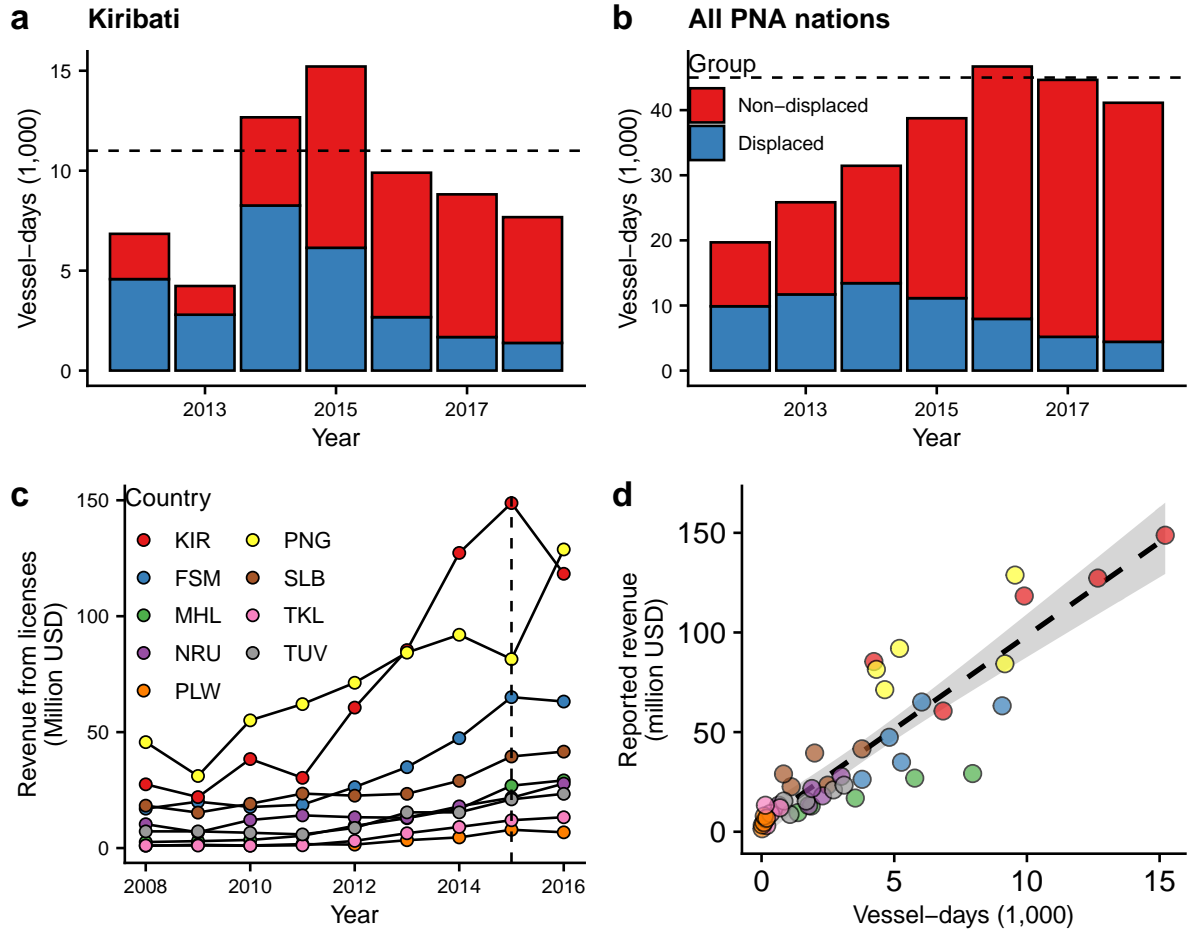


Figure 2.5: Effort displacement and license revenues. Panels (a) and (b) show AIS-derived annual vessel-days for Kiribati and for all Parties to the Nauru Agreement (PNA) by 318 tuna purse seine vessels. Annual effort is broken down by displaced ($n = 64$) and non-displaced ($n = 254$) vessels. The dashed horizontal lines represent the total allowable vessel-days in Kiribati (11,000 days [1]) and the PNA (45,000 vessel-days). Panel (c) shows annual revenue from fishing license fees by country and year (2008 - 2016) and panel (d) shows the correspondence between FFA-reported revenues and AIS-derived vessel-day observations (2012 - 2016). The dashed line in panel (d) represents line of best fit, and the shaded area represents the standard error around the regression. Colors in panels (c) and (d) are given by ISO3 country codes for PNA members (PLW: Palau, PNG: Papua New Guinea, FSM: Federal States of Micronesia, SLB: Solomon Islands, NRU: Nauru, MHL: Marshal Islands, KIR: Kiribati, TUV: Tuvalu, TKL: Tokelau).

fishing vessels. For example, as El Niño events develop, tuna species are known to shift longitudinally across PNA waters, causing vessels to redistribute [13, 19]. However, the aggregate decrease that we observe for Kiribati in Fig. 2.5a is driven by the relocation of vessels that historically fished within PIPA, not by the entire fleet. Oceanographic conditions should be influencing the entire fleet whereas the closure of PIPA should have a stronger impact on vessels that used to fish there. Thus, the large drop in effort within Kiribati for the displaced vessels (relative to the non-displaced vessels) is consistent with the argument that PIPA displaced these vessels to waters outside of Kiribati. One could argue that differences in vessel characteristics between displaced and non-displaced vessels may influence their ability to redistribute or take advantage of different oceanographic conditions in Kiribati. It should be noted that, on average, displaced vessels have smaller crew sizes, more engine power, are larger than non-displaced vessels, fished more in the PNA in 2014, and are more likely to be registered to the Republic of Korea (Supplementary Tables A.1-A.2 and Supplementary Figure A.5). Thus, another alternative explanation for the observed changes in fishing patterns is a change in international relations between Kiribati (or other PNA countries) and the flag country of a particular vessel, although we are not aware of any occurring between 2012 and 2018. Ruling out alternative explanations for observed effects is an important component of careful empirical evaluation of MPAs [23]: as such, our results should not be interpreted as the direct causal impacts of PIPA but are better viewed as patterns that are consistent with the predictions of our theoretical model.

As predicted by our model, the implementation of PIPA resulted in a decrease in fishing effort within Kiribati's water without large revenue losses. Kiribati's reported revenue increased from US\$127.3 million in 2014 to US\$148.8 million in 2015, before decreasing to US\$118.3 million in 2016 (Fig. 2.5c). The increase and subsequent decrease in revenues matches the vessel-day patterns observed for Kiribati from 2014 to 2016

(Fig. 2.5d). But, critically, the drop in revenue in 2016 (20%) is smaller than the drop in vessel-days (35%). This supports a key prediction of our model: with trading, the relative revenue drop will be smaller than the relative effort drop but, without trading, the opposite relationship would hold (Supplementary Figure A.4). At the PNA level, total revenues showed a net increase of \$64.7 and \$28 million USD for 2015 and 2016 respectively (Supplementary Figure A.6), despite the PIPA closure.

2.4 Discussion

Our findings may help inform management and implementation of existing and upcoming MPAs in the PNA. In January 2020, Palau will close nearly 80% of its EEZ to commercial fishing to create the Palau National Marine Sanctuary (PNMS): the 14th largest protected area in the world (Fig. 2.1). Vessel-tracking data (2012 to 2018) shows that, on average, the proposed PNMS boundaries have historically contained $86 \pm 5.30\%$ ($\pm 1SD$) of longline vessel-days (non-tradable) and $91.3 \pm 5.03\%$ ($\pm 1SD$) of purse seine vessel-days (tradable) in Palauan waters (Extended Data Figures A.10 - A.11).

While trading would allow Palau, Kiribati, and other PNA members to reduce revenue losses from large-scale conservation, our model indicates that moving from the current 40% biomass-based allocation rule to a 100% biomass-based rule would ensure long-term financial security in the presence of large-scale MPAs, and further incentivize conservation within the PNA. A 100% biomass-based allocation rule means that fishing rights will be distributed between nations based on the proportion of total biomass within their waters, regardless of historical fishing intensity. In contrast, an effort-based allocation would reward undesirable behavior by granting more fishing rights to a country that fishes the most. This is a model prediction that cannot be empirically tested in the PNA context because the allocation rule has not been experimentally modified. Nevertheless,

the PNA countries have already shown that rights-based management of transboundary resources can result in large management and economic benefits [12, 13]. By facilitating trade and allocating rights based on biomass, they may also have become pioneers in effective large-scale marine conservation in a market-based setting.

There are, however, a series of important considerations to take into account. First, in our model only one of the countries considers the implementation of a protected area. An interesting extension could consider cooperative conservation. In that setting, a group of countries could coordinate on an optimized, large-scale strategic closure -perhaps using vessel-day trading as a means of compensation- in a manner similar to the model above. Future research could explore the role of heterogeneous costs and benefits between countries, and the way in which these can shape conservation outcomes in a market-based setting. A second consideration is the role of the high seas: environmental markets require secure property rights, which are lacking in the high seas [24]. Benefits accruing to the high seas could potentially be eroded by the prevailing open access conditions. Therefore, a conservation-minded nation has no mechanism to capture the benefits provided to the high seas, highlighting the importance of empowering high seas governance and transboundary cooperation [13, 24]. Finally, our work focuses on fisheries and large-scale conservation, but the framework could potentially be expanded and applied to other systems and natural resources. For example, similar mechanisms could be implemented in markets for tradable water rights [25] or game hunting [26] where secure property rights and the presence of a market may incentivize users to conserve the resource in question.

The use of environmental markets for conservation is a common but contentious approach among conservation scientists and resource managers [27]. One of the driving concerns is that markets may create incentives that lead to undesirable outcomes, thus emphasizing the need for careful design. We show that without cross country markets, individual countries have little incentive to undertake large-scale marine conservation, but

that this incentive can be reversed if those countries are in an appropriately-designed market-based setting. For the market to create these incentives, certain design features are paramount. In the case of fishing rights and large-scale MPAs, cross-country transferable fishing rights and a biomass-based allocation rule are two necessary conditions to achieve the conservation incentive. International goals over the next decade have set ambitious targets for terrestrial and marine conservation, which will provide benefits ranging from preserving biodiversity to enhancing human well-being [3, 4, 28, 29]. Our work shows how well-designed environmental markets can provide the right incentives for effective large-scale marine conservation.

Chapter 3

A global market for marine conservation

Abstract

International coordination can help reduce the cost of marine conservation, but no institution currently allows for nations to cooperate over the conservation of the marine environment. Here, we use ecological principles, global empirical data on biodiversity and fisheries, and environmental economics to propose and analyze a new institution where nations can trade conservation obligations within reasonable ecological constraints: a global market for marine conservation. We describe the challenges and solutions to designing a market for marine conservation, and provide an example of how to build such a market and estimate the gains from trade. We find that the high spatial heterogeneity in habitat quality, costs, and sheer area across nations implies large efficiency gains are possible. For a 30% conservation target, the market-based approach would reduce the global cost of conservation by 98%, relative to the case of unilateral conservation. We consider several bubble policies (where trading is spatially restricted on the basis of habitat representation) and alternative conservation targets and find that a market always reduces the costs to all nations.

3.1 Introduction

Even when the global benefits of marine conservation are unequivocal [30, 31, 32, 33, 34], the costs of conservation, which are borne by individual countries, often dominate the debate and lead to little or no ambition and commitment. The consequence is that little conservation actually ensues, with some notable exceptions. This paper specifically addresses this mismatch for marine conservation: less than 3% of the ocean is protected under no-take marine reserves [35]. We posit that if the cost of conservation could be dramatically reduced, this would incentivize nations to undertake substantially more of it.

Previous work has shown that international coordination could reduce the costs of meeting conservation targets [36, 37, 38] and ensure protection of transboundary marine life [39]. Yet, no institution exists that would allow nations to meaningfully engage in coordinated conservation. We propose, design, and analyze a new institution in which nations' conservation obligations are transferable: a global market for marine conservation. This institution allows countries who can provide high quality conservation cheaply to conserve more and countries for whom it is very expensive to conserve. The basic principle is borrowed from successful market-based approaches to environmental improvement which have led to significant benefits to air quality [40, 41], fisheries [42, 43], water provision and quality [44, 45]. The main allure of market based approaches, as opposed to mandates or other regulations, is that their allocative efficiency has the potential to substantially reduce compliance costs [46].

In this paper, we show how such an institution can be designed to adhere to MPA design guidelines. We use ecological principles, global data on biodiversity and fisheries, spatial modelling, and economic theory to propose and analyze this new institution, where nations can trade conservation obligations within reasonable ecological constraints. We

find that the high heterogeneity in habitat quality, costs, and sheer area across nations implies potentially large efficiency gains. For a 30% conservation target, the market-based approach would reduce the global cost of conservation by 98%, relative to the business as usual (BAU) case of unilateral conservation. We also consider several "bubble" policies where trading is restricted to spatially-delineated biogeographic units and find that cost savings are still large (76% - 97%) compared to BAU. Across a range of protection targets, a market approach always produces cost-savings to all nations participating in it.

Our proposed approach has three compelling attributes. First, it dramatically lowers the cost of meeting global conservation targets, minimizing the main obstacle to support and ratification of conservation targets. Second, it provides net financial benefits for all coastal nations. Third, it generally implies that nations who tend to specialize in fishing will financially compensate nations who tend to specialize in biodiversity protection. Our work is particularly relevant as we enter the United Nations "Decade of Ocean Science for Sustainable Development", where innovative approaches will be required if we are to meet ambitious conservation targets.

3.1.1 Leveraging heterogeneity to reduce costs

There are at least three reasons to be optimistic that the market approach could substantially lower the cost of meeting any conservation target. First, suitable habitat is heterogeneously distributed around the planet, creating biodiversity hot-spots and areas with lower conservation value [47, 48, 49]. Second, fishing activity –and the cost of displacing it– is also heterogeneous in space, with some areas of the ocean containing several orders of magnitude more fishing than others [50]. Finally, what ultimately matters for the cost effectiveness of trading is the ratio of conservation benefit divided by cost, and its spatial distribution. This important metric has not been empirically

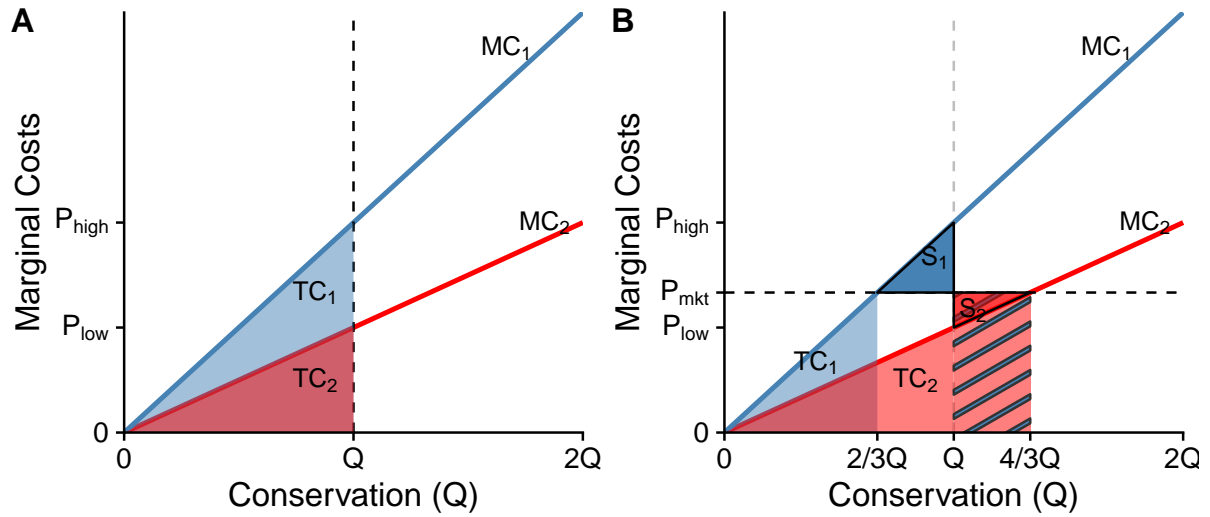


Figure 3.1: Stylized conservation supply curves and market outcomes, which are assumed to be linear for illustrative purposes. MC_1 and MC_2 indicate the marginal costs curves to each nation. The opaque triangles labeled TC_1 and TC_2 indicate the total costs to each nation. The solid triangles labeled S_1 and S_2 indicate the savings to each nations under a market.

studied, so it is not clear whether this will exacerbate or mitigate the aforementioned heterogeneity. For example, if places of high conservation priority are also the most costly to protect, then the value of trading will be blunted. But if places of high conservation priority are relatively inexpensive to protect, then trading could deliver large efficiency gains. The magnitude and distributional effects of the gains from trade is ultimately an empirical question which we will explore in this paper.

But how do markets leverage this heterogeneity to reduce the costs of conservation? Consider the stylized example shown in Figure 3.1A, which shows the marginal cost curves for two nations (these are assumed to be linear for illustrative purposes here, but we later relax this assumption). Each curve indicates the change in total cost that arises from producing an additional unit of conservation (the marginal cost). Note that the two curves have different slopes, which arises due to heterogeneity in conservation benefits and costs. To attain Q units of conservation, Nation 1 (in blue) would face a marginal

cost of P_{high} when protecting its last unit of conservation, and would incur total costs TC_1 (blue triangle). Note that Nation 2 faces a lower marginal cost of P_{low} for the same Q , and that its total cost TC_2 are lower than the costs incurred by Nation 1. Together, they produce $2Q$ units of conservation, at an aggregate cost of $TC_{bau} = TC_1 + TC_2$. The differences in these marginal cost curves imply that there may be a more cost-effective way to attain the same level of conservation.

Under perfectly competitive markets, the marginal cost curves are the same as the supply curve [51] and indicate the quantity a nation is willing to conserve for a given price. Figure 3.1B shows the conservation outcome when trade with each other. For a price P_{mkt} , Nation 1 would conserve $\frac{2}{3}Q$ in its waters, and then pay Nation 1 to protect an extra third in its name (shown in red-blue hashed area). Nation 2 now protects $\frac{4}{3}Q$ of its water. As in the case of unilateral conservation above, this outcome also produces $2Q$ units of conservation. However, Nation 1 avoided the the costs of paying the high price, and Nation 2 was paid to protect. The market gains are therefore $S_1 + S_2$.

The main allure of trade is that it can lower the costs of conservation to all nations. "Buying" nations could benefit from trading because it lowers their cost of compliance, and "Selling" nations could benefit from trading if the selling price more-than-offsets the cost of expanded protection. We outline the steps to design a market that 1) produces the same amount of conservation as would be mandated by unilateral conservation, 2) maintains the principle that each nation is treated fairly and equally but introduce flexibility via *voluntary* trade in conservation obligations, and 3) adheres to marine reserve design principles.

In designing such a market, two challenges arise. First, we must construct conservation supply curves for all coastal nations; to the best of our knowledge, this is an empirical task never done before. Second, not all ecosystems are created equally: protecting a hectare of coral reef is not the same as protecting one of kelp forest. A market that ignores

this could inadvertently undermine important habitat representation principles [52, 53]. We show how ecological principles can be used to build conservation supply curves, and how biogeographic regionalization can guide the design of ecologically-coherent policies that ensure habitat representation and avoid perverse incentives.

3.2 Methods

We provide a road map for constructing conservation supply curves and using them in a manner that is consistent with desired conservation outcomes. We begin by describing the data sources that we use to define the conservation benefits and costs faced by nations. These two measures will be crucial in estimating the marginal cost of conservation for every grid cell in the world, which we will use to build conservation supply curves. We then show how to construct conservation supply curves and simulate a market to estimate the gains from trade.

3.2.1 Data description

This work relies on multiple sources of spatial and tabular data to establish the potential benefits and costs of conservation. We use species distribution models, spatially explicit catch data, ex-vessel price of catch, location of existing marine protected areas, political boundaries, and biogeographic regions to construct conservation supply curves and simulate trade outcomes. We provide a detailed description of the data and how we incorporate them in our work. When necessary, data sets were reprojected and rasterized to conform to a 0.5 x 0.5 degree raster with standard WGS84 ellipsoid and datum. In principle, these data and our approach would allow for the construction of conservation supply curves for terrestrial or marine conservation purposes, but we will focus on the latter.

Gridded data sets

We use species distribution models (SDM) from AquaMaps [54]. These provide the probability of a species occurring on any given ocean grid cell along. The entire data set contains information for 33,518 species. We remove 9,819 species for which SDMs were built using less than 10 records – these species are considered data-poor or with extremely restricted distribution and Kashner et al [54] advise not to use them in large-scale analysis. SDM's for the remaining species are used to compute the Habitat Suitability Index as described in Section 3.2.2.

Our cost layer is built by combining annual ex-vessel price of seafood with spatially-explicit data on capture fisheries. We corroborate and update taxonomy across data sets using taxonomic data from FishBase [55] and SeaLifeBase [56] accessed via rfishbase 3.1.9 [57]. The tabular data-set on ex-vessel prices contains 97,293 distinct records taxa-specific annual ex-vessel prices. We removed records identified as "freshwater", records occurring outside the 2005-2015 period, and records with no ex-vessel price reported, leaving us with 17,419 records. We calculate the median annual price for each species, genus, family, order, and ISCAAP code (Acronym for the "International Standard Statistical Classification for Aquatic Animals and Plants", which categorizes species into 50 groups based on taxonomic, ecological and economic characteristics[58]).

We use spatially-explicit taxa-level reconstructions of annual catch by industrial and non-industrial fisheries from Watson et al., [59]. We keep records between 2005 and 2015 and combine industrial and no-industrial reconstructed catch at the grid-cell-year-taxa-level. We then combine these data with the corresponding taxa-specific price data. Price data are not available for all species included in the reconstructed catch data set. We therefore perform a series of hierarchical matching steps based on taxonomy. We first attempt to match at the species-level, then by genus, then family and order, and finally

class. The remaining groups are matched on the basis of ISCAAP groups.

Combining catch and price data allows us to calculate the cell- and species-specific annual fisheries revenue as the product of catch of species j at time t and grid cell i (c_{jti}) and unit prices of species j at time t (p_{it}). We then collapse the temporal dimension by taking the median revenue for each cell and produce a spatially-explicit measure of fisheries revenue R for patch i :

$$R_i = \text{median} \left(\sum_{j=1}^J p_{it} c_{itj} \right) \quad (3.1)$$

The resulting gridded data are shown in in Fig B.2.

Vector data

The gridded data described above will allow us to identify benefits and costs of conserving a given marine grid cell. But to construct national conservation supply curves, we must assign jurisdiction to each cell. And to simulate bubble policies, we must also assign each grid cell to a hemisphere, realm, and province. We assign jurisdiction based on Version 11 of the "Maritime Boundaries and Exclusive Economic Zones" produced by the Flanders Marine Institute [60]. We define "nation" as the nation state indicated by the standard 3-letter code of the territory for each polygon in the data set. When territory data were missing for a polygon, we used sovereign attribute instead. We assign biogeographic attributes based on Spalding's biogeographic regionalization which divides the world into 12 realms and 60 provinces [61]. All vector data were rasterized onto a 0.5 x 0.5 degree and matched on a cell-by-cell basis to the cost and benefit gridded data sets described above.

Finally, our work must account for areas that have already been protected. We use Marine Protected Area (MPA) boundaries from MPAAtlas (mpaatlas.org) and keep

only strongly-protected areas as defined by IUCN protected area management categories, which classify areas based on their management objectives. We keep only polygons belonging to categories Ia (Strict nature reserve), Ib (Wilderness area), and II (National park). These three categories are largely. These are the three most stringent categories, and while they have slight differences in their objectives, they generally seek to conserve a "particular natural feature" or "whole ecosystem and ecosystem processes" [62]. The resulting data set contains 2,866 spatial features.

3.2.2 Building conservation supply curves

Our description of the benefits of conservation must capture spatial heterogeneity: the fact that some ocean grid cells are inherently more suitable for biodiversity than others [47]. We use species distribution models for 23,699 species available from Aquamaps, which provide the probability of occurrence of a species across a 0.5-by-0.5 degree grid. The probability of occurrence is modeled from the abiotic characteristics of the grid cell, such as temperature, dissolved oxygen, salinity, and depth [54]. Importantly, these abiotic factors are unaffected by the protection status of the grid cell or the protection status of adjacent grid cells.

Let p_{ij} be the probability of occurrence of species j in grid cell i . We retain only grid cells for which $p_{ij} \geq 0.5$, thus represent a species' core habitat [54]. We then calculate the habitat suitability of grid cell i as the average probability of occurrence across all species that inhabit it:

$$HSI_i = \frac{1}{S_i} \sum_{j=1}^{S_i} p_{ji} \quad (3.2)$$

This represents the average suitability of grid cell i for species that reside in it. In the extreme, all species in the grid cell i have a probability of 1.0, then $HSI_i = 1$. Thus,

HSI_i is bounded between 0.5 and 1.

If the area of grid cell i is α_i (in km^2), then our measure of conservation benefit produced by protecting grid cell i is given by:

$$Q_i = \alpha_i HSI_i \quad (3.3)$$

This measure combines the area of a grid cell (α_i) with the suitability of that pixel for the biodiversity distributed in it (HSI_i). Therefore, it aligns with the current wording of international area-based targets for marine conservation [63], but without the downside of creating a perverse incentive to conserve areas of little or no conservation benefit [64, 65, 66]. We calculate Q_i for all 52,879 oceanic grid cells that occur within the Exclusive Economic Zone of 186 coastal nations (Fig B.1).

Multiple prioritization studies have indicated where MPAs should be sited to meet a variety of objectives, ranging from protecting biodiversity hot-spots to blue carbon stocks [47, 67, 53, 38]. Regardless of the goal, a prevailing barrier to action are the large political costs that policy makers face when potentially displacing economic activities, such as fisheries [68, 69]. Even if conservation were to create fishery benefits in the long-run, immediate costs halt action. We therefore use fisheries revenue as a measure of the political cost faced by policymakers. We combine high-resolution spatio-temporal data on fisheries catch[70] and ex-vessel prices[71] to produce a spatially-explicit data set of average fisheries revenue observed between 2000 and 2015 (Fig B.2).

With these measures of costs and benefits in hand, we proceed to build conservation supply curves. We calculate the per-unit cost of conservation benefit for each grid cell by taking the ratio of benefits to costs, and then rank all grid cells within a nation in ascending order. The amount of conservation attained by protecting a grid cell is simply Q_i , which moves us along the x-axis (See Fig. 3.1). The per-unit cost of protecting that

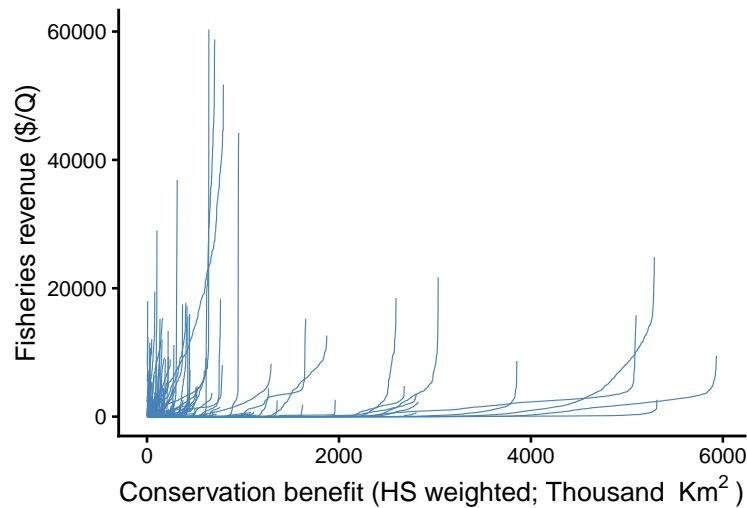


Figure 3.2: Conservation supply curves for 186 coastal nations. Note the large heterogeneity in potential conservation benefits and marginal costs of conserving.

grid cell is the marginal cost (how many dollars of fishery revenue would be displaced for each unit of conservation attained), our y-axis (See Fig. 3.1).

Importantly, we account for presence of existing protected areas and adjust the conservation supply curves by excluding grid cells within strongly protected areas (specifically, MPAs IUCN Class Ia, Ib, and II [62]). We do this to eliminate the possibility of downgrading or down-sizing existing protected areas [72]. Nations that have already met their target by protecting *in situ* are therefore not required to protect any additional units, but are allowed to produce additional conservation by selling conservation credits to other nations. The resulting conservation supply curves are shown in Figure 3.2.

3.3 Results

With the conservation supply curves at hand, we now turn to the task of quantifying the potential gains from trade. As in the stylized example in figure 3.1, we use these supply curves to simulate a business as usual scenario (labeled *BAU*) where nations can

only protect habitat within their waters, and one where nations are allowed to trade (labeled *MKT*). We calculate the total costs incurred by each nation under each scenario as the sum of fisheries revenue that would be displaced by the implementation of marine protected areas, and calculate the gains from trade as the difference between scenarios. In the market-based scenario, we also trace the cost-savings to each nation, and note whether these arise through avoiding costs by purchasing conservation credits (these are the "buyers"), or through transfers that arise from conserving in other nations' name (these are the "sellers").

3.3.1 Gains under a 30% target

How much of the oceans should be protected remains unclear, and a diversity of targets exist. However, there seems to be increasing support to protect at least 30% of the marine environment under no-take marine reserves [73]. This target has been incorporated into the Post-2020 Global Biodiversity Framework draft, and would seek to meet it by 2030 [74]. We run BAU and market-based simulations with a global conservation target of 30%. Under the BAU scenario, each nation is required to protect habitat in its waters, while the market-based simulation allows nations to trade and allocate protection in the most cost-effective way. We find that trade would help nations avoid 98% of the costs. Importantly, every nation participating in the market stands to gain from this cooperative approach (Fig 3.3).

The market-based approach reduces the costs of conservation by changing the location where MPAs are sited (Fig. B.9). These alternative locations will either have higher HSI and less surface area or vice versa. We track the surface area and HSI of grid cells protected under each scenario, and find the market-based approach requires up to 0.77 - 1.23% less surface area than a BAU scenario (Fig. B.10). This indicates that a market-

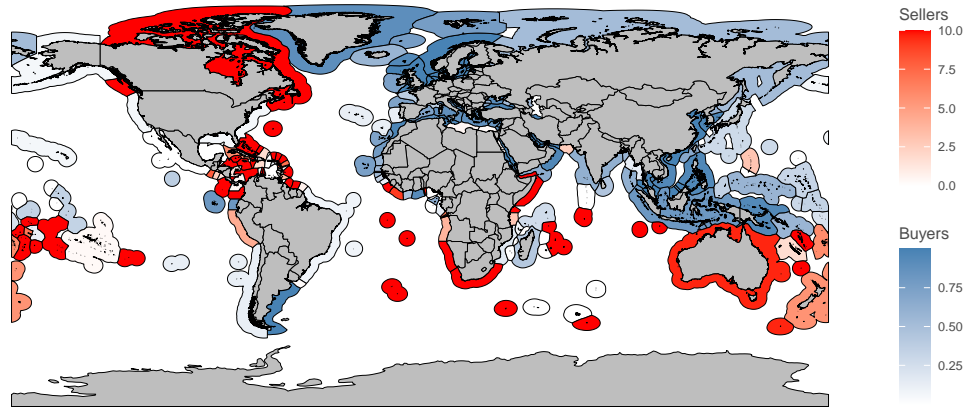


Figure 3.3: Map of savings. The color indicates whether a firm buys (blue) or sells (red) conservation credits, and the hue indicates the magnitude of the savings, similar to the area of the stylized "savings triangles" described in Fig 3.1C.

based approach relocates MPAs to grid cells with more suitable habitat (*i.e.* higher HSI).

3.3.2 Bubble policies

Not all ecosystems are created equally. We therefore need a way to ensure that protection targets are met within spatial units of similar ecological characteristics. In environmental economics, the spatial delineation of a market is known as a bubble policy [75, 76]. One way to divide the World is on the basis of geographic location. For example, we can divide the World into four hemispheres. Another alternative is to divide the world on the basis of biogeographic regionalization. Biogeographic principles have been adopted by conservation planning to design and implement marine protected areas [67, 77]. We use the biogeographic regions defined by Spalding et al [61] to divide the world into ecologically-coherent trading bubbles. Specifically, we implement two additional bubble policies that restrict trade within realms (12 bubbles), and provinces (60 bubbles; Fig B.5).

The rules of a bubble policy warrant further explanation. A bubble policy determines the spatial basis for the segmentation of the global market. For example, a hemisphere policy creates four distinct markets, one for each hemisphere. A nation holds rights (and conservation obligations) to a segment if its Exclusive Economic Zone intersects the hemisphere. Under a 30% global target, 30% of each segment has to be protected. Therefore, conservation credits can not be traded between hemispheres and nations can only engage in trade on markets to which they hold rights. A nation that holds rights to more than one market segment may be a net buyer in one segment and a net seller in another.

But ensuring ecological representation will come at a cost. Segmentation of a market reduces its allocative efficiency (*e.g.* A "nation" bubble policy would in fact divide the world into 186 segments on the basis of Exclusive Economic Zones, making the BAU and market-based scenario identical). How much of the cost savings will be reduced by dividing the world into hemispheres, realms, and provinces is indeed an empirical question of great interest and its answer may ultimately determine the potential support for this new institution. We repeat the process of building conservation supply curves but now do it at the nation-hemisphere, nation-realm, and nation-province levels (B.6,B.7,B.8). Like before, we simulate the outcomes of a 30% protection target under business as usual and a market. We find that the gains from trade decrease as the numbers of segments increases. But even under a strict division of the world into 60 biogeographic provinces reduces the costs of conservation by 77.12%, relative to BAU (Fig 3.4).

3.3.3 Other conservation targets

Multiple targets, agreements, and commitments seek to dramatically increase global marine conservation from the current 3% up to 10% (UN Sustainable Development Goals

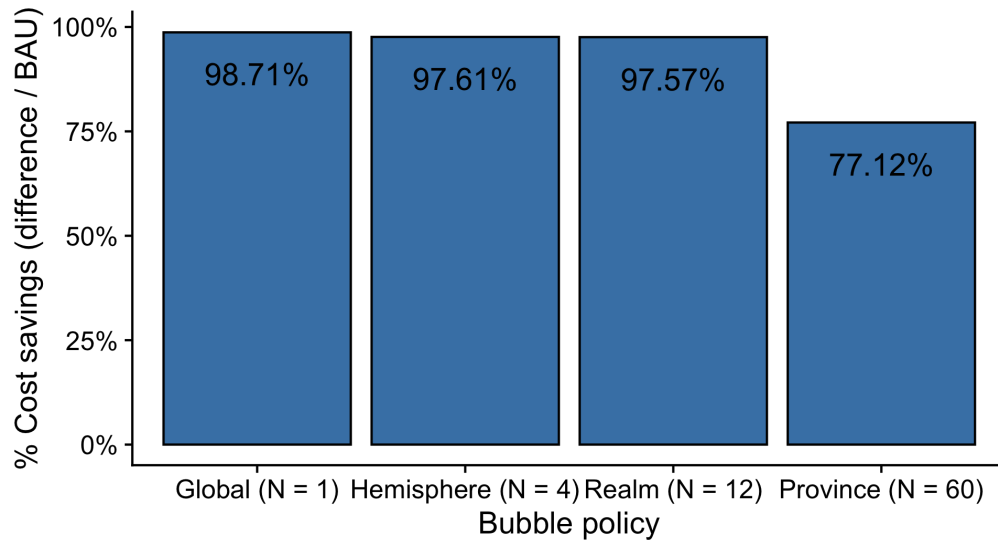


Figure 3.4: Gains from trade of a market for marine conservation under four bubble policies. The y-axis shows the difference between the total costs under market and total costs under BAU, relative to the total costs under BAU. The x-axis shows the bubble policy implemented, with numbers in parentheses indicating the number of bubbles implemented under each policy.

and Convention on Biological Diversity), 30% (International Union for the Conservation of Nature), or even 50% (Half-Earth Coalition) of the ocean. These targets are all ambitious and highlight the diversity of potential targets.

Whatever the combination of conservation target or bubble policy may be, we can use our conservation supply curves to calculate its cost-savings. We simulate a range of protection targets between 10% and 99% under a global market and the same three bubble policies as before. Independent of target or bubble policy, we find that a market always reduces the cost of conservation (Fig. 3.5). For example, 90-99% of the costs can be avoided for the lower bound of a 10% conservation target, depending on the bubble policy. The gains from trade decrease for a 50% target, but are still large and range between 67-97%.

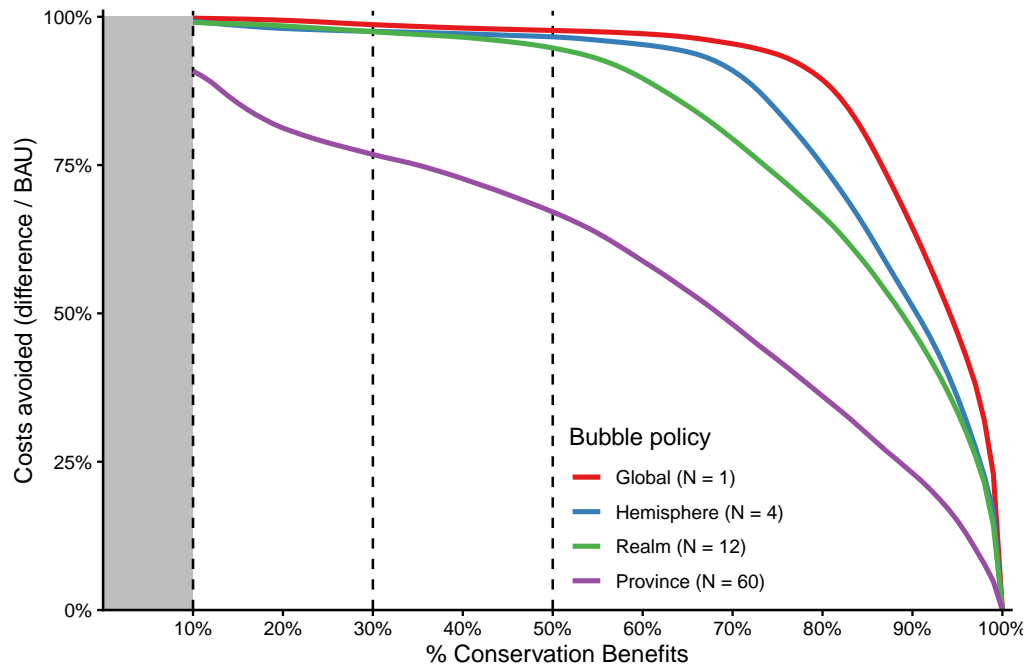


Figure 3.5: Gains from trade (y-axis) for a range of conservation targets (10% to 99%; x-axis), under four different bubble policies (colors). Each line shows the percent of the costs that can be avoided by allowing trade between nations within each segment. The dashed horizontal lines mark the often-cited conservation targets of 10%, 30%, and 50%.

3.4 Discussion

Twice now, we have failed to attain Marine Protected Area coverage targets in time. And while some nations have made notable advances, the ocean as a whole remains largely under-protected [73, 35, 78]. We posit that the main impediment is the high political cost of closing large swaths of ocean to economic activities, and propose an institution where nations can engage in trade to lower the costs of marine conservation. We find that a global market for marine conservation substantially reduces the costs of attaining any conservation target. This result holds across a range of bubble policies, although market segmentation reduces the potential gains from trade. Under our simulations, the market-based approach relocates MPAs to locations that would displace less fishing revenue, requires less surface area, and sites MPAs in areas with a higher suitability

index.

An important feature of a market-based approach is the voluntary nature of transactions. This has two broad implications. Firstly, that no nation can be forced to buy or sell conservation credits from other nations. For example, a nation with large swaths of valuable habitat may choose not to sell conservation credits if sovereignty concerns were to arise [79, 80]. And, secondly, every nation voluntarily participating in the market would be better-off, relative to the BAU scenario. The extent to which nations are willing to engage in trade will ultimately determine the cost-savings potential of a market.

Nations may be more willing to engage in trade with nations with which they already collaborate on other fronts. We showed how biogeography could be used to guide the design of bubble policies, but alternative bubble policies could be created on the basis of international coalitions that jointly manage marine resources. Notable examples include the Parties to the Nauru Agreement via the Palau Arrangement [81, 82] or the European Union via the Common Fisheries Policy [83, 84]. Moreover, political boundaries and biogeographic regions are not mutually exclusive, and bubble policies could be implemented based on their spatial intersection. As we show, this further segmentation of the market would reduce the gains from trade but could ensure that habitat representation guidelines remain present within international coalitions, thus helping incentivize conservation action.

A prevailing concern surrounding Marine Protected Areas is that these can displace users and reallocate spatial property rights from resource users to the public interest [85], which has raised concerns around their distributional impacts [79]. A global market for marine conservation may help alleviate some of these concerns by placing MPAs in areas that would produce similar conservation benefits but imply a lower displacement cost. Importantly, this implies that nations who generally specialize in fisheries would compensate those who specialize in biodiversity conservation. On the other hand, a

market-based approach may generate the concern that the government's appraisal of a "patch" could not accurately capture the cost borne by individual resource users who may be displaced. To assuage this concern, nations could allocate spatial property rights to fishers or fishing cooperatives who would in turn participate in the global market.

We make no attempt to identify optimal conservation targets, prioritize locations, nor we advocate for a particular measure of costs and benefits. The purpose of this work is the more modest one of presenting the steps for designing a global market for marine conservation and calculating the gains from trade under certain simplifying assumptions. Our choice of measures of benefits and costs measures used to build the supply curves therefore warrants a discussion.

We use habitat-suitability-weighted area as a measure of benefits because it aligns with the international area-based measures [63], but incorporates a flexible way of adjusting for the differential value of habitat; the HSI allows us to discern between to grid cells of equal-area, and assigns a greater value to the one that would be more suitable on average. We construct our HSI assuming equal weighs for all species under the assumption that MPAs seek to protect ecosystems and ecosystem processes, rather than individual species or populations. However, the habitat suitability index could be re-calculated as a weighed average that includes, for example, the species conservation status or the inverse of the area of a species' distribution as weighs, as previous assessments of at-risk marine biodiversity have done [86]. Alternatively, other measures could also be used to weigh the area of a pixel. For example, the quality of a habitat in a grid cell as determined by bottom-up (*e.g.* ecological surveys) or top-down (*e.g.* the Ocean Health index [87]) methods.

We use fisheries revenue as a measure of the political cost that policy makers would face when displacing fishing effort to give way to conservation. However, this excludes other potential sources of forgone revenue, such as extraction of mineral resources or the

potential to develop offshore infrastructure (*e.g.* wind farms or mariculture plants). The extent to which costs are heterogeneously distributed in space, and their relationship to the benefits of protection, will ultimately dictate the potential gains from trade. Using different measures of costs and benefits will ultimately change the magnitude of cost-savings. But a market will result in gains so long as the ratio of costs to benefits is heterogeneously distributed in space.

Finally, we must address the potential role of climate change. We use present-day species distribution models and recent fisheries revenue, which implicitly ignores the redistribution of biodiversity and losses in fishery productivity that are induced by climate change [88, 89]. While the effect of climate change on both measures is idiosyncratic [90, 89], there is evidence that present-day MPAs might be exposed to novel conditions by 2050 [91, 92]. The extent to which the design and implementation of MPAs will be able to account for these changes depends on our ability to predict environmental conditions in the ocean and the redistribution of marine biota [77, 93].

It is widely acknowledged that the ocean can play an important role in the livelihood of millions of people, carbon sequestration, food security, among other benefits; this has prompted calls to significantly increase global marine conservation from the current 3% up to 10%, 30%, or even 50% of the ocean¹. Under most of these proposals, conservation obligations would be spread uniformly across nations, but the costs of meeting a given target will differ dramatically across nations. Our work shows that the total costs of attaining any of these targets can be drastically reduced by implementing a global market for marine conservation, in which all nations stand to benefit. Moreover, meeting these ambitious targets will require equally ambitious and innovative approaches that promote international collaboration towards equitable conservation of the oceans.

¹Sustainable Development Goals, International Union for the Conservation of Nature, Half Earth Coalition

Chapter 4

The implied carbon cost of human-induced whale mortality

Abstract

Nature-based climate solutions seek to remove Carbon from the atmosphere by sequestering it into biomass, often in the form of trees. Whales, however, store large amounts of Carbon in their body, sequester it when they die, and stimulate primary production through nutrient recycling. What is the monetary value of a whale's contribution to the Carbon cycle? The value of a whale will depend not only on the amount of Carbon stored in its body, but also on the ecological and demographic processes associated with each organism. I build a model that couples an age-structured whale population, its contributions to the Carbon cycle, and economic principles to calculate the implied cost of human-induced whale mortality in terms of the forgone Carbon sequestration potential. I find that the cost ranges from $\$3,820 \pm 1,440$ (M \pm SD) per Minke whale to $\$51,700 \pm 16,000$ per Fin whale. Importantly, the main Carbon cost of removing a whale accrues due to the ensuing population dynamics of its removal, not due to the Carbon that was once stored in said whale. Combining our estimates with catch data reported by the International Whaling Commission, I estimate the implied Carbon cost of whaling to be in the order of $\$5.9$ M USD per year. These numbers may inform cost-benefit analysis of whale conservation programs, or help design institutions that would link them to nature-based climate change mitigation strategies.

4.1 Introduction

Humans have altered the Earth's climate by increasing atmospheric concentration of green-house gasses, such as CO₂ [94]. Pollution, habitat fragmentation and degradation, and direct resource extraction, have significantly reduced population sizes of many plants and animals [95]. Today, climate and conservation scientists would generally agree that we have too much CO₂ in the atmosphere, and not enough plants and animals alive. Nature-based solutions can help respond to the drivers and implications of climate change and provide a way to conserve life on Earth [96]. In the context of climate change mitigation, nature-based solutions seek to remove Carbon from the atmosphere and sequester it into biomass [97, 96]. Linking conservation actions to Carbon benefits can help monetize the gains. This can contribute to cost-benefit analysis of policy interventions, and provide additional sources of funding.

Sequestering Carbon into biomass is a goal of many forestry policies, and has the potential to contribute to the conservation and climate mitigation agendas [98, 99, 100]. For example, Carbon sequestration capacity in the United States alone could be increased by 187.7×10^6 ($\pm 9.1 \times 10^6$) tonnes per year by fully stocking productive forestland [101]. Many have studied the Carbon storage and sequestration potential of other terrestrial and coastal ecosystems, such as savannas [102], marshes [103], and mangroves [104], highlighting the potential to link climate change mitigation and conservation policies. However, the role of marine biota has been largely neglected, with only a few studies focusing on fish [105] or algae [106, 107].

A growing body of literature suggests that whales once played a significant role in the Ocean's Carbon cycle. Pershing et al., [108] estimate that present-day whale populations of baleen whales store 9.1×10^6 tonnes less Carbon than pre-whaling populations, and that rebuilding whale populations could remove 1.6×10^5 tonnes per year through sinking

whale carcasses. These numbers are modest relative to other nature-based Carbon sequestration alternatives, but a better understanding of whale's role in the Carbon cycle could contribute to their conservation by informing cost-benefit analysis or by linking conservation programs with funding sources like Carbon markets. But monetizing the value of a whale requires careful consideration of the inter-generational dynamics and ecological processes in wild populations.

An important distinction between Carbon stored in managed forests and Carbon stored in animal populations lies in the growth and management of the underlying stock. Estimates of Carbon sequestration potential by forests often focus on comparing policies that affect the growth of individual trees –or use broad measures of Carbon density– in a managed forest [109]. This loosely implies that the maximum number of trees a replanted, and that sequestration comes from tree growth. In wild animal populations this is akin to somatic growth: the accumulation of biomass as an individual grows in age and size. However, wild populations –especially those with low present-day abundances– can also grow in size; not only do organisms grow, but they also produce offspring (which also grow and reproduce). These inter-generational dynamics imply that the Carbon value of a whale is composed of the Carbon stored in a whale and the Carbon sequestration potential of the demographic and ecological processes. The value of each of these processes remains understudied, and estimating their relative contributions is one of our contributions.

Among animals, whales are some of the best candidates to link conservation and Carbon sequestration policies. Their persistent low population sizes imply large potential for recovery. And there are at least three reasons that make whales suitable candidates for Carbon sequestration policies: 1) they are some of the largest and longest-living organisms on earth, which means Carbon in their bodies remains stored for decades or even centuries [108], 2) when they die, a large portion of this in-body Carbon is sequestered in deep-ocean sediments [110, 111], and 3) recent advances have shown that whales also

enhance primary production in the ocean by recycling nutrients [112, 113] and stimulating primary production in above the mixed-layer depth [106, 107]. The combination of these processes implies that whale conservation strategies may also contribute to climate change mitigation via Carbon storage and sequestration [114].

Today, the Carbon sequestration potential of most whale species is limited by prevailing low population values [108]. Present-day whale populations face multiple sources of direct and indirect human-related mortality. Direct sources include harvesting, vessel strikes, debris, and entanglement with fishing gear [115]. Indirect sources include nutritional stress and disease, that result from noise pollution or poor water quality [115]. It is difficult to precisely quantify the rate of human-induced whale mortality, but observational data can still provide some information. For example, an assessment of whale entanglements on the U.S. west coast found that at least 10% of whales entangled in human-made materials were found dead [116]. And data on vessel collisions show that an average of two blue whales per year were killed by ship strikes off California [117]. Importantly, ship strikes have been historically more frequent and prevalent on the U.S. East coast and amongst more abundant whale species, such as fin and humpback whales [118]. These numbers should be interpreted as lower bounds of human-induced whale mortality, since many dead whales likely go unreported or undetected and fishers and boat captains often face an incentive to not disclose these types of information.

Whales store Carbon in their body, sequester it when they die, and stimulate productivity through nutrient transport [119, 108, 112, 113]. Human-induced whale mortality halts somatic growth of the deceased individual, prevents the further stimulation of productivity, and may also prevent the body from being sequestered depending on how and where they are killed. But importantly, it also prevent it from having offspring which would contribute to these processes, therefore highlighting the dynamism of inter-generational Carbon sequestration. What is implied Carbon cost of human-induced

whale mortality? Here, I build a model that couples an age-structured whale population, its contributions to the Carbon cycle, and economic principles to calculate the implied Carbon cost of human-induced whale mortality for five baleen whale species.

The cost will ultimately depend on which whale is removed from the population, the fate of the removed whale's biomass, and the population size from which it is removed. The first point relates to the fact that survival, fecundity, and mass change with whale age. The second point recognizes that Carbon stored in a whale that is harvested for human consumption will have a different fate than that of a whale that has been struck by a ship and has a probability of sinking. Finally, the third reason points at the density-dependence dynamics that arise in animal populations – removing an individual from a small population has a larger impact on population growth than removing an individual from a large population.

4.2 Methods

A simple framework to establish the implied Carbon cost of human-induced whale mortality requires at a minimum three components: i) a model of whale population dynamics, ii) a model of Carbon storage and sequestration, and iii) a way to calculate the net-present value of whale Carbon. The first component captures the fact that a whale and its offspring will capture Carbon over their lifetimes. The second component addresses the process by which whales directly and indirectly contribute to the Carbon cycle. Finally, the third component monetizes these dynamics by connecting them to the social cost of Carbon.

4.2.1 Model description

I use bold symbols to denote matrices and vectors, and Greek letters to denote parameters in the model. When relevant, I use sub-indices to denote specific times (t) or age-classes (i).

Population dynamics

The general discrete-time, density-dependent, deterministic age-structured population model builds on Jensen [120], and is given by:

$$\mathbf{N}_{t+1} = \mathbf{N}_t + \delta(\mathbf{M} - \mathbf{I})\mathbf{N}_t \quad (4.1)$$

\mathbf{N}_t is a $\alpha \times 1$ vector of age-specific population sizes at time t . Parameter α denotes the terminal age-class of the population. The parameter δ is a scalar that induces density-dependence via total population biomass, and takes the form $\delta = \frac{K-B}{K}$ (where B is the total biomass of the population and K is the carrying capacity of the population).

Finally, \mathbf{M} is an $\alpha \times \alpha$ population projection matrix and \mathbf{I} is the identity matrix. Letting μ_i and σ_i be the age-specific fecundity and survival, respectively, M can be defined as follows:

$$\mathbf{M} = \begin{bmatrix} \mu_1\sigma_0 & \mu_2\sigma_1 & \dots & \mu_\alpha\sigma_{\alpha-1} & 0 \\ \sigma_0 & 0 & \dots & 0 & 0 \\ 0 & \sigma_1 & \dots & 0 & 0 \\ 0 & 0 & \dots & \sigma_{\alpha-1} & 0 \end{bmatrix}$$

Note that I use the birth-pulse form of the model in which reproduction occurs following survival, so that the number of offspring produced by age-class x is given by: $\mathbf{N}(x, t)s_{x-1}m_x$ [121]. When simulating human-induced mortality, organisms are removed

prior to any survival and growth. Age-specific survival and fecundity parameters are not available for all whale populations, but general parameter estimates are available for juveniles and adults. All age classes lower than age at maturity are assigned a fecundity of zero, and an equal probability of survival associated with juveniles. Adults receive a constant fecundity rate, described as the inverse of calving interval, and a constant probability of survival (See Table 4.1). The probability of survival for the last age class is exactly zero.

Abundances can be converted into biomass using the von Bertalanfy mass-at-age formulation:

$$M(a) = M_{\infty} (1 - e^{-k(a-a_0)}) \quad (4.2)$$

I then define a vector \mathbf{M} of length α that contains the corresponding mass-at-age values for our species of interest. Total biomass at each time step is then $\mathbf{B}_t = \sum_{i=1}^{\alpha} \mathbf{N}_t \mathbf{M}$. All demographic parameters are shown in Table 4.1.

Carbon dynamics

The stock of whale Carbon at time t is then given by:

$$\bar{C}_t = \underbrace{\sum_{i=1}^a N_{it} M_i C^b}_{\text{In-body Carbon}} + \underbrace{\sum_{i=1}^a N_{it} M_i C^p}_{\text{Stimulated}} + \underbrace{\sum_{i=1}^a (1 - \sigma_i) N_{it} M_i C^s}_{\text{Whalefall}} \quad (4.3)$$

C^b , C^p , and C^s are represent the per-kilogram parameters of in-body storage of Carbon, Carbon storage via productivity enhancement, and sequestration due to death and sinking, respectively. While biological and physical activity may result in remineralization of these Carbon, these processes are time-invariant and independent of whale abundance, and thus not relevant to this exercise.

Valuation

We must monetize the costs of damages associated to the forgone Carbon sequestration potential. The social cost of Carbon (SCC) quantifies these damages by characterizing how additional CO₂ emissions today impact future economic outcomes. Specifically, it is the discounted value of annual damages caused by 1 additional metric ton of CO₂ released in period t , summed over the number of years that it is present in the atmosphere, and discounted to period t .

The total value of whale Carbon over a horizon of length T is then given by:

$$PV = \sum_{t=1}^T \frac{\theta_t \bar{C}_t \psi}{(1 + \rho)^t} \quad (4.4)$$

Haight et al [109] use the same formulation to estimate the present value of Carbon sequestration in US forests when evaluating the climate change mitigation potential of three forest management policies. Here, θ_t represents the Social Cost of CO₂, the \$ per ton CO₂ emitted in period t (See Table C.1), and ρ is the discount rate associated with its estimation ($\rho = 2.5\%$). Finally, ψ is the ratio of the molecular weight of Carbon dioxide to that of Carbon (44:12), and acts as a conversion factor between C and CO₂ ($\psi = \frac{3.67tCO_2}{1tC}$).

A business as usual scenario –where current whale populations grow with no human-induced mortality– allows me to generate a benchmark, C^{bau} . By simulating different policy interventions (*e.g.* harvesting a single whale of age α at time t), I can calculate the net value of said intervention, PV^{mrt} . It follows that the difference, $PV^{mrt} - PV^{bau}$, is the implied Carbon cost of human-induced whale mortality.

4.2.2 Parameterization

The first module pertains to whale population dynamics (Eq. 4.1). Pershing et al., [108] provides a summary of present-day whale population size and demographic parameters required to construct \mathbf{M} matrices (See Table 4.1). Survival-at-age (σ_α) and fecundity-at-age (μ_α) are assumed to be constant across the two life stages (juveniles and adults) as indicated by the age-at-maturity by species (α_m).

The second part of the model tracks the ways in which whales contribute to the Carbon cycle. The first term in Eq. 4.3 points at Carbon stored in a whales body. Jelmert and Oppen-Berntsen [122] provide the information to calculate the in-body Carbon content of a whale: A whale has a dry-weight content of 40%. From this dry biomass, proteins and lipids account for 20% each, and have a Carbon content of 54% and 77%, respectively. Thus, $C^b = 0.4 \times 0.2 \times (0.54 + 0.77) = 0.1048$ (Kg C / Kg Whale biomass).

The second term term in Eq. 4.3 pertains to the possible stimulation of primary production induced by whales. Savoca et al [123] empirically estimate feeding rates of baleen whales (whales eat 5 - 30% of their body-weight daily, and feed for 90 - 120 days / yr), which I combine with data on excretion rates and iron-content of whale feces from Ratnarajah et al., 2014 [113], we can derive the per-Kg contribution of whales to primary production via iron fertilization. Specifically, 1 ton of whale biomass mass results in the fixation of 8.28 g of Carbon by Phytoplankton (*i.e.* $C^p = 8.28$ g C / Kg whale).

Finally, I must account for Carbon sequestered due to whales dying and sinking (third term in Eq. 4.3). The estimates of whale falls vary by species and location, and can range from 10% (for right whales) to 90% (most whales; [111, 108]). I therefore use a conservative estimate and assume that only 50% of natural mortality events will become whale falls (Thus $C^s = 0.5 \times C^b$).

The last part of the model monetizes the Carbon contributions of whales (Eq. 4.4). I

Table 4.1: Demographic and mass-at-age parameters for five baleen whale species. K represent the pre-whaling biomass (in thousand tonnes) estimates used as carrying capacity. N_0 are the present day (2011) estimates of abundance. α_m is the age at maturity, α is the maximum age attained, μ is the fecundity, σ_{juv} and σ_{adt} are the juvenile and adult survival rates, and m_∞ , k , and a_0 are the von Bertalanfy parameters for mass-at-age conversions. All parameters come from Pershing et al., 2010.

Species	K	N_0	α_m	α	μ	σ_{juv}	σ_{adt}	m_∞	k	a_0
Fin	43,340	110	8	118	0.12	0.854	0.976	64.5	0.2	-4.8
Humpback	6,151	42	7	74	0.13	0.856	0.977	30.0	0.1	-9.4
Minke	5,060	507	9	86	0.15	0.850	0.974	6.0	0.2	-1.0
Gray	674	16	7	97	0.12	0.846	0.976	30.0	0.1	-9.4
Right	3,075	9	8	97	0.13	0.858	0.977	40.0	0.1	-9.4

Table 4.2: Other model parameters.

Parameter	Symbol	Value	Source
Proportion of body as carbon	C^b	0.1048	[122]
Productivity stimulation (g Phytoplankton / T whale biomass)	C^p	8.28	[123]
Proportion of dead biomass sequestered	C^s	0.0524	[108]
Discount rate	ρ	2.5%	[124]

use the 2021 estimates of the social cost of Carbon produced by the Interagency Working Group [124]. As previous estimates, these are produced from multiple runs of DICE, FUND, and PAGE across a series of scenarios. The latest interim update seeks to incorporate a lower discount rate in the calculation of the SCC, identified as more appropriate for inter-generational analysis. They provide social cost of Carbon under three discount rates (5%, 3%, and 2.5%). Here, I use the values obtained with a 2.5% discount rate (See Table C.1).

4.2.3 Simulations

I am interested in how the Carbon cost of human-induced whale mortality changes with population size, fate of the whale removed from a population, and age of the whale

harvested. I perform a series of *in silico* experiments to answer each of these questions for five baleen whale species for which population status, demographic parameters, and von Bertalanfy growth parameters are available (Table 4.1).

I use the standard computational experiment hierarchical nomenclature:

- **Experiments** are designed to answer a question by individually manipulating specific parameters of interest across scenarios.
- **Scenarios** are akin to *treatments* in laboratory experiments. The treatment effect is defined as the difference between outcomes from a treatment and a control. In our case, a "treatment" group is a scenario with human-induced whale mortality; a "control" is a business as usual (BAU) scenario using identical parameter values as the treatment scenario, but no human-induced whale mortality. Each scenario can be composed of one or more simulations.
- A **simulation** is an individual model run, where a population is simulated over a time horizon.

Stable age distributions

While current population estimates exist, the number of individuals in each age class—known as the age structure of the population—are not available. This information is crucial, as age-structured population models can exhibit oscillations in age structure at the beginning of simulations (See Fig. C.1). To ensure that changes observed between scenarios are attributable to the simulated intervention—and not to the dynamics of age-structure stabilization—we must first identify the stable age structure of the population.

One can identify the stable age structure by simulating the population until the population reaches carrying capacity and the number of organisms in age class is also stable. However, this is a computationally intensive task, since the time to reach that

equilibrium is unknown (See Fig. C.1). Alternatively, the stable age structure of the population can be identified via eigenanalysis. For an $\alpha \times \alpha$ matrix \mathbf{M} , there are α eigenvalues. The dominant eigenvalue λ of \mathbf{M} is the long-term population growth rate. From the matrix model we can find the right (ω) and left (μ) eigenvectors of \mathbf{M} associated with the dominant eigenvalue λ . These eigenvectors satisfy the conditions:

$$\begin{aligned}\mathbf{M}\omega &= \lambda\omega \\ \mu^T\mathbf{M} &= \lambda\mu^T\end{aligned}$$

The right eigenvector ω of \mathbf{M} is the stable age distribution or the long-term equilibrium states (Fig. C.2). The left eigenvector μ is the reproductive value; the contribution of age-class α to long-term population size (Fig. C.3; [125]).

I use the demographic parameters for each species to construct the population matrices \mathbf{M} and find the eigenvector ω associated with the dominant eigenvalue λ of each population. I then use the identified stable age distribution on the last time step to generate a vector of relative population sizes, which we'll use to determine the age structure with which to prime our BAU and intervention simulation: $\mathbf{N} = N_0 \times \frac{\mathbf{N}}{\sum \mathbf{N}}$. Stable age distributions for all five baleen whale species are shown in Figure C.2.

Scenarios with human-induced mortality

Eigenanalysis allows me to determine the stability conditions of the system. But I am concerned with the transitory dynamics of the population, and how these translate to contributions to the Carbon cycle and discounting of costs through time. I therefore run simulations where human-induced mortality occurs at the beginning of the simulation; remaining organisms then survive and reproduce based on Eq. 4.1. The following sections

describe the computational experiments and manipulation of parameters in each of them.

Source of mortality

As discussed before, whales face multiple sources of direct and indirect mortality, which determine the fate of a whale's carcass. For example, ship-whale collisions are a well-documented phenomenon in which the carcass often sinks. To capture this potential difference, I run two different mortality scenarios. One of them assumes that the whale is removed from the ocean and the Carbon in its body is no longer sequestered into the deep-sea sediments. The other scenario assumes a whale would follow the same fate as if it had died of natural causes and has a probability of sinking [111, 108]. I run factorial combinations between source of mortality and age at which mortality occurs. All scenarios assume a biomass-based density-dependent function, and initial population sizes reflect the estimates of current population size reported by Pershing et al., 2010 [108].

Initial population size

The previous experiment uses current population sizes to estimate the cost of human-induced mortality across two types of fates for the whale carcass. However, the forgone sequestration potential is influenced by population size, because a small population has a greater net sequestration potential than one that is already at carrying capacity. I run scenarios for the factorial combinations between initial population sizes and age classes at which a whale is removed from the population. I use ten initial population sizes (N_0), such that $\frac{N_0}{K} \in (0.1, 0.2, \dots, 0.9, 1)$. For each possible value of initial population size, I run a series of simulations where a single whale is removed from a single age class at the beginning of each simulation. For example, Gray whales have a life expectancy of 97 years. The population size experiment is thus made up of 970 independent model runs. This experiment assumes that whales removed do not sink and therefore do not sequester Carbon into deep-sea sediments.

Simulating business as usual BAU

Each experiment needs a business as usual scenario against which to compare the effect of mortality. I run the required simulations to provide the business as usual (BAU) for each of the scenarios above. These BAU scenarios are identical to the mortality scenarios, absent the human-induced mortality. An example of BAU population trajectories for the density-dependence experiment are shown in figure C.4. A summary of the experiments is shown in Table 4.3.

I run all simulations in the BAU and mortality scenarios out to 2050, the last year for the Inter-agency Working Group on the Social Cost of Green House Gases reports the annual social cost of Carbon [124]. At each time step I calculate population size, biomass, and the contributions to the three Carbon processes (Eqs. 4.1-4.3). I can calculate the present value of Carbon sequestration (Eq. 4.4) of each treatment scenario and compare it to its corresponding BAU to obtain the forgone Carbon sequestration attributed to the intervention.

Table 4.3: Summary of experiments (rows), scenarios (columns), and simulations (cells) used to explore the costs of human-induced whale mortality. This protocol is applied to all five baleen whale species. Note that human-induced mortality is not present in the Business As Usual (BAU) column.

Experiment	BAU	Treatment
Mortality source	<ul style="list-style-type: none"> • Default parameters • 1 run 	Factorial combinations of: <ul style="list-style-type: none"> • Two mortality sources: harvesting and ship-whale collisions • Mortality at age $M_a \in (1, 2, \dots, \alpha - 1, \alpha)$ • $2 \times \alpha$ simulations
Population size	<ul style="list-style-type: none"> • Initial population sizes of $\frac{N_0}{K} \in (0.1, 0.2, \dots, 0.9, 1)$ • No human-induced mortality • 10 simulations 	Factorial combinations of: <ul style="list-style-type: none"> • $\frac{N_0}{K} \in (0.1, 0.2, \dots, 0.9, 1)$ • Mortality at age $M_a \in (1, 2, \dots, \alpha - 1, \alpha)$ • $10 \times \alpha$ simulations

Average value of a whale

The above scenarios independently manipulate a parameter of interest. The rationale behind running these is that we have a reason to believe the implied Carbon cost of removing a whale from a population will depend on population status, source of mortality, and the age of the whale removed. But given current population sizes, what is the cost of human-induced whale mortality? Using the current population estimates reported by Pershing *et al.* [108], I run 1000 simulations for each species. At the beginning of each simulation I remove one whale from a randomly-sampled age class. The probability of sampling a whale from an age class is proportional to the number of organisms in it. All simulations are run to year 2050 and assume the removal of a whale's body from the system.

4.3 Results

Present-day whale populations of the five baleen whale species studied here store 1.12×10^6 tonnes of Carbon in their body, stimulate the storage of 89.2 tonnes through nutrient transport and fertilization, and sequester 34.4×10^3 tonnes annually. If allowed to recover, these values would increase to 1.46×10^6 tonnes of C stored in biomass, 115 tonnes via productivity stimulation, and 44.4×10^3 tonnes per year by 2050 (Fig C.5). Importantly, if the whale-fall process remains undisturbed, it would sequester a total of 1.13×10^6 tonnes of Carbon by 2050. The following results explore how human-induced whale mortality causes deviations from these baselines.

We are concerned with how the cost of human-induced whale mortality changes across sources of mortality (and fate of the deceased whale) and initial population sizes. Importantly, we also explore how the cost varies with age of the deceased whale, and decompose the portion of the cost that comes from in-body Carbon of the deceased whale and the

forgone growth and reproduction potential. These processes operate in the same way across species, and differences are driven by changes in species-specific whale longevity, fecundity, survival rates, and mass-at-age. To maintain the focus on the parameters and processes of interest, I present results using Gray whales (*Eschrichtius robustus*) as an example.

4.3.1 Cost by source of mortality and fate of whale carcass

The implied Carbon cost of human-induced whale mortality for gray whale species ranges between \$2,764 and \$23,352 per whale for ship strikes, and between \$3,220 and \$23,808 per harvested whale (Fig. 4.1A). The highest cost is attained when whales of age 81 are removed from the population. Mortality events that prevent a carcass from sinking can be between \$294 to \$455 costlier, depending on the whale's age (Fig. 4.1B). Note that these difference between scenarios is driven by changes in the sequestration term in the Carbon dynamics (Fig. 4.1C; with losses of in-body Carbon and productivity stimulation being constant across mortality scenarios). This result already hints at the relative contribution of in-body Carbon vs the Carbon sequestration that arises from demographic and ecological dynamics.

The age at which a whale is removed produces different population recovery pathways, which largely govern the cost estimates. The highest immediate cost occurs for a whale of terminal age being harvested (Right-side panel on Fig. 4.2). The intuition behind this is that, had that whale not been extracted, it would have certainly died (Note that $M(\alpha, \alpha) = 0$), sequestering a portion of its biomass into deep-sea sediments. However, a whale of this age does not contribute to population growth via reproduction, and the population quickly rebounds and converges with the BAU scenario of no mortality. On the other hand, removing a whale of age 1 has a smaller impact on the first year (it

contains little Carbon in it's body), but results results in a greater long-term reduction in Carbon sequestration.

These results highlight the importance of fate of the whale's carcass in the estimation of the Carbon value of whales, but also shed light on the relative value of in-body Carbon vs. the Carbon that accrues due to ecological and demographic processes. The Carbon stored in a whale's body only accounts for \$589 to \$911 per whale, representing 3.4-28.3% of the total implied Carbon costs (Fig. 4.3). In other words, the main Carbon cost of whaling is due to the ensuing population dynamics, not due to the Carbon emitted from the harvested whale. This highlights the important role that population dynamics play in the sequestration of whale Carbon

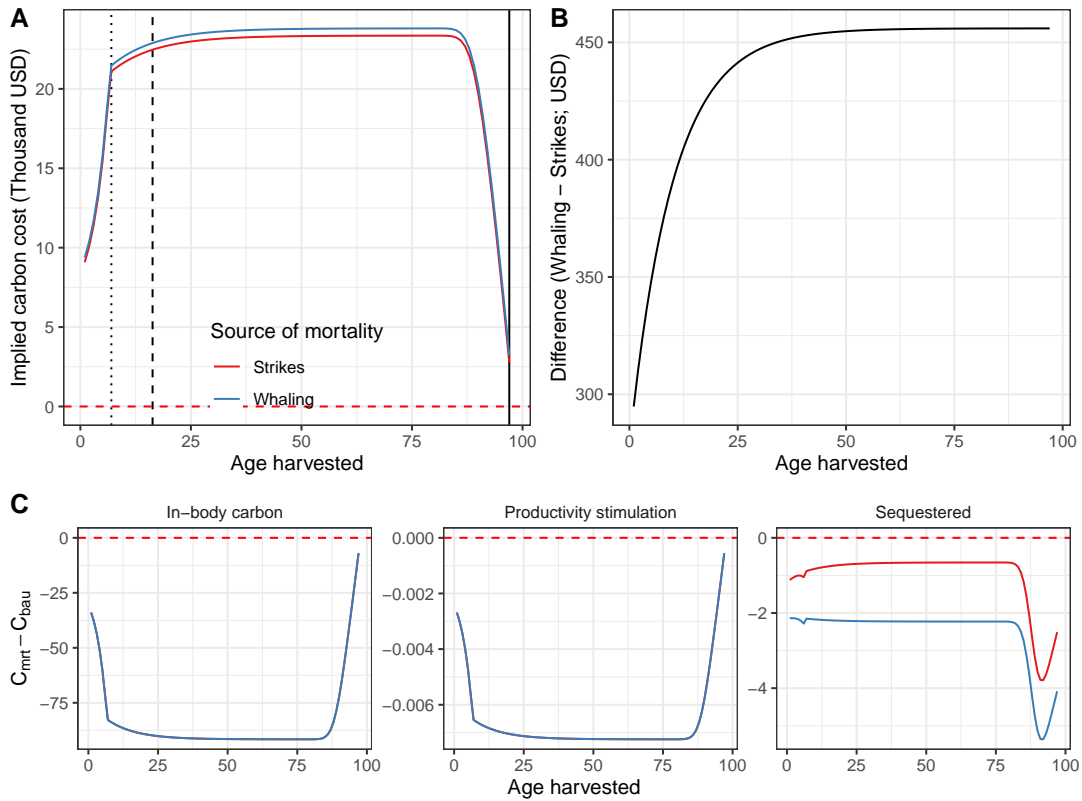


Figure 4.1: Fate of removed whales determine cost. A) Implied costs (y-axis) of whale mortality due to harvesting (blue) or shipstrikes (red) across age-ranges. Panel B shows the difference between the red and blue lines in panel A. Panel C) shows the differences in Carbon contributions (y-axis) for a whale harvested at a given age (x-axis) for the three different contribution pathways. The difference is calculated as Carbon under the mortality scenario minus the Carbon under the BAU scenario. The dotted vertical line indicates the age at maturity (α_m), the dashed vertical line indicates $a_{m50} = a_0 + \frac{\ln(0.5)}{-k}$ the age at which organisms reach 50% of the theoretical maximum mass (m_∞) according to the von Bertalanfy weight-at-age relationship, and the solid vertical line shows the maximum age (α).

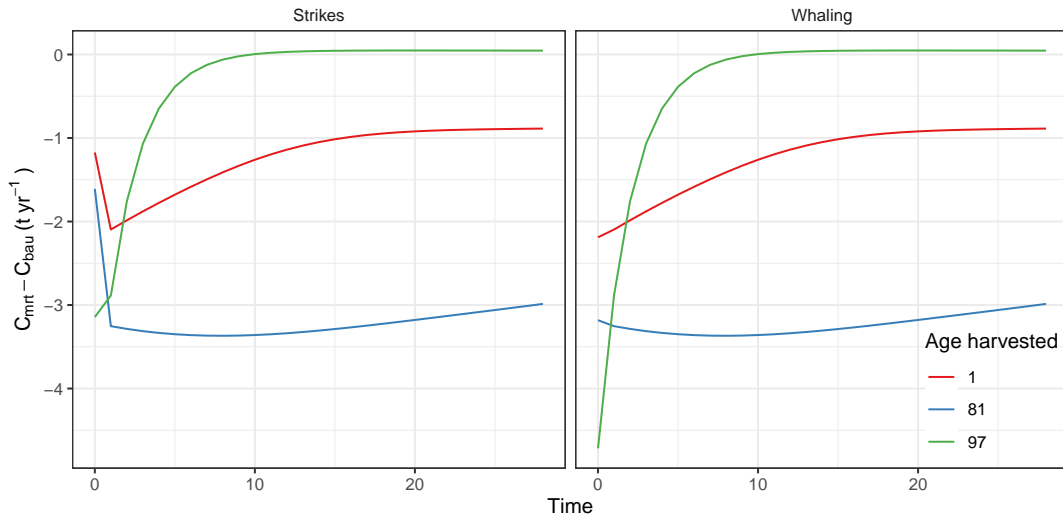


Figure 4.2: Difference in Carbon sequestration pathways ($C_{mrt} - C_{bau}$) for two selected runs under each mortality source scenario. Positive values indicate greater sequestration under the given mortality scenario, relative to BAU. The simulations were selected to show the pathway of simulations where a whale is removed from the first age class ($\alpha = 1$) and the terminal age class ($\alpha = 97$). The panel on the left shows a scenario where the whale sinks, the panel on the right shows a scenario where the whale does not sink.

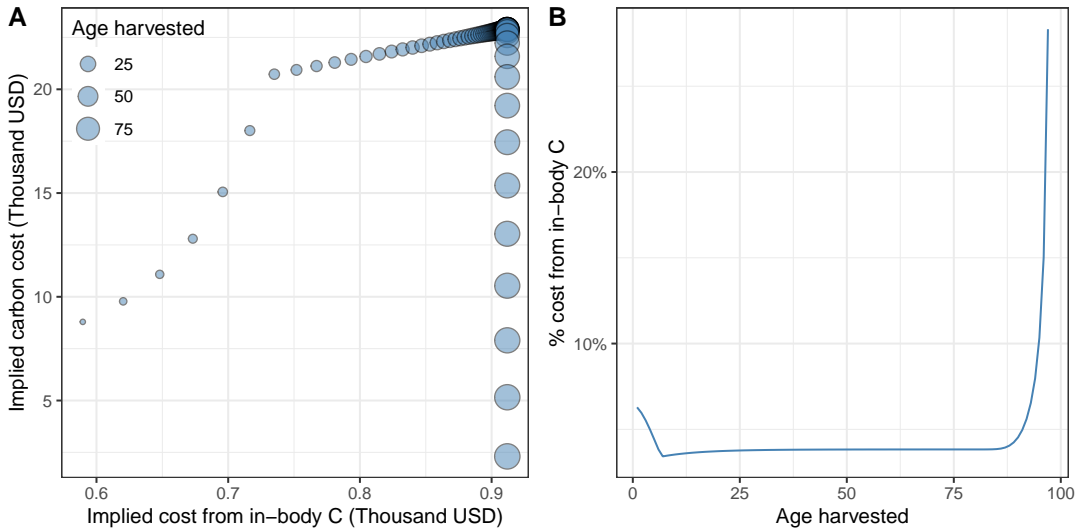


Figure 4.3: Comparison of value of somatic growth and reproductive growth. Panel A) shows the implied Carbon cost for Carbon stored in a whale’s body (x-axis) and the inter-generational Carbon sequestration potential due to reproduction and growth (y-axis), exclusive of in-body Carbon of the harvested whale for each harvested age (marker size). Panel B shows the in-body Carbon value of a harvested whale as a percent of the total value of a whale (y-axis).

4.3.2 Cost across population sizes

The initial population size from which a whale is removed also affects the recovery pathway, and therefore the cost of losing a whale. The implied cost of a gray whale ranges between \$1,505 to \$29,767 per whale, depending on its age and the number of individuals in the population (Fig 4.4). The costs are greater for populations with low population status, because removal of an individual induces a lag in the recovery of the population. However, note that the age of the costliest whale also changes depending on the initial population size.

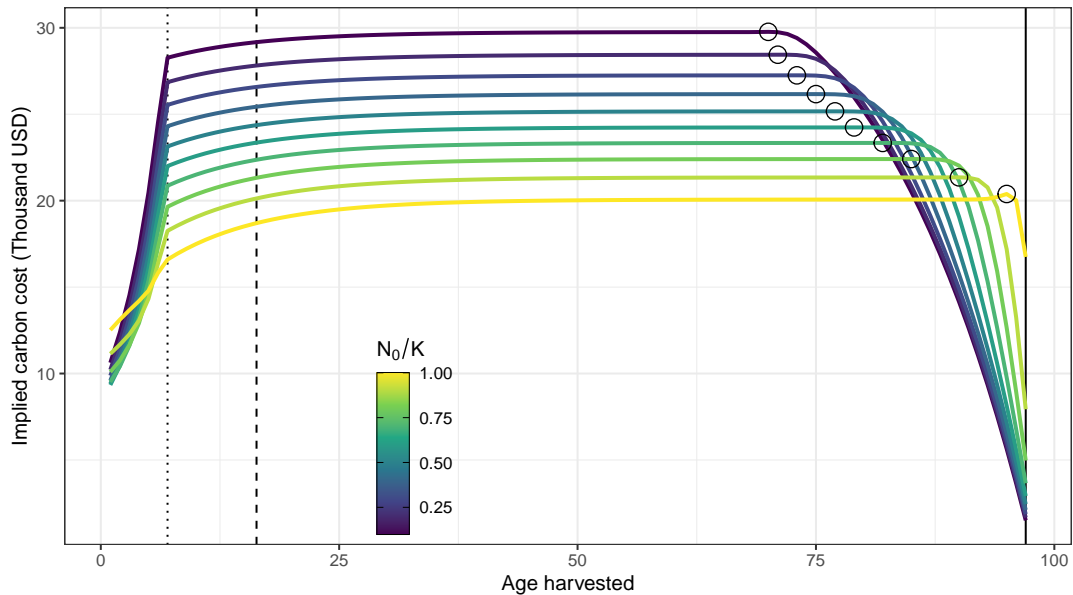


Figure 4.4: Implied costs (y-axis) for ten different initial population sizes (colors) across all possible age-classes (x-axis). The circle markers indicate the highest value along each line; the age at which costs are largest for a given initial population size. The dotted vertical line indicates the age at maturity (α_m), the dashed vertical line indicates $a_{m50} = a_0 + \frac{\ln(0.5)}{-k}$ the age at which organisms reach 50% of the theoretical maximum mass (m_∞) according to the von Bertalanfy weight-at-age relationship, and the solid vertical line shows the maximum age (α).

4.3.3 Average value of a whale

The previous sections explored the role of source of mortality and fate of whale carcass, initial population size, and age at which a whale is removed from the population. But how do these translate to possible human-induced mortalities experienced by present-day whale populations? By simulating random human-induced mortalities for all five baleen whale species, I find that the average Carbon cost lies between $\$3,820 \pm 1,440$ (M \pm SD for Minke whales *Balaenoptera acutorostrata*) and $\$51,700 \pm 16,000$ (M \pm SD for Fin whales *Balaenoptera physalus*; Fig 4.5). Minke whales are relatively smaller ($m_\infty = 6$ tonnes), and their estimated present-day population size is around 80% of it's carrying capacity (See Fig C.4 and Table 4.1). The combination of small body sizes and high abundances imply that the forgone Carbon sequestration potential from human-induced mortality in Minke whales are small, relative to other species. On the other hand, current estimates of Fin whale populations indicate they are around 14% of pre-whaling biomass, and adult Fin whales can weigh up to 64.5 tonnes. This simulations, however, only induce mortality in the first year of model-time and do not allow for density-dependent interactions between whale populations and sources of mortality, or for climate feed-backs between continued climate change and population carrying capacity.

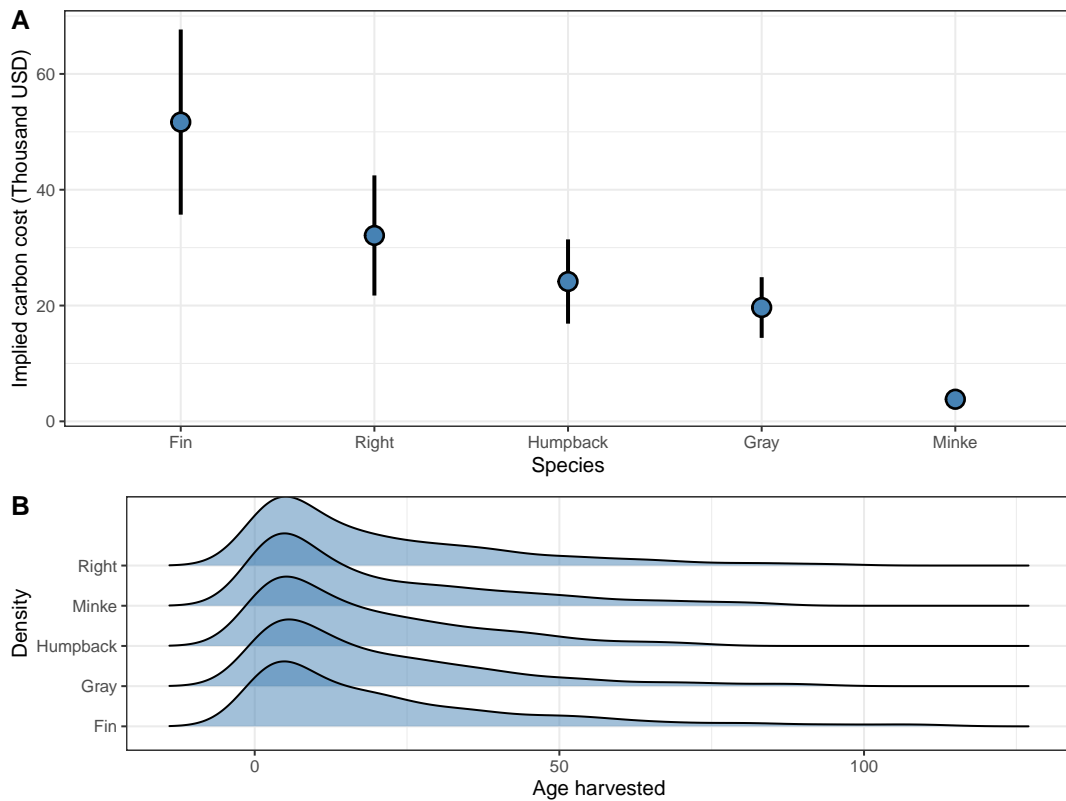


Figure 4.5: Implied Carbon cost of human-induced whale mortality for five species of baleen whales. Panel A) shows the mean (\pm SD) implied Carbon cost resulting from 1000 simulations where one organism is randomly removed from the population. The age at which an organism is removed is proportional to the age-class-specific abundance. Panel B) shows the kernel density distribution (using a bandwidth of 5 years) of ages at which mortality is induced by species.

4.4 Discussion and Conclusions

My work produces two important findings that can help guide whale conservation policies that seek to leverage their Carbon sequestration potential. The first one pertains to identifying the processes that contribute the most to Carbon sequestration, and the second one to the demographic characteristics that determine the sequestration potential. Most of the Carbon value of a whale is determined by its contributions to population dynamics, and less by the Carbon stored in its body. This important result highlights that the value of ecological dynamics is greater than that of the carbon stored in the removed organism. It follows, then, that it is the population status and demographic characteristics of a species what will determine whales' role in the Carbon cycle.

The implied Carbon cost of human-induced whale mortality varies depending on the age at which a whale is removed from the population. But a general pattern prevails: there is a sharp discontinuity at the age of maturity. After this age, adult whales are sexually mature and therefore contribute to the Carbon cycle not only by somatic growth, but also by producing offspring that in turn also accumulate Carbon and stimulate productivity. Organisms in the terminal age class only contribute to the Carbon cycle via sequestration into deep-sea sediments. This point reiterates the finding that a whale's value comes from the dynamics, not the Carbon stored in its body.

My estimates suggest that present-day whale populations of five baleen whale species store 1.12×10^6 tonnes of Carbon in their body, stimulate the storage of 89.2 tonnes through nutrient transport and fertilization, and sequester 34.4×10^3 tonnes annually. Previous estimates of a whales' contributions to the Carbon cycle suggest that recovered whale populations could help sequester an additional 1.6×10^5 tonnes of Carbon per year [108], but current recovery rates indicate that it would take at least two centuries before attaining such numbers C.1, which become less relevant once their value is discounted.

These values are modest compared to other coastal and marine Carbon sinks. For example, mangrove forests in the Everglades National Park have been estimated to store 48.47×10^6 tonnes of Carbon [126]. Similarly, seagrass meadows world wide store between 4.2×10^9 and 8.4×10^9 tones [127], and global deep sea sediments store around $2,322 \times 10^9$ tonnes of Carbon in the first meter of sediment [128]. The value and contribution of whales to the carbon cycle is modest when compared to other nature-based solutions for carbon sequestration in the oceans, but can nonetheless be used when estimating the cost of direct and indirect mortality that arises from economic activities, such as whaling and ship strikes.

A moratorium on whaling was implemented in 1985, which significantly reduced the number of whales caught each year. However, data from the International Whaling Commission (IWC) show that contemporaneous (2010 - 2020 average) whaling harvests an average of 1,470 whales per year, and that most of the catch is comprised of Minke whales (Fig 4.6). These numbers are attributed to commercial and non-commercial catches by non-member nations, whales harvested under an "Aboriginal subsistence" provision, and sporadic reports of illegal catch by IWC member nations. A simple calculation combining the IWC catch data with our cost estimates indicates that the implied Carbon cost of whaling for Minke, Gray, Humpback, and Fin whales in 2020 was in the order of \$5.9 million USD. This cost is likely to be higher, because whaling operations don't randomly extract whales and likely focus on the extraction of larger organisms.

Some have proposed using philanthropic funds to buy an annual whaling quota, and estimate that per-whale profits to whalers range between \$13,000 and \$85,000 for Minke or Fin whales harvested, respectively [129]. In contrast, our estimates of the Carbon cost for these species are much lower, at $\$3,820 \pm 1,440$ for Minke whales and $\$51,700 \pm 16,000$ for Fin whales (Fig 4.5). This shows that the Carbon value of a whale alone would not cover the cost of buying a whaling quota, and that additional funding would

be required.

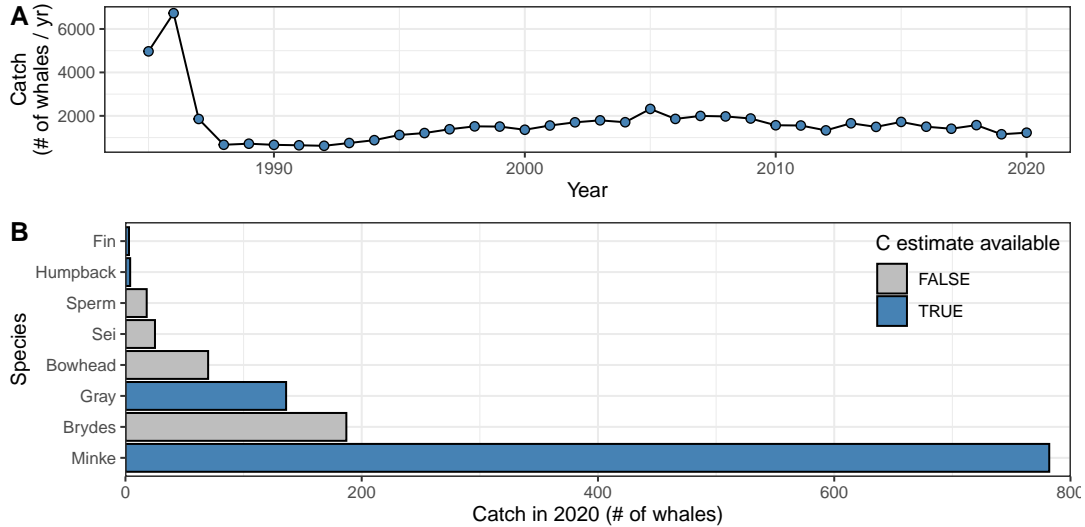


Figure 4.6: Whale catch from the International Whaling Commission. Panel A) shows a time series of catch since the moratorium on whaling came into place (1985). Panel B) shows the number of whales caught in 2020 for each species.

Another important source of whale mortality comes from non-extractive uses, such as ship strikes and entanglements with fishing gear. An exact quantification of the magnitude of these sources of mortalities is difficult. And while multiple groups agree on the general point of addressing these sources of mortality, the targets, policy interventions, and priorities remain idiosyncratic. One way to reduce mortality from ship strikes is by reducing the cruising speed of large vessels in areas of high whale density (*i.e.* via "Vessel Speed Reduction programs" [130]). An often-cited shortcoming of this measure is that it leads to sub-optimal cruising speeds, which increase engine load and results in increased emissions. An exact quantification of these is still lacking, but could be directly compared against the value of reducing speed (which reduces the likelihood of mortality due to ship strikes [130]).

Other policies that seek to reduce whale mortality include real-time spatio-temporal regulation of fishing and shipping activity [131]. However, these programs have only

approached the issue of whale mortality from the conservation angle and operate on a voluntary basis. Incorporating the Carbon value of whales may help guide the design of alternative policy instruments. One possible approach would be to link whale conservation with existing nature-based climate change mitigation strategies. For example, the United Nations REDD+ initiative seeks to finance conservation of Carbon-capturing ecosystems [132]. While this program focuses on reducing deforestation, there is opportunity to incorporate other forms of nature-based Carbon storage to it, or to develop alternative and more general systems that allow for the incorporation of whales.

Much of the concerns around nature-based solutions for climate change mitigation focus on the uncertainty around the accounting of Carbon stocks and flows [96]. I use the best-available estimates to parameterize a model, but further research can help reduce some of the sources of uncertainty. For instance, increasing the resolution of age-specific survival and fecundity [108] will undoubtedly modify the projected stable age distributions and reproductive value, which underpin the estimates of implied Carbon costs reported here. I use general estimates of in-body Carbon rates for all species, but the extent to which these differ across species been only briefly studied [113]. And while differences in average whale value are largely driven by whale age (*i.e.* size), increasing the precision of in-body Carbon estimates and species-specific demographic parameters will ultimately reduce variation between-species. Finally, further research on the fate of whale carcasses from ship strikes and entanglement with fishing gear can help discern cost differences between sources of mortality [111].

My results show modest contributions of whales to the Carbon cycle, and highlight the relative importance of ecological dynamics over in-body carbon storagewich has two broad implications. One is that whales could potentially be incorporated to the portfolio of nature-based solutions that seek to sequester Carbon into living biomass. The second is that it can provide help informing estimates of non-use values of whales [133].

Appendix A

Supplementary materials for Ch. 2

A.1 Supplementary methods

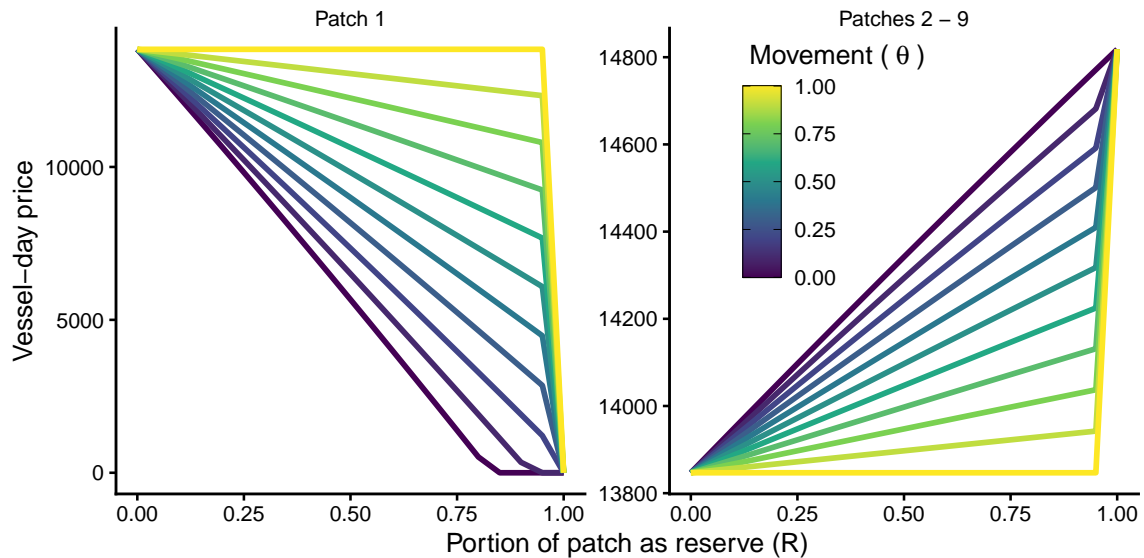
A.1.1 Balance on observables

We observe six characteristics for every vessel: flag, crew size, engine power, vessel length, tonnage capacity, and fishing hours within PNA waters in 2014. Figure A.5 shows the distribution of the numeric variables for each group of vessels. Table A.1 presents the mean and standard deviation of each observable, and table A.2 shows the composition of each group by flag. On average, displaced vessels have smaller crew sizes, more engine power, are larger than non-displaced vessels, and fished more in PNA waters during 2014. The largest relative difference is in terms of gross tonnage.

Supplementary Table A.1: Mean values on observable characteristics by vessel for displaced ($n = 64$), and non-displaced vessels ($n = 254$). Numbers in parentheses indicate standard deviation. The last column contains the difference in means (t-scores), with asterisks indicating significant differences as indicated by a two-tailed t-test (* $p < 0.1$; ** $p < 0.05$; *** $p < 0.01$).

Characteristic	Displaced	Non-displaced	Difference
Crew size (n)	26.38 (3.94)	30.46 (6.25)	4.08 (6.49) ***
Engine Power (KW)	2983.6 (558.76)	2559.89 (588.28)	-423.71 (-5.36) ***
Length (m)	74.23 (9.71)	68.97 (8.42)	-5.25 (-3.97) ***
PNA fishing in 2014 (hours)	667.57 (489.24)	529.33 (380.11)	-138.24 (-1.89) *
Tonnage (GT)	1718.14 (653.38)	1383.41 (533.56)	-334.73 (-3.79) ***

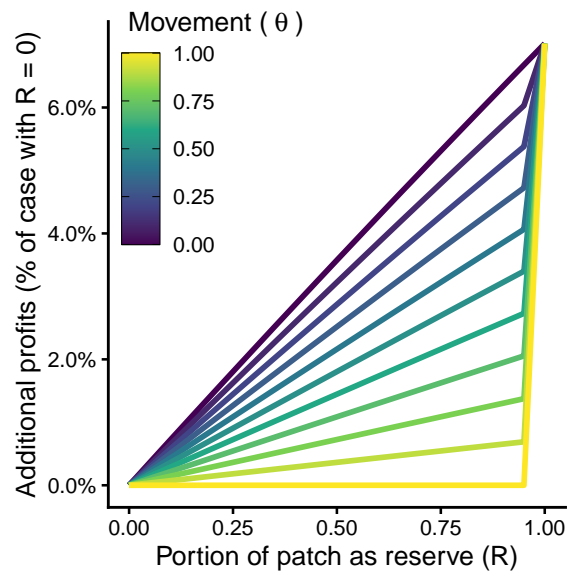
A.2 Supplementary figures



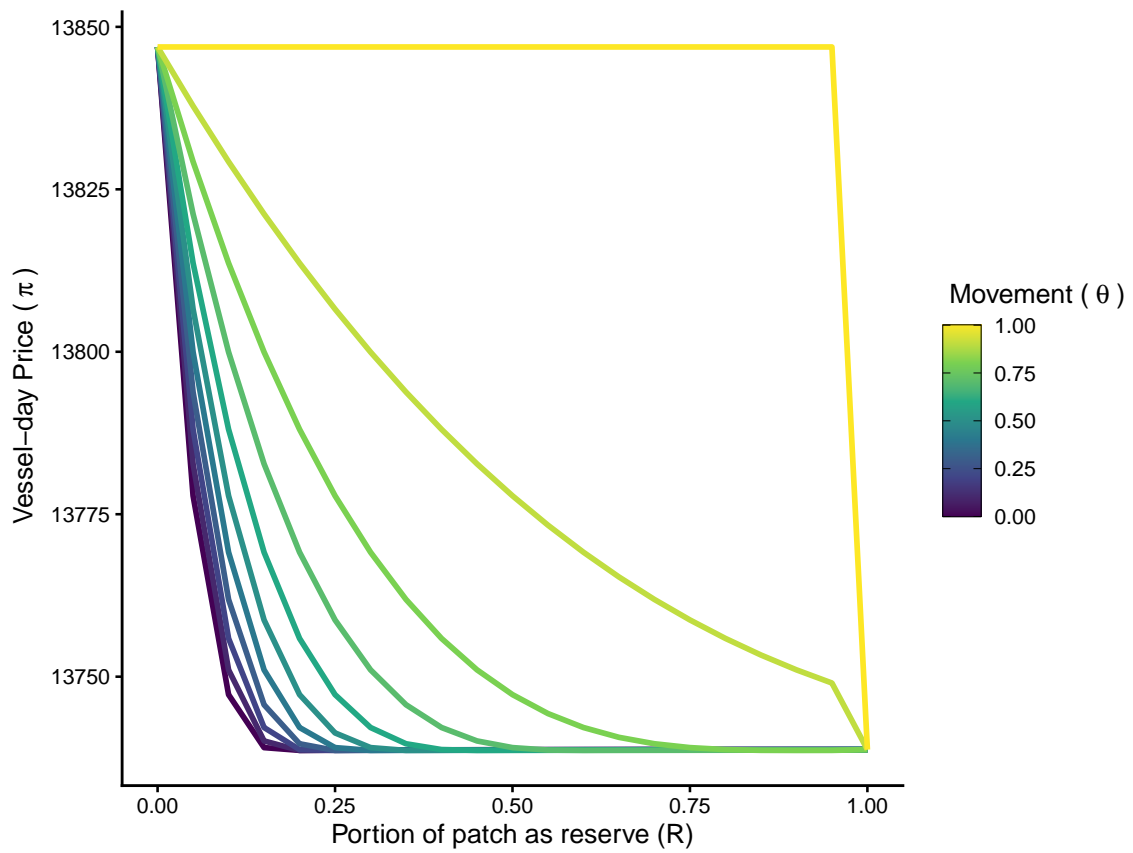
Supplementary Figure A.1: Vessel-day prices with conservation and no trading. Vessel-day prices (vertical axis) are shown for a combination of reserve sizes (R in the horizontal-axis) and different within-country movement (θ) for the country with spatial closure and other countries (left - right, respectively) when there is no trading.

Supplementary Table A.2: Proportion of vessel flags by group. Note that we do not observe the flag for two vessels (0.78%) in the non-displaced group.

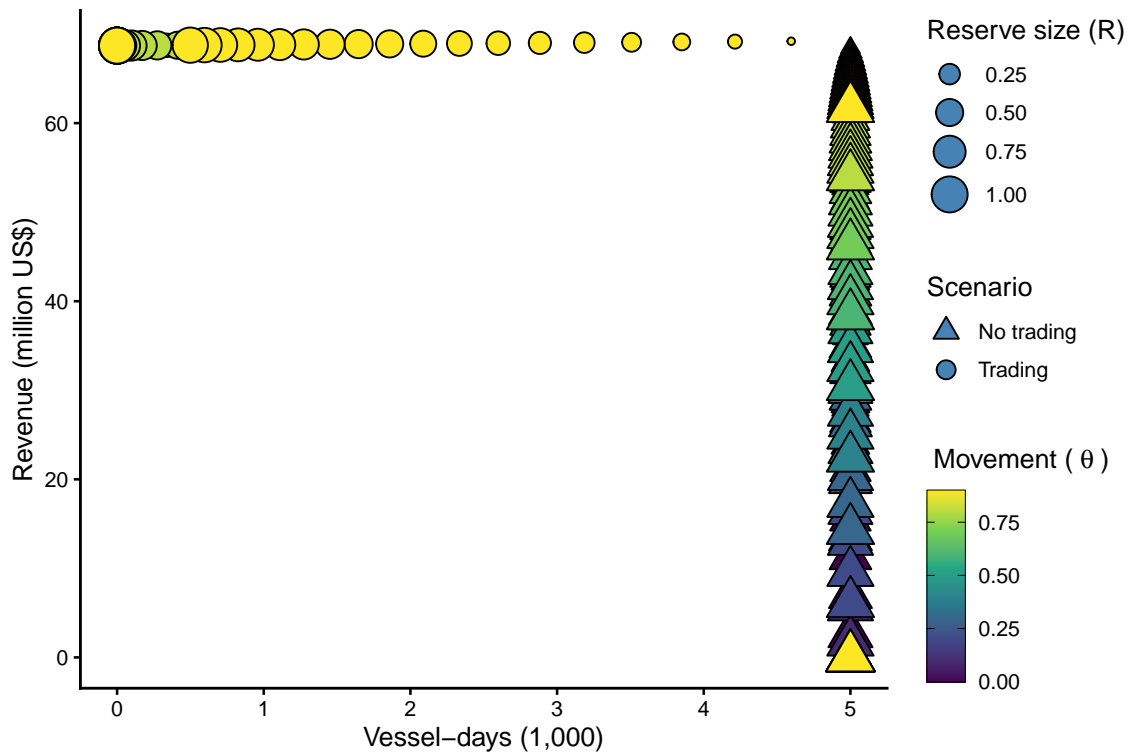
Flag	Non-displaced	Displaced
CHN	10.24	0.00
ECU	1.57	4.69
ESP	0.39	4.69
FSM	8.27	3.12
GTM	0.39	1.56
JPN	16.93	0.00
KIR	2.76	12.50
KOR	3.54	45.31
MEX	1.18	0.00
MHL	3.54	1.56
NIC	0.39	0.00
NRU	0.39	0.00
NZL	1.18	3.12
PAN	0.79	0.00
PHL	7.87	1.56
PNG	11.42	1.56
SLB	1.57	0.00
SLV	0.79	0.00
TWN	11.81	3.12
USA	12.20	17.19
VUT	1.97	0.00
Not reported	0.79	0.00
Total	100.00	100.00



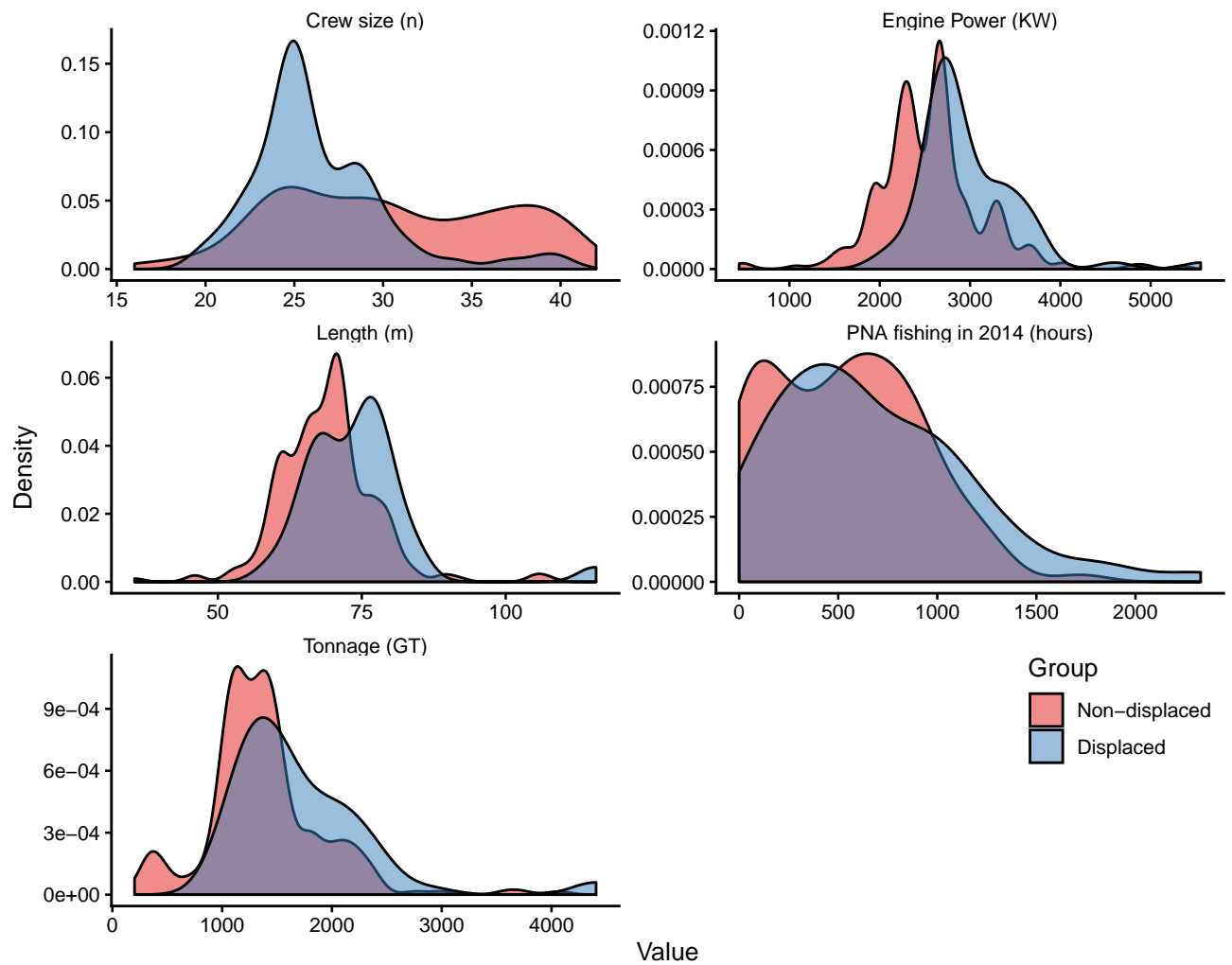
Supplementary Figure A.2: Change in revenues to non-conserving countries. Relative change in revenue for countries 2 - 9 (vertical axis) for a combination of reserve sizes (R in the horizontal-axis) and different within-country movement (θ) when there is no trading.



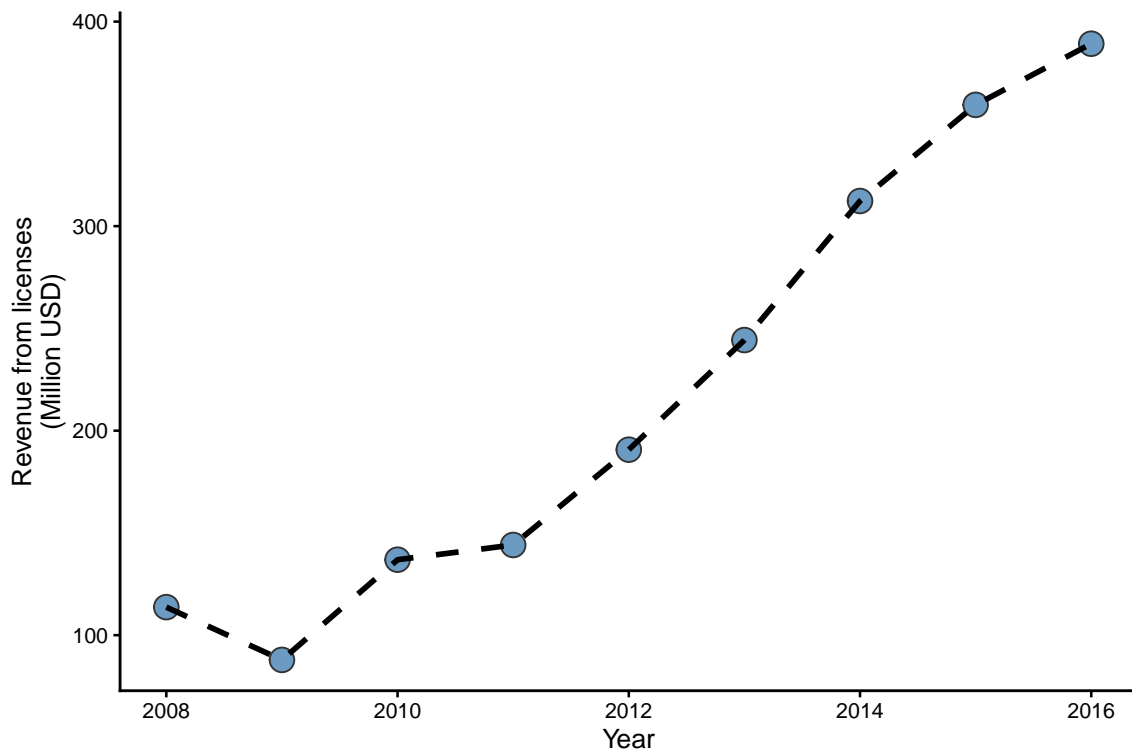
Supplementary Figure A.3: Vessel-day prices with conservation and trading. PNA-wide vessel-day prices (vertical axis) with trading, for a combination of reserve sizes (R in the horizontal-axis) and different within-country movement (θ).



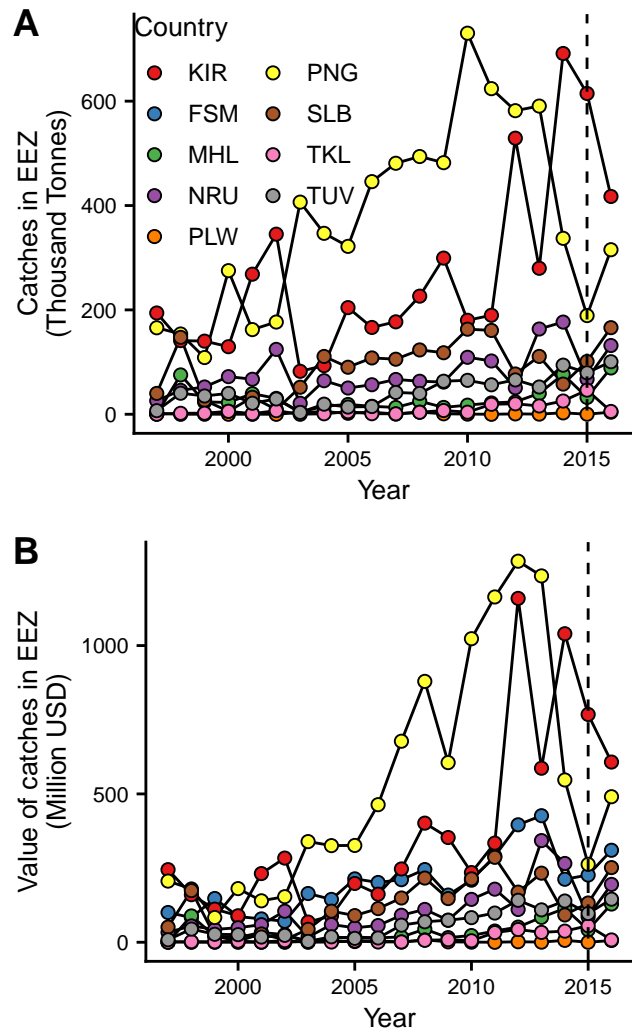
Supplementary Figure A.4: Effort and revenues to the conserving country with and without trading. Effort and revenue in Country 1 are shown for a combination of reserve sizes (R), different within-country movement (θ), and with and without trading. With trading, the relative drop in effort is always larger than the relative drop in revenue as R increases. The exact opposite relationship holds without trading: effort remains fixed as revenue declines with increasing R .



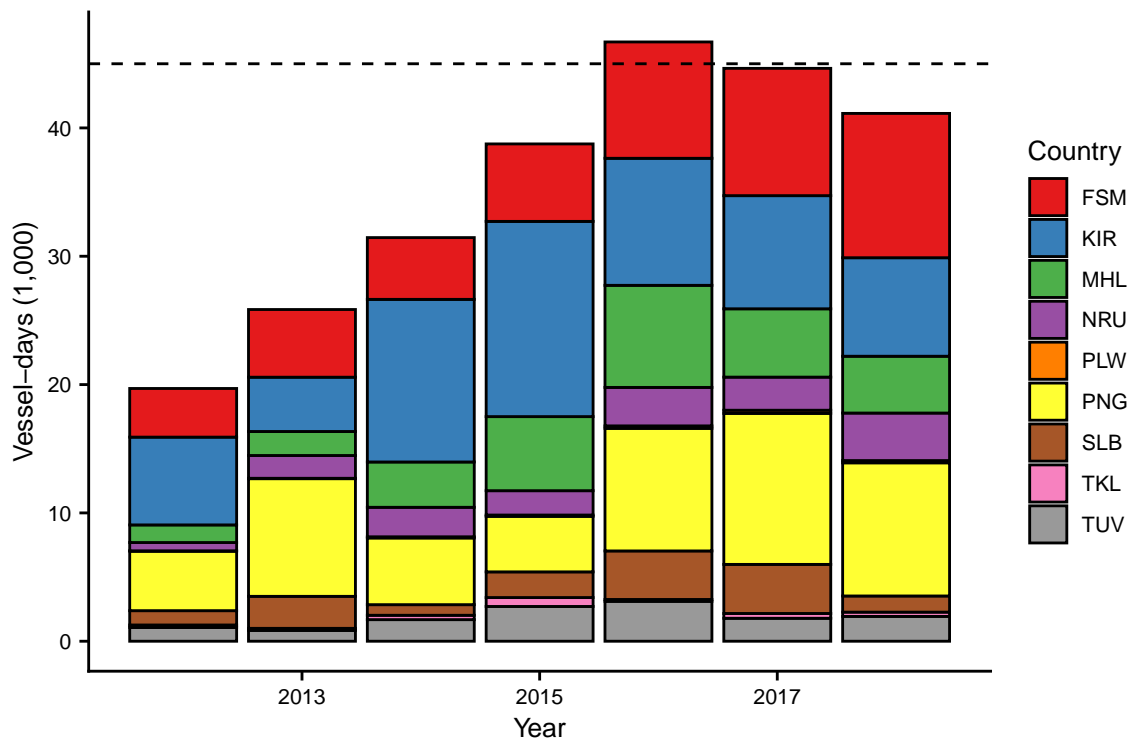
Supplementary Figure A.5: Vessel characteristics for 318 tuna purse seiners. Distribution of observable characteristics by vessel for displaced ($n = 64$), non-displaced vessels ($n = 254$).



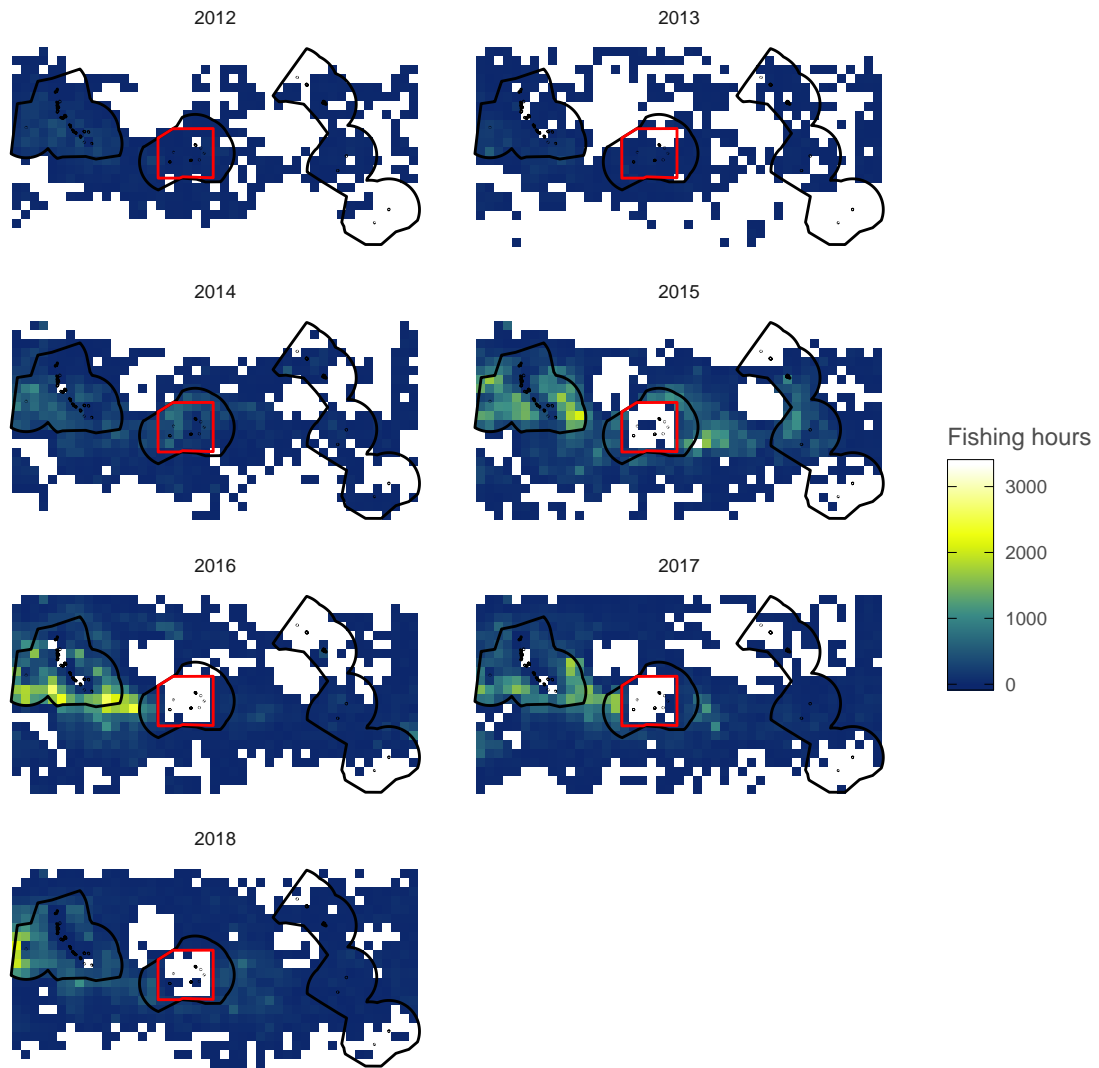
Supplementary Figure A.6: Total revenues for all PNA countries combined.



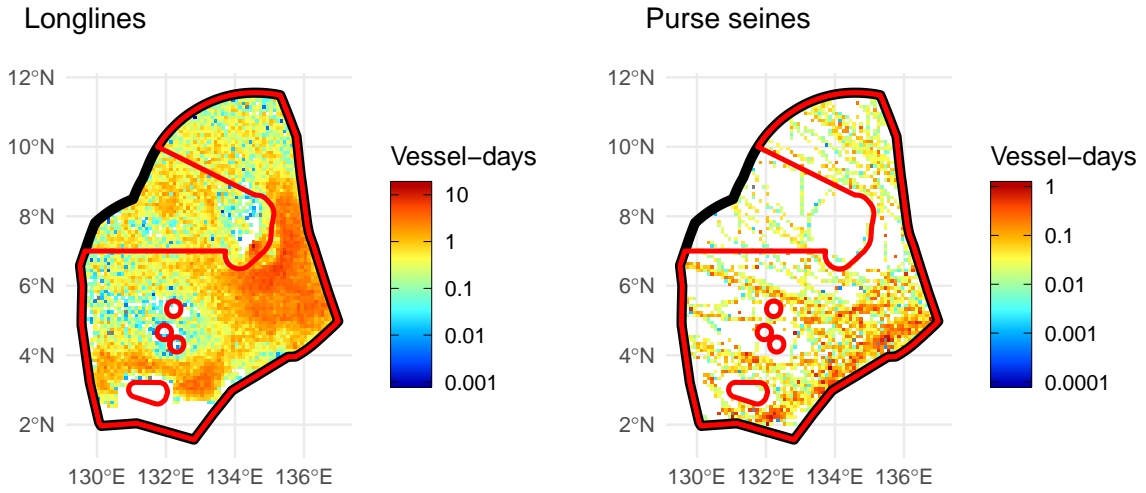
Supplementary Figure A.7: Financial indicators for PNA countries. A) Total annual purse seine catch by EEZ and, B) Total annual value of purse seine catch by EEZ. Vertical dashed line in both plots denotes implementation of PIPA.



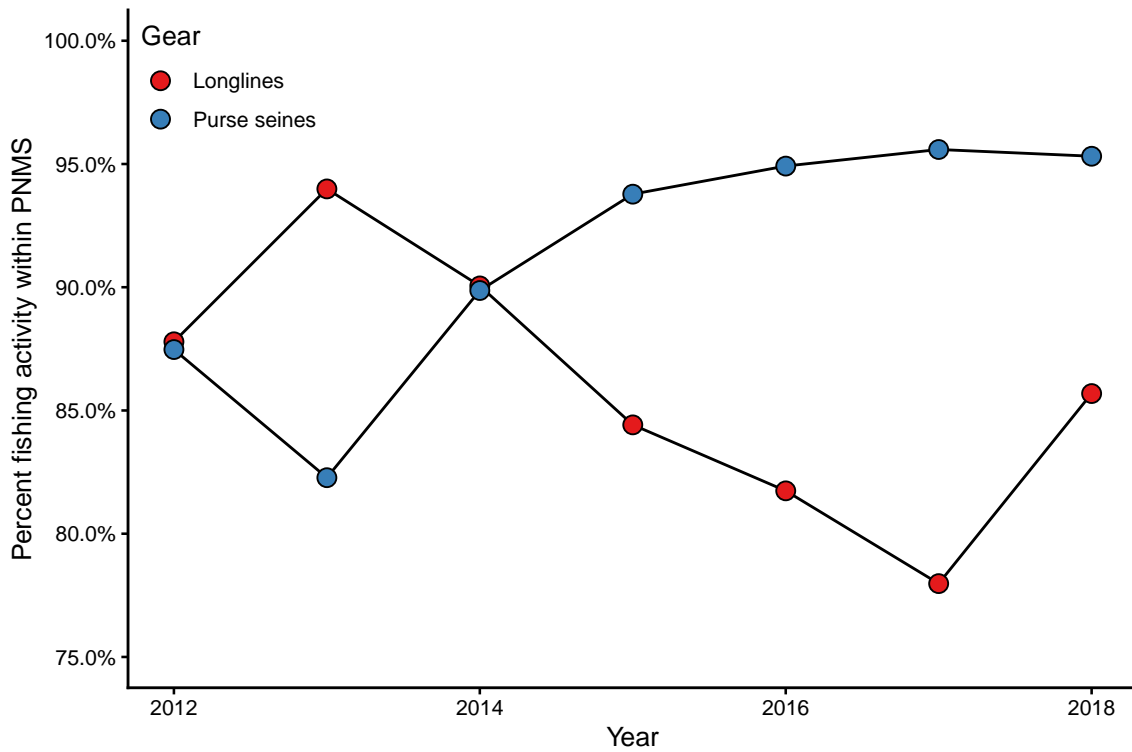
Supplementary Figure A.8: Annual country-level vessel-days for all PNA countries by 318 tuna purse seiners.



Supplementary Figure A.9: Annual fishing effort (hours) on a 1-degree grid around PIPA (red polygon) and Kiribati (black polygons).



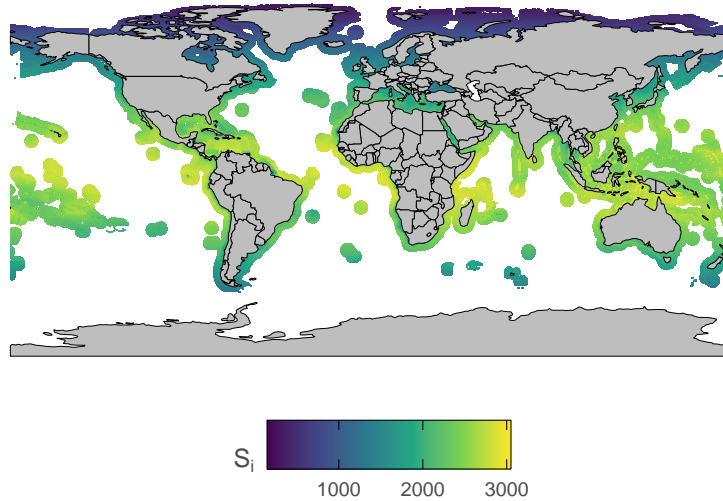
Supplementary Figure A.10: Longline and purse seine vessel-days in Palau during 2018 at a 0.5 degree resolution.



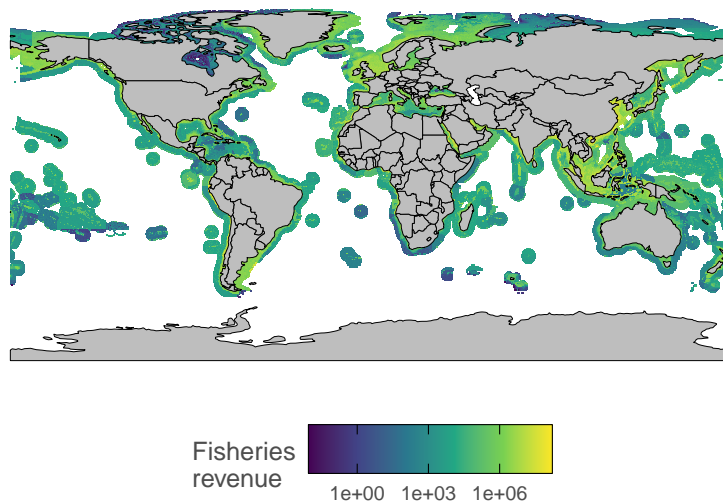
Supplementary Figure A.11: Time series of the annual proportion of longline and purse seine vessel-days within the proposed PNMS boundaries.

Appendix B

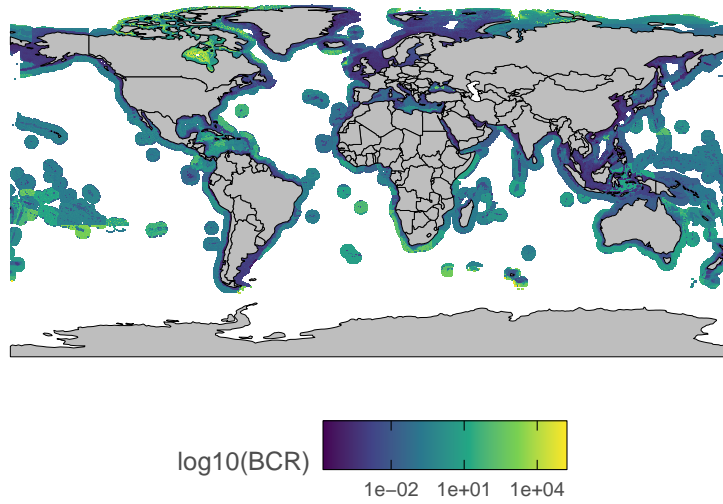
Supplementary materials for Ch. 3



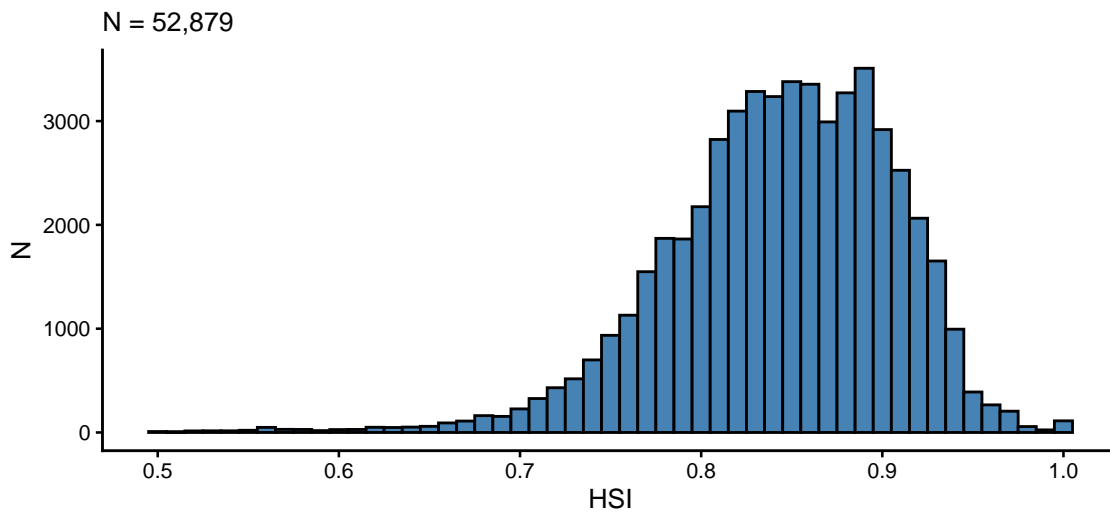
Supplementary Figure B.1: Construction of our measure of conservation benefits using a 0.5×0.5 grid cell. Panel A) shows the Habitat Suitability Index (HSI_i), panel B) shows the area (α_i in Km^2), and panel C) shows the conservation benefit ($Q_i = HSI_i \times \alpha_i$) for each grid cell.



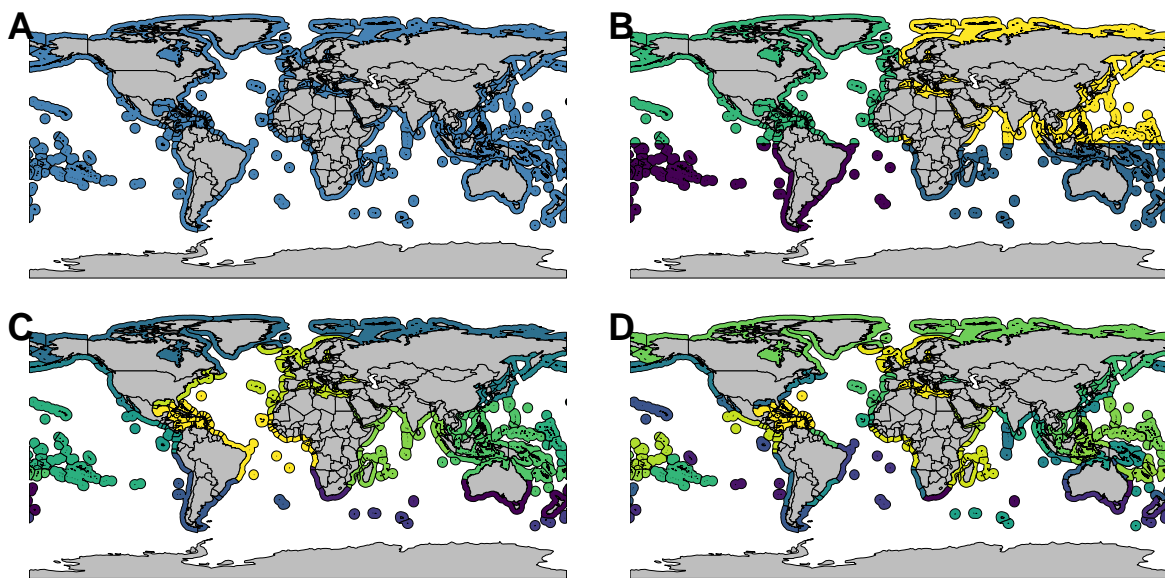
Supplementary Figure B.2: Median fisheries revenue (M USD; 2005 - 2015) along a 0.5×0.5 grid.



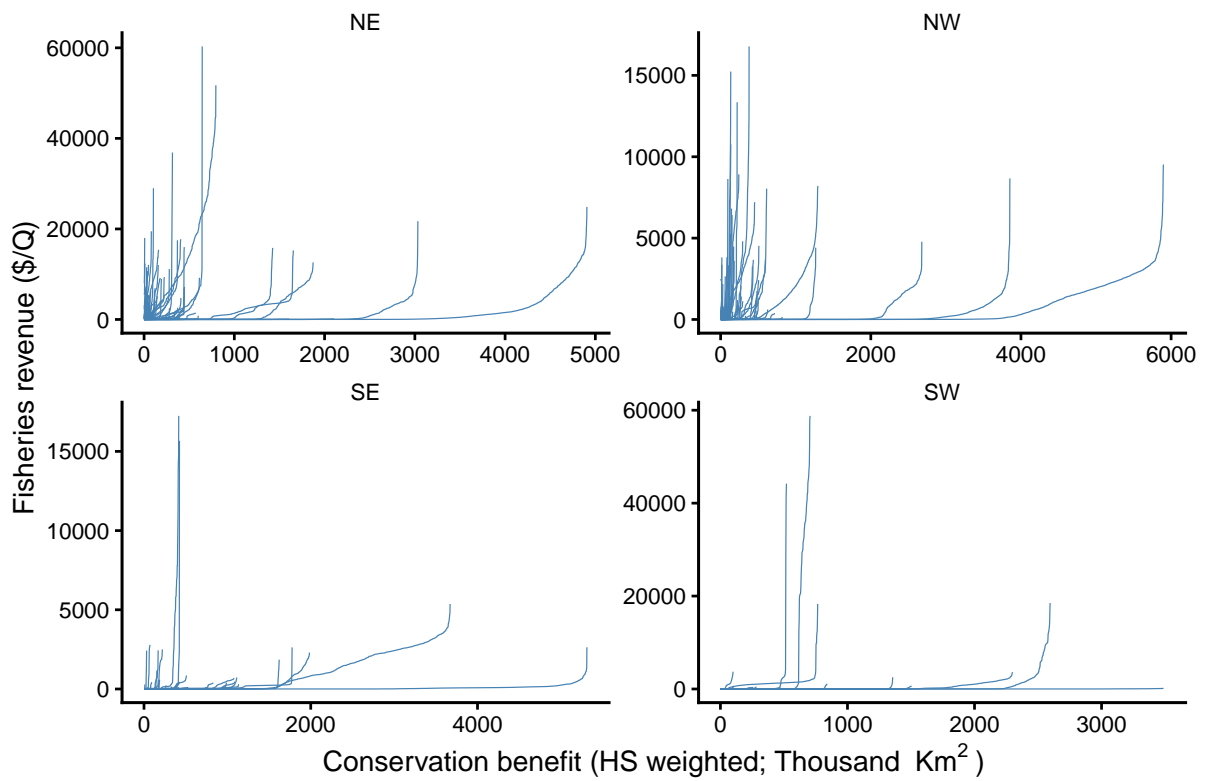
Supplementary Figure B.3: Benefit to cost ratio (log-10 transformed HSI-weighted KM2 / M USD) on a 0.5 x 0.5 grid cell.



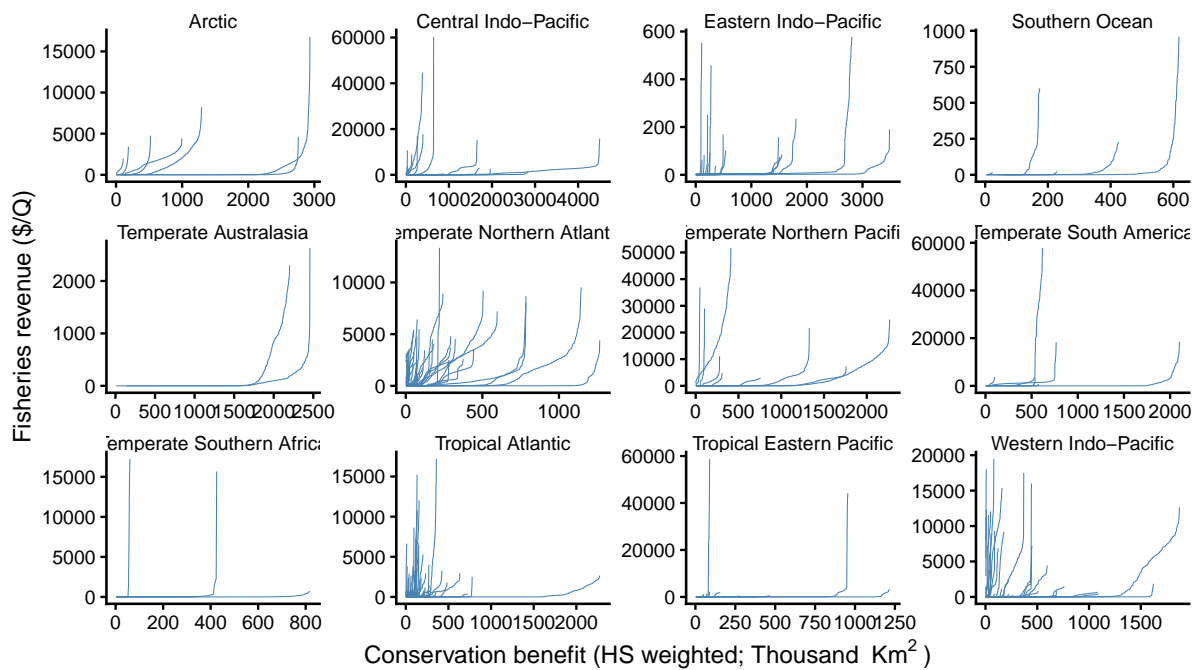
Supplementary Figure B.4: Histogram of habitat suitability index "HSI"



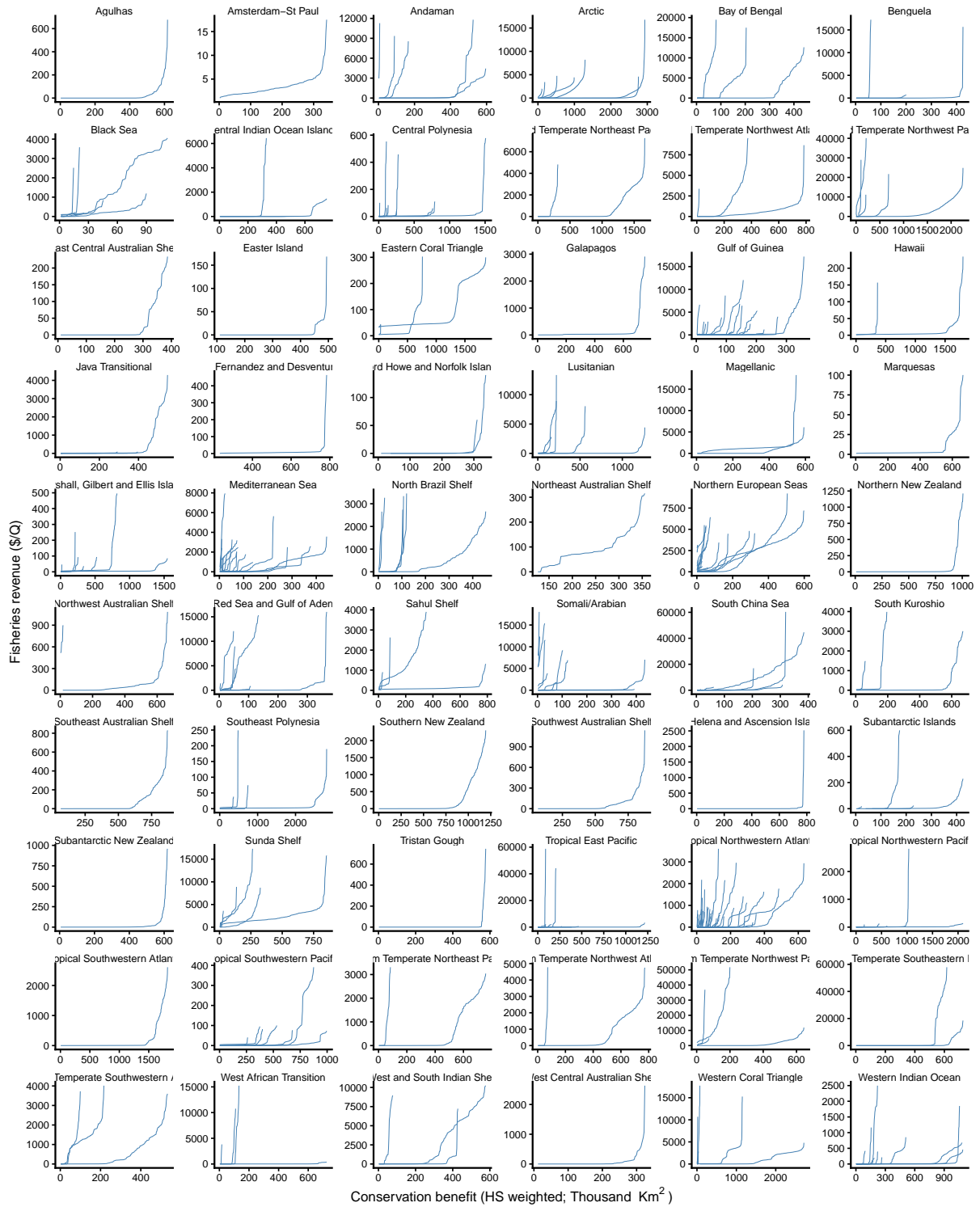
Supplementary Figure B.5: Spatial distribution of the four bubble policies intersected with the Exclusive Economic Zones of 186 coastal nations. A) Shows a global bubble policy, where all nations participate in a single market. B) Shows the oceans are divided into four market segments on the basis of geographic hemispheres. C) Shows the 12 biogeographic realms defined by Spalding et al., 2007, and D) shows the sub-division of realms into 60 provinces.



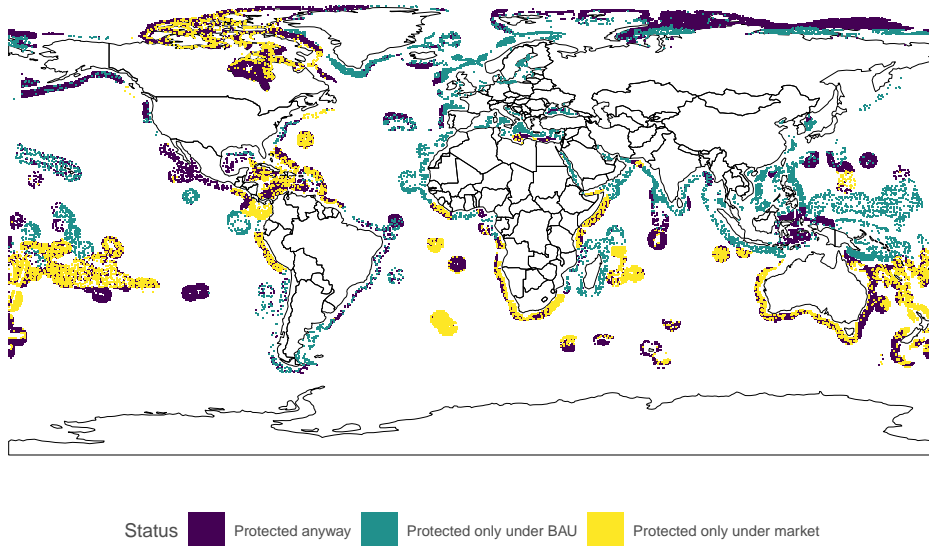
Supplementary Figure B.6: Conservation supply curves for nations across four hemispheres.



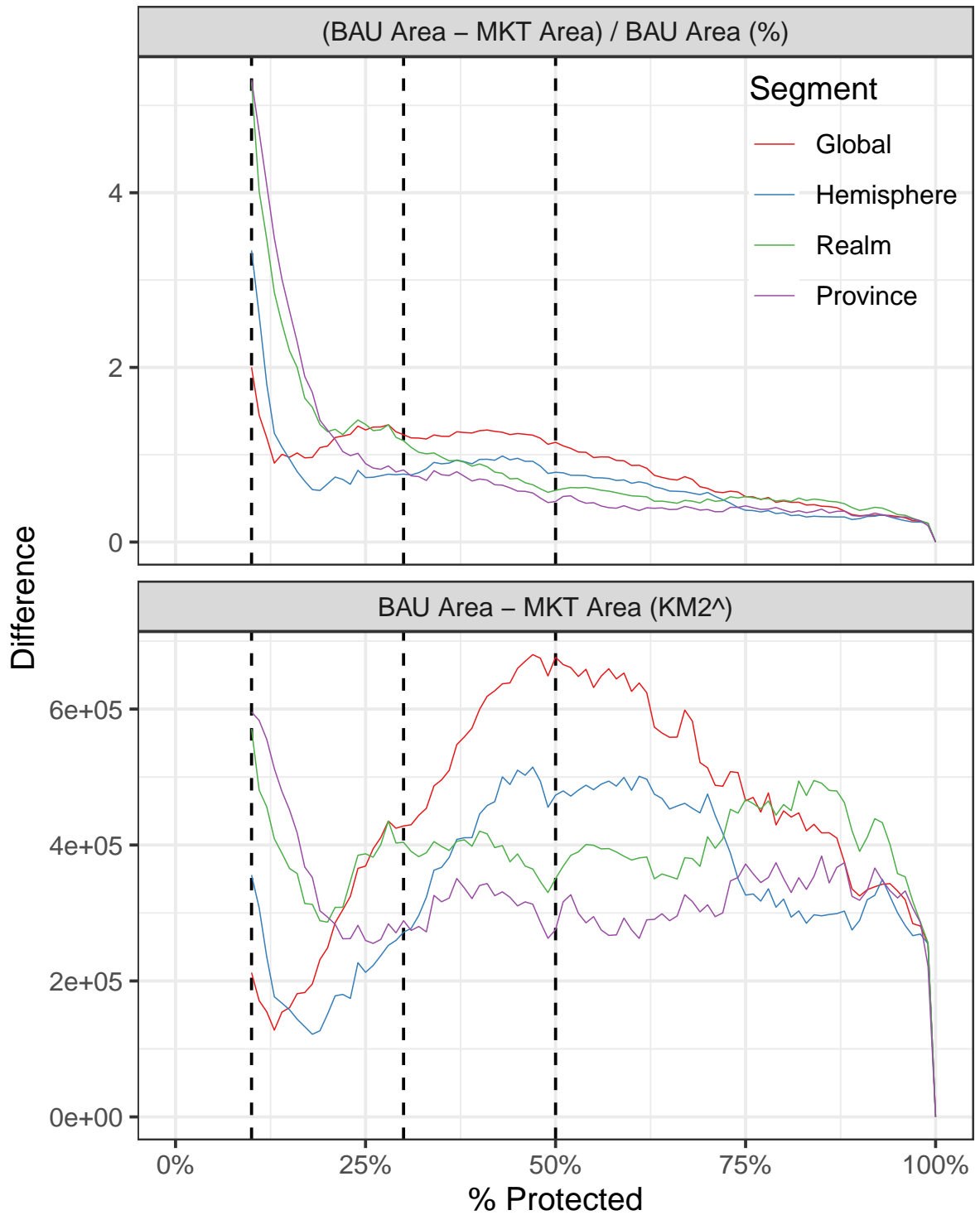
Supplementary Figure B.7: Conservation supply curves for nations across 12 biogeographic realms.



Supplementary Figure B.8: Conservation supply curves for nations across 60 biogeographic provinces.



Supplementary Figure B.9: A market-based approach relocates some Marine Protected Areas. Colors on the map indicate whether a grid cell is protected regardless of strategy, protected only under unilateral conservation, or protected only under a market (yellow).



Supplementary Figure B.10: Differences in surface area (y-axis) needed to meet a given conservation target (x-axis). The top panel shows change in area relative to BAU, and is represented as a percentage. The bottom panel shows the absolute difference. Each line shows a bubble policy.

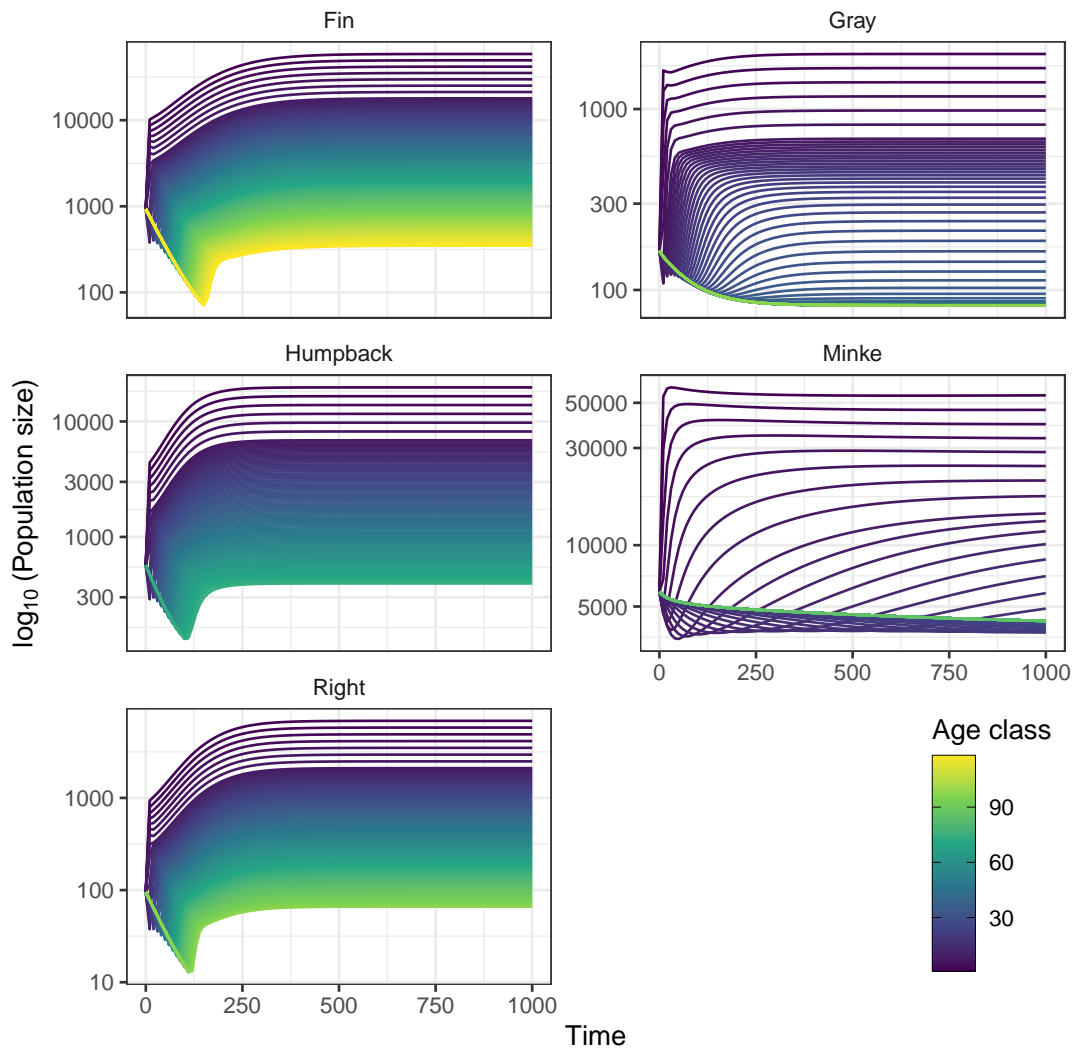
Appendix C

Supplementary materials for Ch. 4

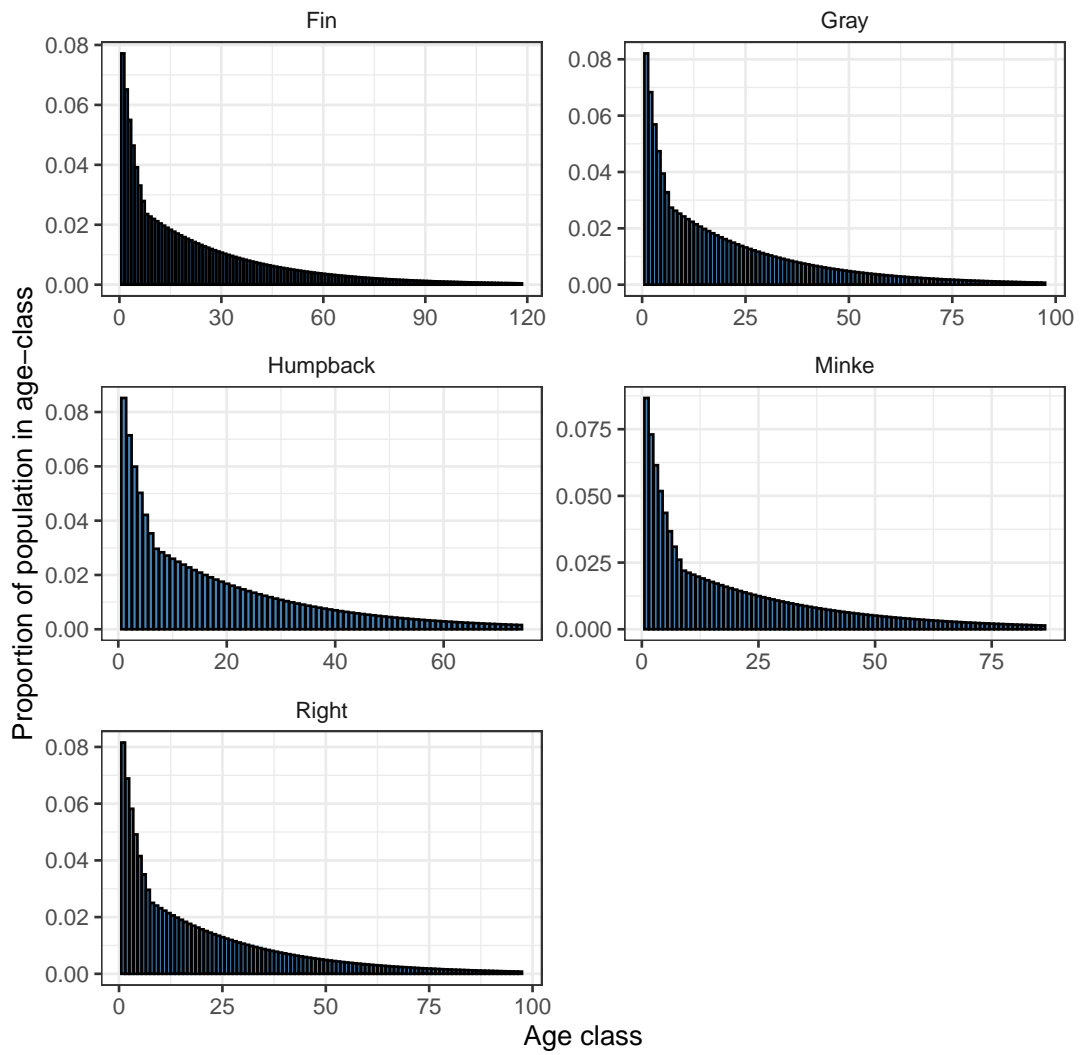
Using simulation to find the stable equilibrium is computationally expensive. For example, here I simulate each population over 1000 years. All populations exhibit the known oscillations in age distributions at the beginning of the simulation. After 1000 years, population structure is visually stable for all species (lines are horizontal) except Minke whales.

Supplementary Table C.1: Annual Social Cost of Carbon, 2020-2050 (in 2020 dollars per metric ton of CO₂) for three different discount rates. Model output by the Interagency Working Group reports values in five-year increments, they then use linear interpolation to fill-in missing years (Interagency Working Group, 2021).

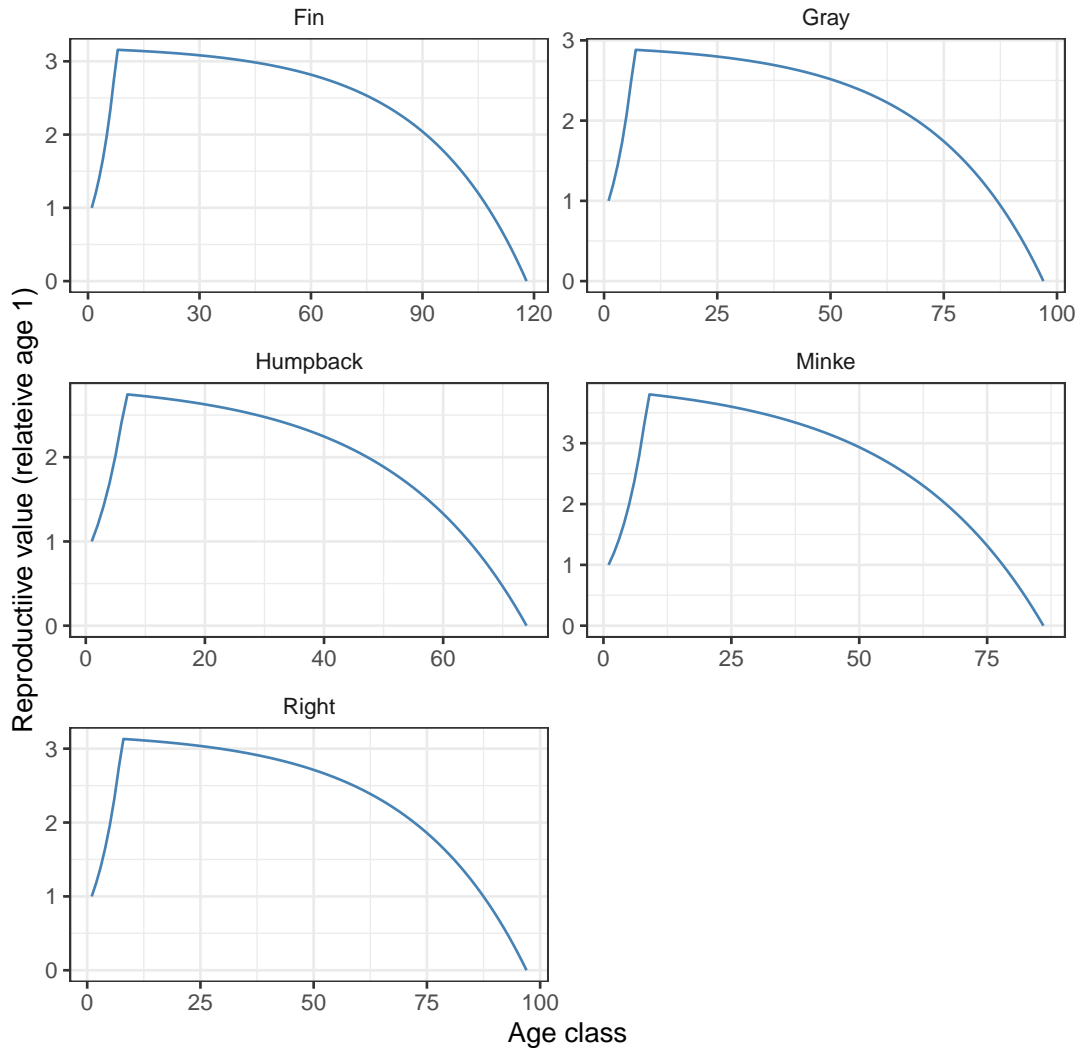
Year	5% Average	3% Average	2.5% Average
2020	14.48	51.08	76.42
2021	14.96	52.15	77.73
2022	15.45	53.22	79.03
2023	15.94	54.29	80.34
2024	16.43	55.35	81.64
2025	16.92	56.42	82.95
2026	17.41	57.49	84.26
2027	17.90	58.56	85.56
2028	18.39	59.63	86.87
2029	18.87	60.70	88.17
2030	19.36	61.76	89.48
2031	19.95	62.91	90.84
2032	20.53	64.05	92.21
2033	21.11	65.20	93.57
2034	21.70	66.34	94.93
2035	22.28	67.48	96.30
2036	22.86	68.63	97.66
2037	23.45	69.77	99.02
2038	24.03	70.92	100.39
2039	24.61	72.06	101.75
2040	25.20	73.20	103.11
2041	25.84	74.35	104.45
2042	26.49	75.50	105.78
2043	27.14	76.64	107.12
2044	27.78	77.79	108.46
2045	28.43	78.93	109.79
2046	29.08	80.08	111.13
2047	29.72	81.22	112.46
2048	30.37	82.37	113.80
2049	31.01	83.52	115.14
2050	31.66	84.66	116.47



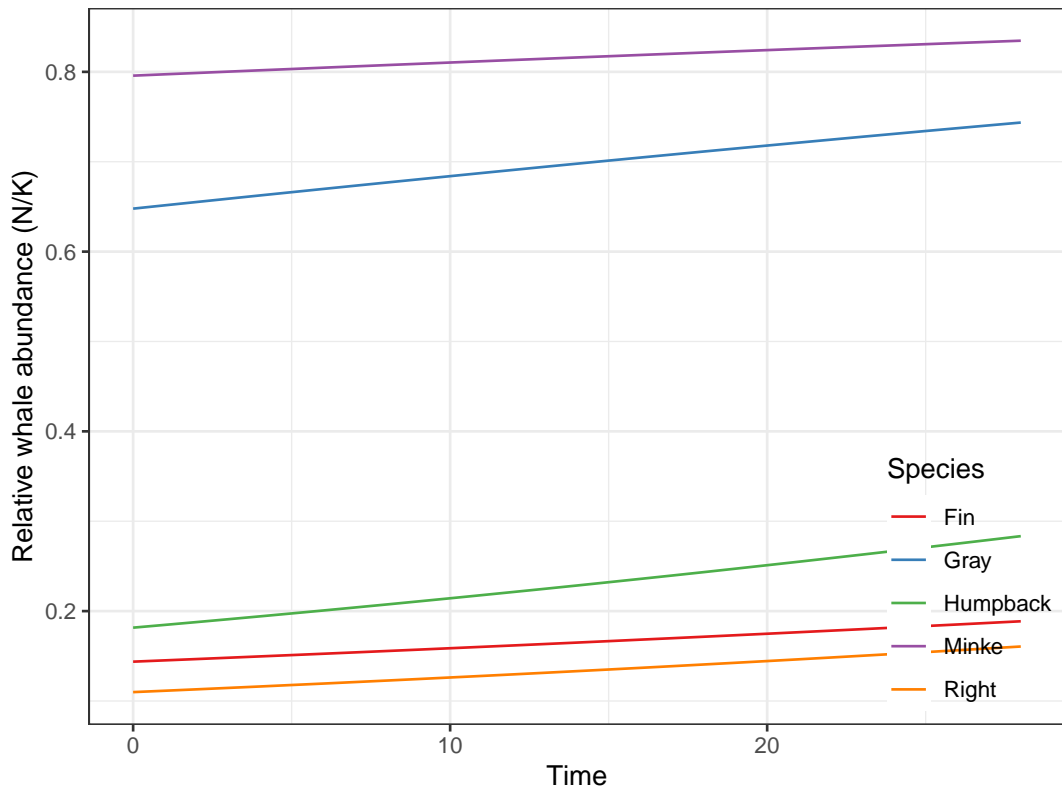
Supplementary Figure C.1: Age-specific population trajectories (y-axis) in time (x-axis) for five baleen whale species. Age structure becomes stable (slopes are parallel for across age classes). Note how Minke whales do not achieve stable age distribution.



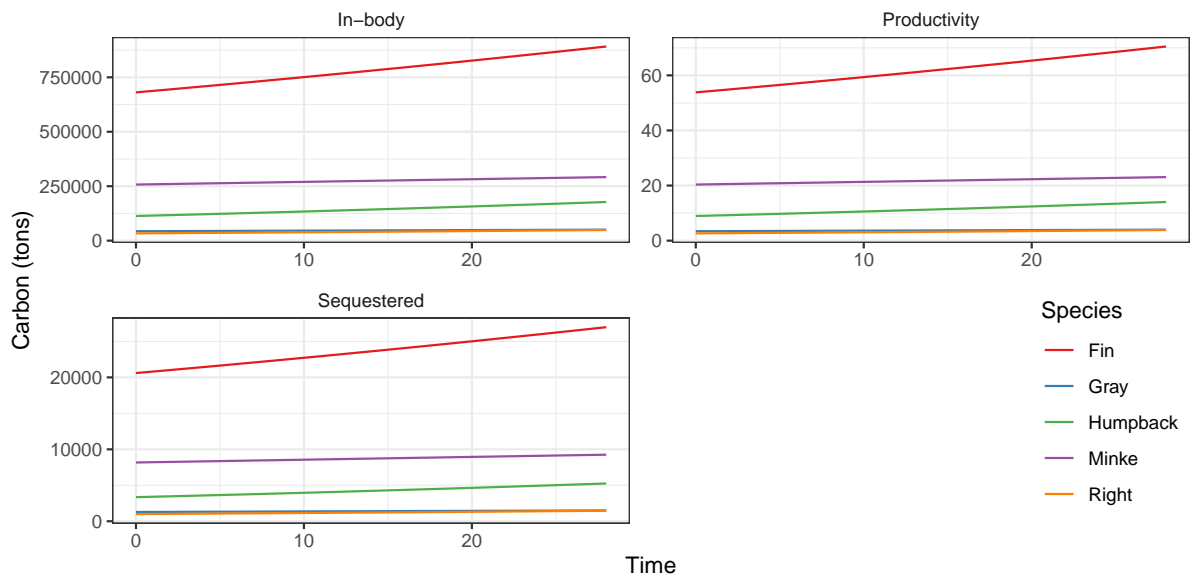
Supplementary Figure C.2: Stable age distributions for five baleen whale species. The x-axis shows age, the y-axis shows the proportion of individuals contained in each age class.



Supplementary Figure C.3: Reproductive value (y-axis) by age (x-axis) for five baleen whale species.



Supplementary Figure C.4: Time series of relative abundance (abundance normalized by carrying capacity) for five whale populations. These population trajectories are used as a baseline for the subsequent simulations where human-induced whale mortality is introduced.



Supplementary Figure C.5: Contribution of whales to the carbon cycle through time. Note that the sequestration plot shows annual values, not the cumulative sequestration.

Bibliography

- [1] A. D. Yeeting, H.-P. Weikard, M. Bailey, V. Ram-Bidesi, and S. R. Bush, *Stabilising cooperation through pragmatic tolerance: the case of the parties to the nauru agreement (pna) tuna fishery*, *Regional Environmental Change* **18** (2018), no. 3 885–897.
- [2] R Core Team, *R: A Language and Environment for Statistical Computing*. R Foundation for Statistical Computing, Vienna, Austria, 2021.
- [3] B. C. O’Leary, M. Winther-Janson, J. M. Bainbridge, J. Aitken, J. P. Hawkins, and C. M. Roberts, *Effective coverage targets for ocean protection*, *Conservation letters* **9** (nov, 2016) 398–404.
- [4] E. Dinerstein, C. Vynne, E. Sala, A. R. Joshi, S. Fernando, T. E. Lovejoy, J. Mayorga, D. Olson, G. P. Asner, J. E. M. Baillie, N. D. Burgess, K. Burkart, R. F. Noss, Y. P. Zhang, A. Baccini, T. Birch, N. Hahn, L. N. Joppa, and E. Wikramanayake, *A global deal for nature: Guiding principles, milestones, and targets*, *Sci. Adv.* **5** (apr, 2019) eaaw2869.
- [5] E. Sala, J. Lubchenco, K. Grorud-Colvert, C. Novelli, C. Roberts, and U. R. Sumaila, *Assessing real progress towards effective ocean protection*, *Marine Policy* **91** (may, 2018) 11–13.
- [6] E. Sala and S. Giakoumi, *No-take marine reserves are the most effective protected areas in the ocean*, *ICES Journal of Marine Science* **75** (2018), no. 3 1166–1168.
- [7] E. Mcleod, M. Bruton-Adams, J. Förster, C. Franco, G. Gaines, B. Gorong, R. James, G. Posing-Kulwaum, M. Tara, and E. Terk, *Lessons from the pacific islands – adapting to climate change by supporting social and ecological resilience*, *Frontiers in Marine Science* (2019).
- [8] N. Ramesh, J. A. Rising, and K. L. Oremus, *The small world of global marine fisheries: The cross-boundary consequences of larval dispersal*, *Science* **364** (2019), no. 6446 1192–1196.

- [9] C. M. Hernández, J. Witting, C. Willis, S. R. Thorrold, J. K. Llopiz, and R. D. Rotjan, *Evidence and patterns of tuna spawning inside a large no-take marine protected area*, *Scientific reports* **9** (2019), no. 1 1–11.
- [10] T. Agardy, *Justified ambivalence about mpa effectiveness*, *ICES Journal of Marine Science* **75** (2018), no. 3 1183–1185.
- [11] E. Havice, *The structure of tuna access agreements in the western and central pacific ocean: Lessons for vessel day scheme planning*, *Marine Policy* **34** (sep, 2010) 979–987.
- [12] E. Havice, *Rights-based management in the western and central pacific ocean tuna fishery: Economic and environmental change under the vessel day scheme*, *Marine Policy* **42** (nov, 2013) 259–267.
- [13] T. Aqorau, J. Bell, and J. N. Kittinger, *Good governance for migratory species*, *Science* **361** (sep, 2018) 1208.2–1209.
- [14] G. D. Libecap, *Distributional issues in contracting for property rights*, *Journal of Institutional and Theoretical Economics* **145** (mar, 1989) 6–24.
- [15] C. Costello, D. Ovando, T. Clavelle, C. K. Strauss, R. Hilborn, M. C. Melnychuk, T. A. Branch, S. D. Gaines, C. S. Szuwalski, R. B. Cabral, *et. al.*, *Global fishery prospects under contrasting management regimes*, *Proceedings of the national academy of sciences* **113** (2016), no. 18 5125–5129.
- [16] Hagrannsoknir, *Review of the purse seine vessel day scheme*, tech. rep., PNA Office, available at: www.pnatuna.com/sites/default/files/IndependentVDS
- [17] PNA, *Parties to the nauru agreement*, 2018.
- [18] D. A. Kroodsma, J. Mayorga, T. Hochberg, N. A. Miller, K. Boerder, F. Ferretti, A. Wilson, B. Bergman, T. D. White, B. A. Block, P. Woods, B. Sullivan, C. Costello, and B. Worm, *Tracking the global footprint of fisheries.*, *Science* **359** (feb, 2018) 904–908.
- [19] Q. Hanich, R. Rotjan, T. Aqorau, M. Bailey, B. Campbell, N. Gray, R. Gruby, J. Hampton, Y. Ota, H. Parris, *et. al.*, *Unraveling the blue paradox: Incomplete analysis yields incorrect conclusions about phoenix islands protected area closure*, *Proceedings of the National Academy of Sciences* **115** (2018), no. 52 E12122–E12123.
- [20] P. Terawasi and C. Reid, *Economic and development indicators and statistics: Tuna fisheries of the western and central pacific ocean*, tech. rep., Pacific Islands Forum Fisheries Agency, Honaira, Solomon Islands, 2017.

- [21] D. J. McCauley, P. Woods, B. Sullivan, B. Bergman, C. Jablonicky, A. Roan, M. Hirshfield, K. Boerder, and B. Worm, *Ending hide and seek at sea*, *Science* **351** (mar, 2016) 1148–1150.
- [22] G. R. McDermott, K. C. Meng, G. G. McDonald, and C. J. Costello, *The blue paradox: Preemptive overfishing in marine reserves.*, *Proc Natl Acad Sci USA* (aug, 2018).
- [23] P. J. Ferraro, J. N. Sanchirico, and M. D. Smith, *Causal inference in coupled human and natural systems*, *Proceedings of the National Academy of Sciences* (2018) 201805563.
- [24] G. Ortuno-Crespo, D. C. Dunn, G. Reygondeau, K. Boerder, B. Worm, W. Cheung, D. P. Tittensor, and P. N. Halpin, *The environmental niche of the global high seas pelagic longline fleet*, *Sci. Adv.* **4** (aug, 2018) eaat3681.
- [25] M. W. Rosegrant and H. P. Binswanger, *Markets in tradable water rights: Potential for efficiency gains in developing country water resource allocation*, *World development* **22** (1994), no. 11 1613–1625.
- [26] J. M. Hutton and N. Leader-Williams, *Sustainable use and incentive-driven conservation: realigning human and conservation interests*, *Oryx* **37** (2003), no. 2 215–226.
- [27] C. Sandbrook, J. A. Fisher, G. Holmes, R. Luque-Lora, and A. Keane, *The global conservation movement is diverse but not divided*, *Nature Sustainability* **2** (2019), no. 4 316–323.
- [28] C. M. Roberts, B. C. O’Leary, D. J. McCauley, P. M. Cury, C. M. Duarte, J. Lubchenco, D. Pauly, A. Sáenz-Arroyo, U. R. Sumaila, R. W. Wilson, B. Worm, and J. C. Castilla, *Marine reserves can mitigate and promote adaptation to climate change*, *Proc Natl Acad Sci USA* **114** (jun, 2017) 6167–6175.
- [29] N. C. Ban, G. G. Gurney, N. A. Marshall, C. K. Whitney, M. Mills, S. Gelcich, N. J. Bennett, M. C. Meehan, C. Butler, S. Ban, T. C. Tran, M. E. Cox, and S. J. Breslow, *Well-being outcomes of marine protected areas*, *Nature Sustainability* **2** (jun, 2019) 524–532.
- [30] F. Micheli, B. S. Halpern, L. W. Botsford, and R. R. Warner, *Trajectories and correlates of community change in no-take marine reserves*, *Ecological applications* **14** (2004), no. 6 1709–1723.
- [31] B. Worm, E. B. Barbier, N. Beaumont, J. E. Duffy, C. Folke, B. S. Halpern, J. B. Jackson, H. K. Lotze, F. Micheli, S. R. Palumbi, *et. al.*, *Impacts of biodiversity loss on ocean ecosystem services*, *science* **314** (2006), no. 5800 787–790.

- [32] S. E. Lester, B. S. Halpern, K. Grorud-Colvert, J. Lubchenco, B. I. Ruttenberg, S. D. Gaines, S. Airamé, and R. R. Warner, *Biological effects within no-take marine reserves: a global synthesis*, *Marine Ecology Progress Series* **384** (2009) 33–46.
- [33] C. M. Roberts, B. C. O’Leary, D. J. McCauley, P. M. Cury, C. M. Duarte, J. Lubchenco, D. Pauly, A. Sáenz-Arroyo, U. R. Sumaila, R. W. Wilson, *et. al.*, *Marine reserves can mitigate and promote adaptation to climate change*, *Proceedings of the National Academy of Sciences* **114** (2017), no. 24 6167–6175.
- [34] R. B. Cabral, B. S. Halpern, S. E. Lester, C. White, S. D. Gaines, and C. Costello, *Designing mpas for food security in open-access fisheries*, *Scientific reports* **9** (2019), no. 1 1–10.
- [35] E. Sala, J. Lubchenco, K. Grorud-Colvert, C. Novelli, C. Roberts, and U. R. Sumaila, *Assessing real progress towards effective ocean protection*, *Marine Policy* **91** (2018) 11–13.
- [36] S. Kark, N. Levin, H. S. Grantham, and H. P. Possingham, *Between-country collaboration and consideration of costs increase conservation planning efficiency in the mediterranean basin*, *Proceedings of the National Academy of Sciences* **106** (2009), no. 36 15368–15373.
- [37] T. Mazor, H. P. Possingham, and S. Kark, *Collaboration among countries in marine conservation can achieve substantial efficiencies*, *Diversity and Distributions* **19** (2013), no. 11 1380–1393.
- [38] E. Sala, J. Mayorga, D. Bradley, R. B. Cabral, T. B. Atwood, A. Auber, W. Cheung, C. Costello, F. Ferretti, A. M. Friedlander, *et. al.*, *Protecting the global ocean for biodiversity, food and climate*, *Nature* **592** (2021), no. 7854 397–402.
- [39] L. A. Roberson, H. L. Beyer, C. O’Hara, J. E. Watson, D. C. Dunn, B. S. Halpern, C. J. Klein, M. R. Frazier, C. D. Kuempel, B. Williams, *et. al.*, *Multinational coordination required for conservation of over 90% of marine species*, *Global Change Biology* **27** (2021), no. 23 6206–6216.
- [40] B. G. Colby, *Cap-and-trade policy challenges: a tale of three markets*, *Land economics* (2000) 638–658.
- [41] R. Schmalensee and R. N. Stavins, *Lessons learned from three decades of experience with cap and trade*, *Review of Environmental Economics and Policy* (2020).
- [42] R. Arnason, *Property rights in fisheries: Iceland’s experience with itqs*, *Reviews in Fish Biology and Fisheries* **15** (2005), no. 3 243–264.

- [43] C. Costello, S. D. Gaines, and J. Lynham, *Can catch shares prevent fisheries collapse?*, *Science* **321** (2008), no. 5896 1678–1681.
- [44] C. W. Howe, D. R. Schurmeier, and W. D. Shaw Jr, *Innovative approaches to water allocation: the potential for water markets*, *Water resources research* **22** (1986), no. 4 439–445.
- [45] H. Chong and D. Sunding, *Water markets and trading*, *Annu. Rev. Environ. Resour.* **31** (2006) 239–264.
- [46] R. Fujita, J. Lynham, F. Micheli, P. G. Feinberg, L. Bourillón, A. Sáenz-Arroyo, and A. C. Markham, *Ecomarkets for conservation and sustainable development in the coastal zone*, *Biological Reviews* **88** (2013), no. 2 273–286.
- [47] C. M. Roberts, C. J. McClean, J. E. Veron, J. P. Hawkins, G. R. Allen, D. E. McAllister, C. G. Mittermeier, F. W. Schueler, M. Spalding, F. Wells, *et. al.*, *Marine biodiversity hotspots and conservation priorities for tropical reefs*, *Science* **295** (2002), no. 5558 1280–1284.
- [48] T. Morato, S. D. Hoyle, V. Allain, and S. J. Nicol, *Seamounts are hotspots of pelagic biodiversity in the open ocean*, *Proceedings of the National Academy of Sciences* **107** (2010), no. 21 9707–9711.
- [49] C. N. Jenkins and K. S. Van Houtan, *Global and regional priorities for marine biodiversity protection*, *Biological Conservation* **204** (2016) 333–339.
- [50] D. A. Kroodsma, J. Mayorga, T. Hochberg, N. A. Miller, K. Boerder, F. Ferretti, A. Wilson, B. Bergman, T. D. White, B. A. Block, *et. al.*, *Tracking the global footprint of fisheries*, *Science* **359** (2018), no. 6378 904–908.
- [51] N. O. Keohane and S. M. Olmstead, *Markets and the Environment*. Island Press, 2016.
- [52] H. M. Leslie, *A synthesis of marine conservation planning approaches*, *Conservation Biology* **19** (2005), no. 6 1701–1713.
- [53] Q. Zhao, F. Stephenson, C. Lundquist, K. Kaschner, D. Jayathilake, and M. J. Costello, *Where marine protected areas would best represent 30% of ocean biodiversity*, *Biological Conservation* **244** (2020) 108536.
- [54] K. Kaschner, K. Kesner-Reyes, C. Garilao, J. Segschneider, J. Rius-Barile, T. Rees, and R. Froese, *Aquamaps: Predicted range maps for aquatic species*, 2019.
- [55] R. Froese, D. Pauly, *et. al.*, *Fishbase*, 2010.
- [56] M. Palomares, D. Pauly, *et. al.*, *Sealifebase*, 2020.

- [57] C. Boettiger, D. Temple Lang, and P. Wainwright, *rfishbase: exploring, manipulating and visualizing FishBase data from r*, *Journal of Fish Biology* (nov, 2012).
- [58] Fisheries and F. Aquaculture Division, *Asfis list of species for fishery statistics purposes*, 2021.
- [59] R. A. Watson, *A database of global marine commercial, small-scale, illegal and unreported fisheries catch 1950–2014*, *Scientific Data* **4** (2017), no. 1 1–9.
- [60] F. M. Institute, *Maritime boundaries geodatabase: Maritime boundaries and exclusive economic zones (200nm)*, version 11, 2018.
- [61] M. D. Spalding, H. E. Fox, G. R. Allen, N. Davidson, Z. A. Ferdaña, M. Finlayson, B. S. Halpern, M. A. Jorge, A. Lombana, S. A. Lourie, *et. al.*, *Marine ecoregions of the world: a bioregionalization of coastal and shelf areas*, *BioScience* **57** (2007), no. 7 573–583.
- [62] N. Dudley, *Guidelines for applying protected area management categories*. Iucn, 2008.
- [63] W. C. P. A. International Union for the Conservation of Nature, *Recognising and reporting other effective area-based conservation measures*, 2019.
- [64] M. D. Barnes, L. Glew, C. Wyborn, and I. D. Craigie, *Prevent perverse outcomes from global protected area policy*, *Nature Ecology & Evolution* **2** (2018), no. 5 759–762.
- [65] N. Bhola, H. Klimmek, N. Kingston, N. D. Burgess, A. van Soesbergen, C. Corrigan, J. Harrison, and M. T. Kok, *Perspectives on area-based conservation and its meaning for future biodiversity policy*, *Conservation Biology* **35** (2021), no. 1 168–178.
- [66] H. D. Jonas, G. N. Ahmadi, H. C. Bingham, J. Briggs, D. Butchart, J. Cariño, O. Chassot, S. Chaudhary, E. Darling, A. Degemmis, *et. al.*, *Equitable and effective area-based conservation: towards the conserved areas paradigm*, *PARKS: The International Journal of Protected Areas and Conservation* **27** (2021).
- [67] S. A. Lourie and A. C. Vincent, *Using biogeography to help set priorities in marine conservation*, *Conservation Biology* **18** (2004), no. 4 1004–1020.
- [68] M. D. Smith, J. Lynham, J. N. Sanchirico, and J. A. Wilson, *Political economy of marine reserves: Understanding the role of opportunity costs*, *Proceedings of the National Academy of Sciences* **107** (2010), no. 43 18300–18305.

- [69] J. Lynham, A. Nikolaev, J. Raynor, T. Vilela, and J. C. Villaseñor-Derbez, *Impact of two of the world's largest protected areas on longline fishery catch rates*, *Nature communications* **11** (2020), no. 1 1–9.
- [70] R. Watson, A. Kitchingman, A. Gelchu, and D. Pauly, *Mapping global fisheries: sharpening our focus*, *Fish and fisheries* **5** (2004), no. 2 168–177.
- [71] M. C. Melnychuk, T. Clavelle, B. Owashi, and K. Strauss, *Reconstruction of global ex-vessel prices of fished species*, *ICES Journal of Marine Science* **74** (2017), no. 1 121–133.
- [72] M. B. Mascia and S. Pailler, *Protected area downgrading, downsizing, and degazettement (padd) and its conservation implications*, *Conservation letters* **4** (2011), no. 1 9–20.
- [73] B. C. O’Leary, M. Winther-Janson, J. M. Bainbridge, J. Aitken, J. P. Hawkins, and C. M. Roberts, *Effective coverage targets for ocean protection*, *Conservation Letters* **9** (2016), no. 6 398–404.
- [74] C. on Biological Diversity, *A new global framework for managing nature through 2030*, 2022.
- [75] D. M. Costle, *Air pollution control; recommendation for alternative emission reduction options within state implementation plans*, *Federal Register* **044** (1979) 3740–3744.
- [76] M. Deland, *Regulatory alert: The bubble concept*, *Environmental Science & TECHNOLOGY* **13** (1979), no. 3 277–277.
- [77] A. Fredston-Hermann, S. D. Gaines, and B. S. Halpern, *Biogeographic constraints to marine conservation in a changing climate.*, *Annals of the New York Academy of Sciences* **1429** (2018), no. 1 5–17.
- [78] E. Dinerstein, C. Vynne, E. Sala, A. R. Joshi, S. Fernando, T. E. Lovejoy, J. Mayorga, D. Olson, G. P. Asner, J. E. Baillie, *et. al.*, *A global deal for nature: guiding principles, milestones, and targets*, *Science advances* **5** (2019), no. 4 eaaw2869.
- [79] N. J. Bennett, H. Govan, and T. Satterfield, *Ocean grabbing*, *Marine Policy* **57** (2015) 61–68.
- [80] M.-A. F. Mallin, D. C. Stolz, B. S. Thompson, and M. Barbesgaard, *In oceans we trust: Conservation, philanthropy, and the political economy of the phoenix islands protected area*, *Marine Policy* **107** (2019) 103421.
- [81] T. Aqorau, *Recent developments in pacific tuna fisheries: the palau arrangement and the vessel day scheme*, *Int’l J. Marine & Coastal L.* **24** (2009) 557.

- [82] E. Havice, *Rights-based management in the western and central pacific ocean tuna fishery: Economic and environmental change under the vessel day scheme*, *Marine Policy* **42** (2013) 259–267.
- [83] H. Frost and P. Andersen, *The common fisheries policy of the european union and fisheries economics*, *Marine Policy* **30** (2006), no. 6 737–746.
- [84] C. of the European Communities (EC), *Green paper: reform of the common fisheries policy [com(2009) 163 final]*, 2009.
- [85] M. B. Mascia and C. A. Claus, *A property rights approach to understanding human displacement from protected areas: the case of marine protected areas*, *Conservation Biology* **23** (2009), no. 1 16–23.
- [86] C. C. O’Hara, J. C. Villaseñor-Derbez, G. M. Ralph, and B. S. Halpern, *Mapping status and conservation of global at-risk marine biodiversity*, *Conservation Letters* **12** (2019), no. 4 e12651.
- [87] B. S. Halpern, S. Walbridge, K. A. Selkoe, C. V. Kappel, F. Micheli, C. D’Agrosa, J. F. Bruno, K. S. Casey, C. Ebert, H. E. Fox, *et. al.*, *A global map of human impact on marine ecosystems*, *science* **319** (2008), no. 5865 948–952.
- [88] E. S. Poloczanska, M. T. Burrows, C. J. Brown, J. García Molinos, B. S. Halpern, O. Hoegh-Guldberg, C. V. Kappel, P. J. Moore, A. J. Richardson, D. S. Schoeman, *et. al.*, *Responses of marine organisms to climate change across oceans*, *Frontiers in Marine Science* (2016) 62.
- [89] C. M. Free, J. T. Thorson, M. L. Pinsky, K. L. Oken, J. Wiedenmann, and O. P. Jensen, *Impacts of historical warming on marine fisheries production*, *Science* **363** (2019), no. 6430 979–983.
- [90] M. L. Pinsky, B. Worm, M. J. Fogarty, J. L. Sarmiento, and S. A. Levin, *Marine taxa track local climate velocities*, *Science* **341** (2013), no. 6151 1239–1242.
- [91] J. F. Bruno, A. E. Bates, C. Cacciapaglia, E. P. Pike, S. C. Amstrup, R. Van Hoodonk, S. A. Henson, and R. B. Aronson, *Climate change threatens the world’s marine protected areas*, *Nature Climate Change* **8** (2018), no. 6 499–503.
- [92] S. M. Johnson and J. R. Watson, *Novel environmental conditions due to climate change in the world’s largest marine protected areas*, *One Earth* **4** (2021), no. 11 1625–1634.
- [93] A. Fredston-Hermann, R. Selden, M. Pinsky, S. D. Gaines, and B. S. Halpern, *Cold range edges of marine fishes track climate change better than warm edges*, *Global Change Biology* **26** (2020), no. 5 2908–2922.

- [94] IPCC, *Climate Change 2021: The Physical Science Basis. Contribution of Working Group I to the Sixth Assessment Report of the Intergovernmental Panel on Climate Change*. Cambridge University Press, Cambridge, United Kingdom and New York, NY, USA, 2021.
- [95] R. Dirzo, H. S. Young, M. Galetti, G. Ceballos, N. J. Isaac, and B. Collen, *Defaunation in the anthropocene*, *science* **345** (2014), no. 6195 401–406.
- [96] H. Keith, M. Vardon, C. Obst, V. Young, R. A. Houghton, and B. Mackey, *Evaluating nature-based solutions for climate mitigation and conservation requires comprehensive carbon accounting*, *Science of The Total Environment* **769** (2021) 144341.
- [97] U. Nations, *Sustainable development goals 2019. high-level political forum 2018 review of goal 15*, 2019.
- [98] S. Luysaert, E. Schulze, A. Börner, A. Knohl, D. Hessenmöller, B. E. Law, P. Ciais, J. Grace, *et. al.*, *Old-growth forests as global carbon sinks*, *Nature* **455** (2008), no. 7210 213–215.
- [99] Y. Malhi, P. Meir, and S. Brown, *Forests, carbon and global climate*, *Philosophical Transactions of the Royal Society of London. Series A: Mathematical, Physical and Engineering Sciences* **360** (2002), no. 1797 1567–1591.
- [100] R. Sedjo and B. Sohngen, *Carbon sequestration in forests and soils*, *Annu. Rev. Resour. Econ.* **4** (2012), no. 1 127–144.
- [101] G. M. Domke, S. N. Oswalt, B. F. Walters, and R. S. Morin, *Tree planting has the potential to increase carbon sequestration capacity of forests in the united states*, *Proceedings of the National Academy of Sciences* **117** (2020), no. 40 24649–24651.
- [102] A. Victor, N. Valery, and Z. Louis, *Carbon storage and emission factor of savanna ecosystems in soudano-sahelian zone of cameroon*, *J Bot Res* **2** (2020), no. 1 60–67.
- [103] J. B. Kauffman, A. F. Bernardino, T. O. Ferreira, L. R. Giovannoni, L. E. de O. Gomes, D. J. Romero, L. C. Z. Jimenez, and F. Ruiz, *Carbon stocks of mangroves and salt marshes of the amazon region, brazil*, *Biology Letters* **14** (2018), no. 9 20180208.
- [104] D. R. Richards, B. S. Thompson, and L. Wijedasa, *Quantifying net loss of global mangrove carbon stocks from 20 years of land cover change*, *Nature communications* **11** (2020), no. 1 1–7.

- [105] G. Mariani, W. W. Cheung, A. Lyet, E. Sala, J. Mayorga, L. Velez, S. D. Gaines, T. Dejean, M. Troussellier, and D. Mouillot, *Let more big fish sink: Fisheries prevent blue carbon sequestration—half in unprofitable areas*, *Science advances* **6** (2020), no. 44 eabb4848.
- [106] R. Ritschard, *Marine algae as a co2 sink*, *Water, Air, and Soil Pollution* **64** (1992), no. 1 289–303.
- [107] P. Kaladharan, S. Veena, and E. Vivekanandan, *Carbon sequestration by a few marine algae: observation and projection*, *Journal of the Marine Biological Association of India* **51** (2009), no. 1 107–110.
- [108] A. J. Pershing, L. B. Christensen, N. R. Record, G. D. Sherwood, and P. B. Stetson, *The impact of whaling on the ocean carbon cycle: why bigger was better*, *PloS one* **5** (2010), no. 8 e12444.
- [109] R. G. Haight, R. Bluffstone, J. D. Kline, J. W. Coulston, D. N. Wear, and K. Zook, *Estimating the present value of carbon sequestration in us forests, 2015–2050, for evaluating federal climate change mitigation policies*, *Agricultural and Resource Economics Review* **49** (2020), no. 1 150–177.
- [110] C. A. Butman, J. T. Carlton, and S. R. Palumbi, *Whaling effects on deep-sea biodiversity*, 1995.
- [111] M. D. Smith and J. E. Wilen, *Economic impacts of marine reserves: the importance of spatial behavior*, *Journal of Environmental Economics and Management* **46** (sep, 2003) 183–206.
- [112] J. Roman, J. A. Estes, L. Morissette, C. Smith, D. Costa, J. McCarthy, J. Nation, S. Nicol, A. Pershing, and V. Smetacek, *Whales as marine ecosystem engineers*, *Frontiers in Ecology and the Environment* **12** (2014), no. 7 377–385.
- [113] L. Ratnarajah, A. R. Bowie, D. Lannuzel, K. M. Meiners, and S. Nicol, *The biogeochemical role of baleen whales and krill in southern ocean nutrient cycling*, *PloS one* **9** (2014), no. 12 e114067.
- [114] R. Chami, T. F. Cosimano, C. Fullenkamp, and S. Oztosun, *Nature’s solution to climate change: A strategy to protect whales can limit greenhouse gases and global warming*, *Finance & Development* **56** (2019), no. 004.
- [115] E. Oldach, H. Killeen, P. Shukla, E. Brauer, N. Carter, J. Fields, A. Thomsen, C. Cooper, L. Mellinger, K. Wang, *et. al.*, *Managed and unmanaged whale mortality in the california current ecosystem*, *Marine Policy* **140** (2022) 105039.
- [116] L. Saez, D. Lawson, and M. DeAngelis, *Large whale entanglements off the us west coast, from 1982-2017*, .

- [117] M. Berman-Kowalewski, F. M. Gulland, S. Wilkin, J. Calambokidis, B. Mate, J. Cordaro, D. Rotstein, J. St Leger, P. Collins, K. Fahy, *et. al.*, *Association between blue whale (*balaenoptera musculus*) mortality and ship strikes along the california coast*, *Aquatic Mammals* **36** (2010), no. 1 59–66.
- [118] A. S. Jensen, G. K. Silber, and J. Calambokidis, *Large whale ship strike database*, .
- [119] C. R. Smith and A. R. Baco, *Ecology of whale falls at the deep-sea floor*, *Oceanography and marine biology* **41** (2003) 311–354.
- [120] A. Jensen, *Simple density-dependent matrix model for population projection*, *Ecological modelling* **77** (1995), no. 1 43–48.
- [121] H. Caswell, *Matrix population models*, vol. 1. Sinauer Sunderland, MA, 2000.
- [122] A. Jelmert and D. O. Oppen-Berntsen, *Whaling and deep-sea biodiversity*, *Conservation biology* **10** (1996), no. 2 653–654.
- [123] M. S. Savoca, M. F. Czapanskiy, S. R. Kahane-Rapport, W. T. Gough, J. A. Fahlbusch, K. Bierlich, P. S. Segre, J. Di Clemente, G. S. Penry, D. N. Wiley, *et. al.*, *Baleen whale prey consumption based on high-resolution foraging measurements*, *Nature* **599** (2021), no. 7883 85–90.
- [124] I. W. Group *et. al.*, *Technical support document: social cost of carbon, methane, and nitrous oxide interim estimates under executive order 13990*, tech. rep., Tech. rep., White House. URL [https://www.whitehouse.gov/wp-content/uploads . . .](https://www.whitehouse.gov/wp-content/uploads...), 2021.
- [125] H. Caswell, *A general formula for the sensitivity of population growth rate to changes in life history parameters*, *Theoretical population biology* **14** (1978), no. 2 215–230.
- [126] M. Jerath, M. Bhat, V. H. Rivera-Monroy, E. Castañeda-Moya, M. Simard, and R. R. Twilley, *The role of economic, policy, and ecological factors in estimating the value of carbon stocks in everglades mangrove forests, south florida, usa*, *Environmental Science & Policy* **66** (2016) 160–169.
- [127] J. W. Fourqurean, C. M. Duarte, H. Kennedy, N. Marbà, M. Holmer, M. A. Mateo, E. T. Apostolaki, G. A. Kendrick, D. Krause-Jensen, K. J. McGlathery, *et. al.*, *Seagrass ecosystems as a globally significant carbon stock*, *Nature geoscience* **5** (2012), no. 7 505–509.
- [128] T. B. Atwood, A. Witt, J. Mayorga, E. Hammill, and E. Sala, *Global patterns in marine sediment carbon stocks*, *Frontiers in Marine Science* **7** (2020) 165.

- [129] C. Costello, S. Gaines, and L. R. Gerber, *A market approach to saving the whales*, *Nature* **481** (2012), no. 7380 139–140.
- [130] R. Freedman, S. Herron, M. Byrd, K. Birney, J. Morten, B. Shafritz, C. Caldow, and S. Hastings, *The effectiveness of incentivized and non-incentivized vessel speed reduction programs: Case study in the santa barbara channel*, *Ocean & Coastal Management* **148** (2017) 31–39.
- [131] E. L. Hazen, D. M. Palacios, K. A. Forney, E. A. Howell, E. Becker, A. L. Hoover, L. Irvine, M. DeAngelis, S. J. Bograd, B. R. Mate, *et. al.*, *Whalewatch: a dynamic management tool for predicting blue whale density in the california current*, *Journal of Applied Ecology* **54** (2017), no. 5 1415–1428.
- [132] A. Angelsen, S. Brown, and C. Loisel, *Reducing emissions from deforestation and forest degradation (redd): an options assessment report*, .
- [133] D. Cook, L. Malinauskaite, B. Davihottir, H. Ögmundardóttir, and J. Roman, *Reflections on the ecosystem services of whales and valuing their contribution to human well-being*, *Ocean & Coastal Management* **186** (2020) 105100.